NTNU
Norwegian University of Science and Technology
Department of Marine Technology

M.Sc.THESIS

Title:	Delivered:
An investigation of forces and moments from drilling risers on wellheads	21.06.10
	Availability: Open
Student: Camilla Stokvik	**Number of pages:** 71+ Appendices

Abstract:

The technology of retrieving energy in form of oil and gas offshore is in continuous development, and is moving towards larger water depths and more difficult environmental conditions. Challenges regarding the use of deep water rigs in shallow waters have appeared in the industry, it is therefore of interest to investigate what happens when equipment designed for operation in deep water is used in shallow waters. An investigation can be done with a good analysis model. In this thesis an analysis model is created for the drilling riser system used by Deepsea Atlantic on the Troll field, where measurements of strains in the wellhead has been performed. The model results are compared with the measurements, which is done with the intention of optimizing the analysis model.

In this thesis the computer software OrcaFlex is used to perform the riser analysis. In OrcaFlex the riser model is build up from lines, buoys and springs by use of the graphical user interface in the program.

The main focus in this analysis is on the wellhead, but results for the 10ft pup joint is also presented to provide a wider evaluation basis. The model has been run for two cases, corresponding to two measurement sequences. Due to lack of information the current has been implemented from Metocean report from Troll and the waves are taken from logs kept during the operations that correspond to the measurements.

The evaluation of the model shows that at the area of main interest, the wellhead, the model does not provide accurate results. The forces and moments found do not correspond with the full scale measurements obtained. An investigation of the forces and moments in the wellhead is therefore not possible with the current model used. The reason for the deviation from reality is that the model is simplified to a large extent in the wellhead region of the system. In addition waves and current are affecting the analysis system in one direction and in reality the current direction will vary trough the water column.

The investigation of the forces and moments in the 10 ft pup joint shows better results and the results coincide to some extent with the reality, but the analysis results are non-conservative. The energy spectrums generated for all cases show that the model response equals the response of the measured system. The response results combined with the results found for the 10 ft pup joint implies that the model has some correct elements and can be used as a basis for further development. In such a development the correct waves and current should be implemented from measured data; and the soil and wellhead model should be modeled in more detail.

Keyword:

Drilling riser analysis, OrcaFlex,
Full-scale measurements

Advisor:

Carl Martin Larsen

Address:
NTNU
Department of Marine Technology
N-7491 Trondheim

Location
Marinteknisk Senter
O. Nielsens vei 10

Tel. +47 73 595501
Fax +47 73 595697

Master Thesis in Marine Hydrodynamics

An investigation of forces and moments from drilling risers on wellheads

Camilla Stokvik

Spring 2010

NTNU
Norwegian University of
Science and Technology

NTNU
Norwegian University of Science and Technology

Scope of work

M.Sc. thesis 2010

For

Stud.techn. Camilla Stokvik

An investigation of forces and moments from drilling risers on wellheads

The marine drilling riser is connected to the wellhead during drilling. The riser is exposed to dynamic loads from currents, ocean waves and drilling platform motions. Hence, dynamic analysis of the riser and wellhead system is needed in order to find forces and moments in the wellhead. The quality of dynamic riser analysis is therefore crucial to ensure safe operation and avoid excessive loads and damage of the wellhead structure. The objective of this work is to describe analysis models for calculation of dynamic riser and wellhead response, and improve the accuracy of such analyses by comparison between analysis results and full scale measurements.

For a Mobile Offshore Drilling Unit in operation the drilling riser and the BOP are essential parts of the system. These are well investigated, but the interaction between the BOP and the wellhead is an area which has had little attention. Previously it has been assumed that the BOP will not experience significant movements, and hence not transfer significant forces to the wellhead. This has shown not to be true in all cases. A combination of full scale measurements and computer analysis can give better understanding of the forces occurring in the wellhead for specific cases.

This thesis will be completed in collaboration between the candidate, NTNU and Odfjell Drilling Technology AS (ODT). ODT is a division within the Odfjell Drilling group and works, amongst many other things, with riser analyses, mooring analyses and rig motions for the company's Mobile Offshore Drilling Units. An interest for Odfjell Drilling and ODT is to investigate the deformations, forces and moments on the wellhead caused by rig motions and drilling riser dynamics.

The work should be carried out in steps as follows:

Background and literature study

- Describe in brief the drilling rig, marine riser, BOP and wellhead. Why is the topic interesting – set the scene w.r.t. situation in industry today. Describe in particular the DeepSea Atlantic (DSA) rig and relevant equipment.

Theory

- Theory behind modeling the system for calculation purposes. Which simplifications one can assume and the consequences of these simplifications.

- Full-scale measurement; describe measurement set up used, and how to convert the measurement data into parameters which can be used in comparison cases, i.e. transformation from strain to bending moment and force.

Analysis tools

- Computer program for riser analyses (OrcaFlex).
- Describe the element formulation and methods for dynamic analysis in brief and also modelling options for the actual drilling riser system.
- Make a model for the drilling riser on DSA in operation on the Troll field.
- Carry out a set of analysis

Result comparison

- Process measured data.
- Evaluate the model in the program by comparing full-scale measurements from DSA on Troll, with the analysis results

Conclusions and proposal for further work

The work may show to be more extensive than anticipated. Some topics may therefore be left out after discussion with the supervisor without any negative influence on the grading.

The candidate should in her report give a personal contribution to the solution of the problem formulated in this text. All assumptions and conclusions must be supported by mathematical models and/or references to physical effects in a logical manner.

The candidate should apply all available sources to find relevant literature and information on the actual problem.

The report should be well organised and give a clear presentation of the work and all conclusions. It is important that the text is well written and that tables and figures are used to support the verbal presentation. The report should be complete, but still as short as possible.

The final report must contain this text, a preface, abstract, main body, conclusions and suggestions for further work, symbol list, references and appendices. All figures, tables and equations must be identified by numbers. References should be given by author and year in the text, and presented alphabetically in the reference list. The report must be submitted in two copies unless otherwise has been agreed with the supervisor.

The supervisor may require that the candidate should give a written plan that describes the progress of the work after having received this text. The plan may contain a table of content for the report and also assumed use of computer resources.

From the report it should be possible to identify the work carried out by the candidate and what has been found in the available literature. It is important to give references to the original source for theories and experimental results.

The report must be signed by the candidate, include this text, appear as a paperback, and - if needed - have a separate enclosure (binder, diskette or DVD-ROM) with additional material.

Supervisor at NTNU is Professor Carl M. Larsen

Contact persons at ODT is Elin Crombie, Nicolas J. Toynbee and Erik F. Drageset

Trondheim, February 2010

Carl M. Larsen

Submitted: January 2010

Deadline: June 2010

Preface

This report is the result of the MSc thesis which is the last part of the five year master program in Marine Technology at the Norwegian University of Science and Technology (NTNU). The thesis is written in the last semester and is weighted with 30 units. This thesis consists of a literature study and an analysis part.

The common progression of the master program is to write a project-thesis before this main thesis, where a literature study for the subject handled will be performed. I chose to change focus after writing my project thesis. Because of this, and that that drilling was a relative new field for me, a literature study has been performed in an extended degree in the beginning of this thesis.

The literature study is performed to provide an introduction to the subject of drilling and especially drilling risers. This information is gained to obtain insight and overall understanding of the technology and system in focus, as well as finding information that can be used in the analysis part. The analysis in the report is performed in an analysis tool, OrcaFlex, and learning the program has also been a large part of the thesis.

In the section dealing with full-scale measurements and the transformation of the measurements to comparable sizes, theory presented in the project thesis could also be used in this thesis. The theory of the transformation was based on circular cylinders in the project-thesis, which is suited for the marine riser in this thesis.

As the work progressed I learned and failed several times. Among other things the focus on the literature study was to large, this can be seen in the aftermath of the process. So, in addition to the theoretical knowledge gained in this thesis, training in work methods and time prioritizing in a project work has been of great value for the author.

It is assumed that the persons reading this thesis has some background knowledge to the terminology of the theory presented in the report.

I would like to thank Professor Carl Martin Larsen for guidance with the thesis. I would also like to direct thanks to my co supervisors at Odfjell Drilling Technology AS, Elin Crombie, Nicholas Toynbee and Erik F. Drageset for all the support and guidance during the thesis work.

Bergen, 21 June 2010

_____

Camilla Stokvik

Abstract

The technology of retrieving energy in form of oil and gas offshore is in continuous development, and is moving towards larger water depths and more difficult environmental conditions. Challenges regarding the use of deep water rigs in shallow waters have appeared in the industry, it is therefore of interest to investigate what happens when equipment designed for operation in deep water is used in shallow waters. An investigation can be done with a good analysis model. In this thesis an analysis model is created for the drilling riser system used by Deepsea Atlantic on the Troll field, where measurements of strains in the wellhead has been performed. The model results are compared with the measurements, which is done with the intention of optimizing the analysis model.

The typical riser system consists of several components; which have to withstand high tension, bending moments, resist fatigue damage and the weight should to be as small as possible. Marine drilling riser mechanics give the physical and the mathematical aspects of riser theory which include tension, pressure and weight aspects, especially with regard to geometric stiffness and effective tension, as well as stress and strains which occur in the riser structure.

An analysis of marine risers will implement the finite element method and consist of a static and a dynamic analysis part. The objective is to find the equilibrium of the system under the loads it is exposed to and to obtain information of how a structure responds and behaves when exposed to loads varying over time. In this thesis the computer software OrcaFlex is used to perform the riser analysis. OrcaFlex is a program used for static and dynamic analysis of several marine applications, including marine risers. It is a 3D non-linear time domain finite element program, which uses lumped mass element to simplify the mathematical formulation and make the calculation efficient. In OrcaFlex the riser model is build up from lines, buoys and springs by use of the graphical user interface in the program.

In the model the riser line is assumed to start at the upper flex joint and is divided into two main parts, the first stretching to the tension ring and the next stretching from the tension ring to the LMRP. The stack-up used on Troll is the stack-up modeled. The tension cylinders connected to the tension ring are modeled as springs. The LMRP is connected to the lower stack which in turn is connected to the wellhead. The springs that model the vertical and horizontal soil stiffness are connected to top of the wellhead.

The main focus in this analysis is on the wellhead, but results for the 10ft pup joint is also presented to provide a wider evaluation basis. The model has been run for two cases, corresponding to two measurement sequences. Due to lack of information the current has been implemented from Metocean report from Troll and the waves are taken from logs kept during the operations that correspond to the measurements.

The evaluation of the model shows that at the area of main interest, the wellhead, the model does not provide accurate results. The forces and moments found do not correspond with the full scale measurements obtained. An investigation of the forces and moments in the wellhead is therefore not

possible with the current model used. The reason for the deviation from reality may be that the model is simplified to a large extent in the wellhead region of the system. In addition waves and current are affecting the analysis system in one direction and in reality the current direction will vary trough the water column.

The investigation of the forces and moments in the 10 ft pup joint shows better results and the results coincide to some extent with the reality, but the analysis results are non-conservative. The energy spectrums generated for all cases show that the model response equals the response of the measured system. The response results combined with the results found for the 10 ft pup joint implies that the model has some correct elements and can be used as a basis for further development. In such a development the correct waves and current should be implemented from measured data; and the soil and wellhead model should be modeled in more detail.

Table of contents

List of figures

List of tables

List of symbols and acronyms

α	Deflection angle
a	Acceleration vector
A	Area
A_e	External cross-section area
A_i	Internal cross-sectional area
BOP	Blow-out Preventer
C_1	Stress loading factor
C_D	Drag coefficient
C_M	Inertia coefficient
C_m	Mass coefficient/added mass coefficient
C	Damping matrix
C(p,v)	The system damping load
CMC	Crown-mounted compensator
δ	Displacement
dz	Unit length
D	Riser diameter
DSA	Deepsea Atlantic
DSC	Drillstring compensator
ε_i	Phase angle
EI	Bending stiffness
f_D	Drag force
f_H	Hydrodynamic force
f_I	Inertia force

f_y	Distributed hydrodynamic force acting in the y-direction
F	Resulting lateral force
F	Shear force
$F_X(x)$	Rayleigh distribution of the variable x
F_z	Axial force (wall tension from analysis results)
F(p,v,t)	The external load
FFT	Fast Fourier Transformation
$H_x^2(\omega)$	Transfer function
I	Moment of inertia
I_y	Moment of inertia about the y-axis
I_z	Moment of inertia about the z-axis
k	Total stiffness matrix
$\mathbf{k}_E$	Beam stiffness matrix
$\mathbf{k}_G$	Geometric stiffness matrix
k_G	Geometric stiffness
K	Global stiffness matrix
$\widehat{\boldsymbol{K}}$	Efficient stiffness matrix
K(p)	The system stiffness load
L	Length from the bottom to the center of the resulting force
LMRP	Lower marine-riser package
m_{xn}	Spectrum moments
M	Moment/bending moment
M_{tot}	Total mass
M_x	Bending about x-axis/x-bending moment (Bending moment 12 (SP) from analysis results)
M_y	Bending about y-axis/y-bending moment (Bending moment 34 (AF) from analysis results)

M(p,a)	The system inertia load
M	Mass matrix
N	Axial force
NPD	Norwegian Petroleum Directorate
ρ	Fluid density
P	Top tension
P_x	Lateral force component of the top tension
p	Position vector
p_e	External fluid pressure
p_i	Internal fluid pressure
R	Total system load/ vector of external loads
$\widehat{\boldsymbol{R}}$	Effective load
r_i	Inner radius
r_e	Outer radius
r	System displacements/ vectors for displacements
$\dot{\boldsymbol{r}}$	Vectors for velocities
$\ddot{\boldsymbol{r}}$	Vectors for accelerations
$\hat{\boldsymbol{r}}$	Eigenvector/effective displacement
σ	Tension
σ_1, σ_2, σ_3	Axial stresses
σ_{ab}	Total axial stress
σ_b	Bending stress
σ_c	Circumferential stress
σ_r	Radial stress
σ_p	End effect stress

σ_{ST}	Standard deviation
σ_{tw}	Axial stress
σ_{vm}	Equivalent Von Mises' stress
$S_x(\omega)$	Response spectrum
$S_x(\omega_i)$	Spectrum depending on frequency ω
$S_\zeta(\omega)$	Wave spectrum
SWF	Shallow water flow
τ_{12}, τ_{23}, τ_{31}	Shear stresses
t	Simulation time/time
ΔT	Variation of effective tension
T_e	Effective tension
T_{true}	True tension
T_{tw}	True wall tension
T_{xz}	The zero-up-crossing period
UTS	Ultimate tensile strength
u	Instantaneous velocity
$\dot{u}$	Instantaneous acceleration
V	Volume of sphere
v	Velocity vector/lateral velocity of structure
VIV	Vortex induced vibrations
ω	Eigenfrequency
ω_i	Frequency of response component
Δω	Frequency interval
w_a	Apparent weight
w_e	Displaced fluid weight

w_i	Internal fluid weight
w_t	Segment weight
x	Response variable
x_i	Amplitude
x(t)	Realization of a variable
y	Distance from the centre of the element, in calculation of tension
ÿ	$\frac{d^2y}{dt}$
y’	$\frac{\partial y}{\partial x}$
y”	$\frac{\partial^2 y}{\partial x^2}$
y””	$\frac{\partial^2}{\partial x^2}\frac{\partial^2}{\partial x^2}$

1 Introduction

The technology of retrieving energy in form of oil and gas offshore is in continuous development, and is moving towards larger water depths and more difficult environmental conditions. The reason for the development is that large amounts of the oil and gas reserves offshore are located in deep waters. Drilling in deep waters is accompanied by various challenges and the environmental situation is different from shallow water, i.e. different factors will be the main focus and new problems have to be addressed.

A natural result of the move towards larger depths is that equipment and vessels are adjusted and constructed for the increasing depths. That means a longer, larger and heavier marine drilling riser, which again requires a large handling and motion compensating system. In addition, large quantities of materials for drilling fluid require storage space. In other words, when rigs are moved to larger depths the size of the construction increases (Sangesland, 2008).

The development on the Norwegian continental shelf has resulted in the production of a new generation of semi-submersibles, the sixth generation rigs, which are designed for harsh environment and deep water. Most of the new generation rigs that are built today have a large operating area where they can be used in both shallow and deep water. The combination of deep and shallow water operability will induce rigs which are good for all purposes, but not great because of compromises that have to be performed. As issues regarding deep water rigs used in shallow waters have appeared in the industry, it is of interest to investigate what happens when equipment designed for operation in deep water is used on shallow water. This will be of interest for the whole drilling industry, as it is the large deep water sixth generation rigs that are being built nowadays.

In this report the new Odfjell Drilling rig Deepsea Atlantic (DSA) will be discussed. DSA is fronted as a sixth generation deep water and harsh environment semi-submersible, which can operate in water depths from 70m down to 3000m (Odfjell Drilling, 2009). Drilling operations has been attempted with this rig, in shallow waters at the Gullfaks field (133,5m) and on the Troll field (334m). The drilling operation could not be completed as there were problems in the transition between the riser and the wellhead at both sites. The wellhead seemed to loosen from the seabed. This problem is believed to be caused by the large equipment from the rig, and cases like this may occur for several operators/rig owners as the deep water rigs are built.

This thesis starts with a general introduction to the field of drilling, followed by a more detailed section about marine drilling risers. This is done to provide an insight and overall understanding of the system, and its components, discussed in this report. The theory for calculation of riser statics and dynamics is presented, and a riser analysis is performed for DSA at the Troll field.

At the Toll field full-scale measurements have been performed. Full-scale measurements are not performed often; it is therefore of interest to test the validity of the analysis performed by comparing the full-scale measurements with the analysis results. This is done in the latter part of the thesis, and actions for optimizing the model are presented with basis in the comparison.

2 Drilling operations and system

Drilling is the process which starts the penetration of the seabed to find oil or gas. Once oil or gas is found drilling is followed by the production process. In the following sub-chapters a description of the drilling process, as well as the equipment needed to accomplish it, is given.

2.1 The steps of the drilling process

The drilling process will in reality differ from operation to operation, but a general process can be presented. This general drilling process can be coarsely divided in 6 steps; see Figure 2-1. In the following a description of the process is given.

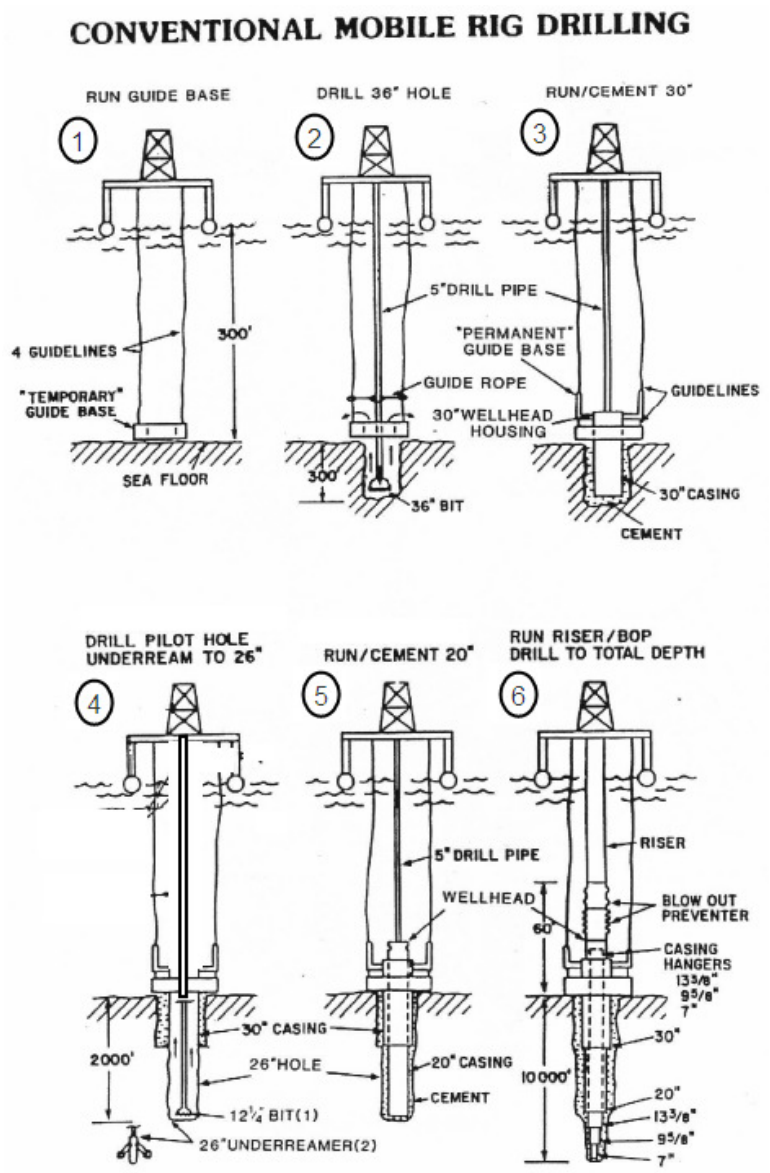

Figure 2-1: The drilling process coarsely divided in 6 steps (Sangesland, 2008)

First the guidebase is lowered; it is connected to 4 guidelines that will be used for lowering the components in the next steps. This will both ease the operation and the position of the next components will be more accurate.

The next step is to start the drilling. A 36” hole is drilled, riserless, for the 30” conductor casing section. The 30” conductor casing is then cemented in the hole and a permanent guide base is installed. The upper part of the 30” conductor will be the wellhead housing.

The drilling continues; a 26” hole will be drilled for the installation of the 20” casing with wellhead. After the 20” casing has been cemented in place, the marine drilling riser and the Blow-out Preventer (BOP) are connected to the wellhead. The Blow-out Preventer (BOP) also includes the lower marine-riser package (LMRP). The marine drilling riser and BOP will stay in place for the rest of the drilling operation. The drilling cuttings from the borehole is circulated and disposed on the seabed for the 36” and 26” borehole operation.

For the next casings that will be installed the drilling riser will be used to divert the drilling fluid back to the drilling vessel, the cuttings will be removed and the drilling fluid circulated back to the borehole. The next casings will have smaller and smaller diameter until the desired depth has been reached, e.g. 20” is followed by 13 3/8”, than 9 5/8” and 7” casings. If the well is used for production, not exploration, more installations have to be performed.

2.2 System components

The drilling process requires a drilling system. There are system components above and below the water surface, which are all vital for the accomplishment of the drilling process. The system is built up of components that can be specialized equipment for use in drilling only or general equipment, which is used for production as well as drilling. Specialized equipment for other operations than drilling will not be described here as drilling is the main focus here. The general components of such a system are sketched in Figure 2-2 and will be presented in the following sub-chapters.

2.2.1 Vessel

The vessel is the part of the system that is located on the water surface; it is the upper attachment point for the riser. For a drilling operation the drilling riser is connected to the vessel, e.g. a drill ship or a semi-submersible (drilling rig), generally called mobile offshore drilling units. The drilling operation is controlled from the vessel. Deepsea Atlantic, the vessel used in this report, is a semi-submersible.

2.2.2 Diverter

The diverter is attached to the rig just below the drill floor round the drill-pipe. The function of the diverter is to direct fluids flowing from the well away from the rig. This is especially useful in cases were shallow gas fields, i.e. high pressures, occur. It also directs the mud returning from the well to the rig so this can be filtered and used again. The high pressures can cause fracture in the formation (Bai & Bai, 2005).

2.2.3 Motion compensators

A drilling vessel will be subjected to motions in all six degrees of freedom, heave, sway, surge, pitch, roll and yaw because of the environment it operates in. All the motions will affect the drilling operation. Motion compensators are used on the rigs to reduce these motions, keep the position and load on the system stable. Normally heave is the most critical motion. Heave compensators are used on several systems, for instance the drillstring, the marine drilling riser, guidelines, winches etc. (Sangesland, 2008).

2.2.4 Tension system

Top tension risers, i.e. drilling risers, require a constant tension in the riser pipe and are therefore sensitive to heave motions. If the top tension is lowered large bending moments can occur in the riser. To avoid this regardless of the vertical motion of the vessel a tension systems is used. Different types of tension systems exist. But a common nominator is that the riser is connected to one part and the vessel to another part of the system, e.g. for tension cylinders where the inner barrel is connected to the riser and an outer barrel is connected to the vessel. The two parts (barrels) can move relative to each other and a constant tension can be maintained by hydraulic systems (McCrae, 2001).

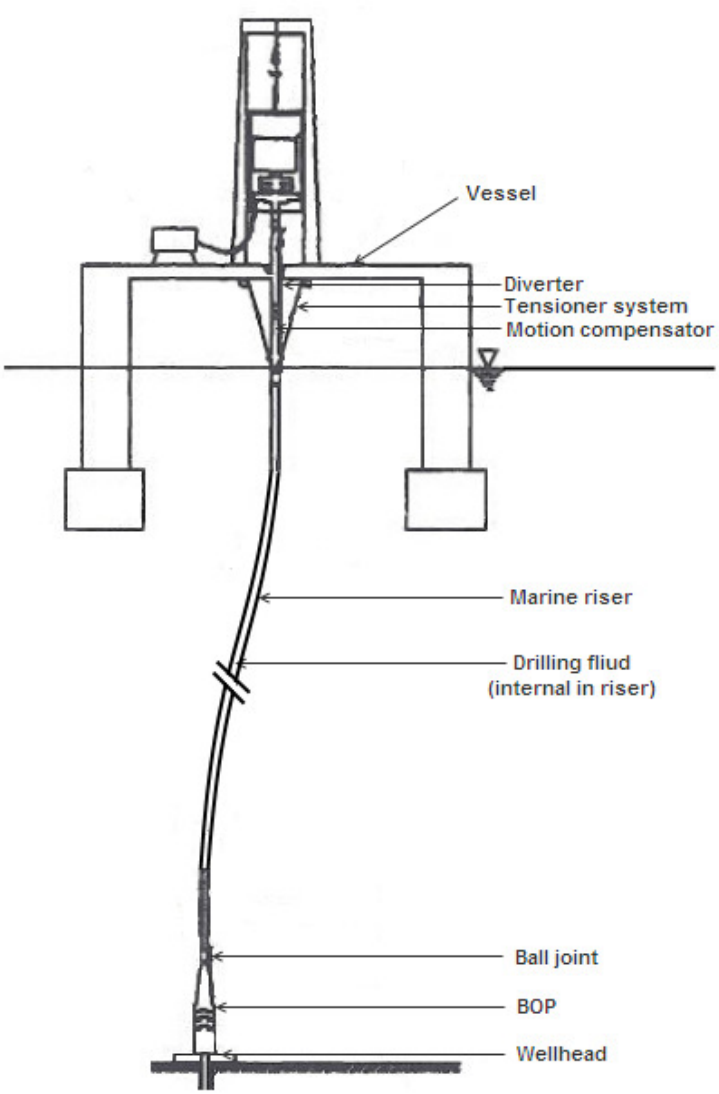

Figure 2-2: Drilling system

2.2.5 Marine riser

The riser is a conductor pipe stretching between two end points, i.e. from the vessel to the BOP for drilling systems. There are several types of risers and more than one way to classify them. Classification by function gives us drilling, production, export and completion/workover risers. Classification by riser structure gives us fixed, tensioned, flexible and catenary risers (Larsen C. M., 2008). In this report the drilling riser, i.e. a tensioned riser, will be in focus. The riser is built up by several parts, mainly riser joints. A more detailed description of a drilling riser build-up will be given in chapter 3.

2.2.6 Ball joints

Movements, i.e. rotations, which are induced by waves and currents cause large bending stresses and moments to occur in the system. This requires the system to have a ball joint. A ball joint, also called a flex joint, is a device that is installed to prevent large bending forces to act on the BOP and the marine riser. The flex joints can bend laterally, i.e. tolerate a limited offset angle from the vertical position, and therefore reduce the effect of the bending on the riser or BOP. Respectively the areas for use are in the connection between the riser and the vessel, and in the lower end connection between the riser and the BOP (McCrae, 2001).

2.2.7 Drilling fluid

Drilling fluid circulates around the drill string, within the riser. The fluid is used to cool down the drill bit, lubricate the drill string, transport the cuttings away by forced circulation upwards, prevent wall cave-ins or intrusions of the formation it passes and provide a hydrostatic head (Bai & Bai, 2005).

2.2.8 Blow-out preventer (BOP)

Just above the seabed there will be a BOP installed during a drilling operation. The BOP ensures pressure control in the well and circulation of drilling fluid. It is the connection link between the riser and the wellhead on the seabed. It consists of two main parts, the lower marine-riser package (LMRP) and the BOP stack. The system on the seabed will not be the focus in this report, but it can be worth mentioning the equipment used here because it will affect the stiffness in the lower part of the riser. An analysis of the riser has to take into account the stiffness of the entire riser (Bai & Bai, 2005).

2.2.9 Wellhead

The wellhead is the connection point between the BOP and the well, it also is a supports the casing string and the casing hangers. The wellhead housing is installed onto the conductor housing. This system on the seabed will not be the focus in this report, but it will affect the stiffness in the lower part of the riser system and has to be taken into account like the BOP.

2.3 Drilling in deep water

Deep water as a describing parameter has no clear definition, but in the drilling aspect it refers to water depths larger than 500 m. Drilling operations in depths that are greater than 2000 m is referred to as ultra deep water drilling (Larsen C. M., 2010). For calculations, the deep water assumptions follow the rule of thumb derived from the dispersion relation. The rule says that if the wave depth is larger than half the wavelength then deep water is a correct assumption (Pettersen, 2004).

Design of drilling rigs has in generations moved towards larger depths. In the 70's 300m water depth was considered deep. The sixth generation rigs designed today is designed for up to 3000m depth. The new rigs encounter some of the same, but also different problems than the rigs designed earlier. The areas that need attention when performing drilling operations in both shallow and deep water are often site and environment specific. The loads include waves, current, vessel motion, system weight, buoyancy etc., see Figure 2-3. But some of the not so obvious areas that can cause additional loads and that should be taken note of are mentioned in the following (Sangesland, 2008):

- *Formation consolidation:* Lack of formation consolidation can cause a non-vertical top section because of weakness in the surrounding formation. This will again cause bending moments and stresses on the wellhead.
- *Formation pressure:* The hydrostatic head of seawater and the mud in the borehole is required to balance the formation pressure after disconnection of the riser and BOP. High pore pressure and low fracture gradient can make this difficult.
- *Shallow water flow (SWF):* Shallow water flow can cause washouts and hole-collapse during drilling after casing has been set. The SWF problem can be prevented by use of weighted drilling mud or eliminated by re-spudding of the well in a new location.
- *Hydrostatic pressure:* Pressure is a critical parameter and effect several parts of the system. During drilling the hydrostatic pressure in the riser can be controlled by regulating the mud weight. In the case of regulation, large pressure drops, fracture and loss of circulation in the system should be avoided. Loss of circulation can in turn cause riser collapse.
- *Riser tensioning:* For increasing depth and larger currents there is a need for larger top tension as the riser is larger and heavier. Computer analysis should determine limiting tension for a given field and for the case of emergency disconnection.

2.4 Operating criteria

For every location a drilling operation is to be executed a riser analysis has to be performed. This analysis will give the risers operation criteria for the specific site and its environment. It is common to give the criteria in green, yellow and red zones. The green zone gives the limits for the general operations, i.e. fatigue failure has to be avoided here. The limit is often set at 67% of yield stress. The yellow zone gives the limits for short term operations, i.e. operations in heavy weather. And the red zone is the zone where a kill and abandon routine has to be performed. The limits here are closer to 85%, given in regulations (Bai & Bai, 2005).

Figure 2-3 shows the loads acting on a riser system. The loads and the effect they have on the riser combined with material used, define the zones in the operation criteria. The external loads have to be within acceptable limits with regard to: Stress and sectional forces, VIV and suppression, wave fatigue and interference (Bai & Bai, 2005).

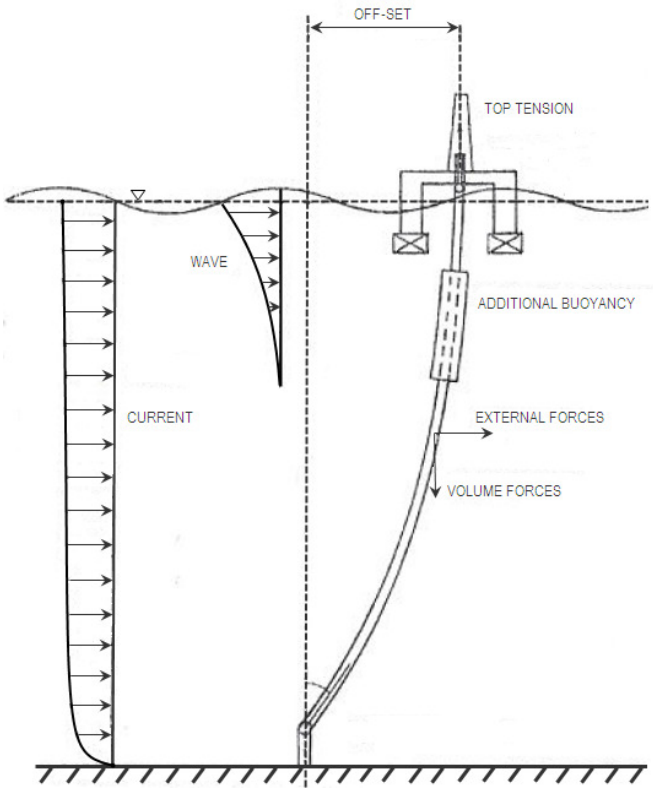

Figure 2-3: Loads on riser system (Larsen C. M., 2008)

3 The marine drilling riser

The choice of riser depends on the area of use, for drilling operations one uses a drilling riser, which is in focus here. The drilling riser is under constant tension, and is approximately vertical. The typical riser system is consist of several components; these have to withstand high tension, bending moments, resist fatigue and the weight of them should to be as small as possible (Bai & Bai, 2005). In this chapter a general description of a marine drilling riser and its components will be given, as well as a specific description of the drilling riser used on DSA.

3.1 Drilling riser components

Figure 3-1 shows a simplified riser system with general components. The equipment may vary with the rig and the purpose of the operation that will be performed. The components in Figure 3-1 are described in the following, from top to bottom in the system.

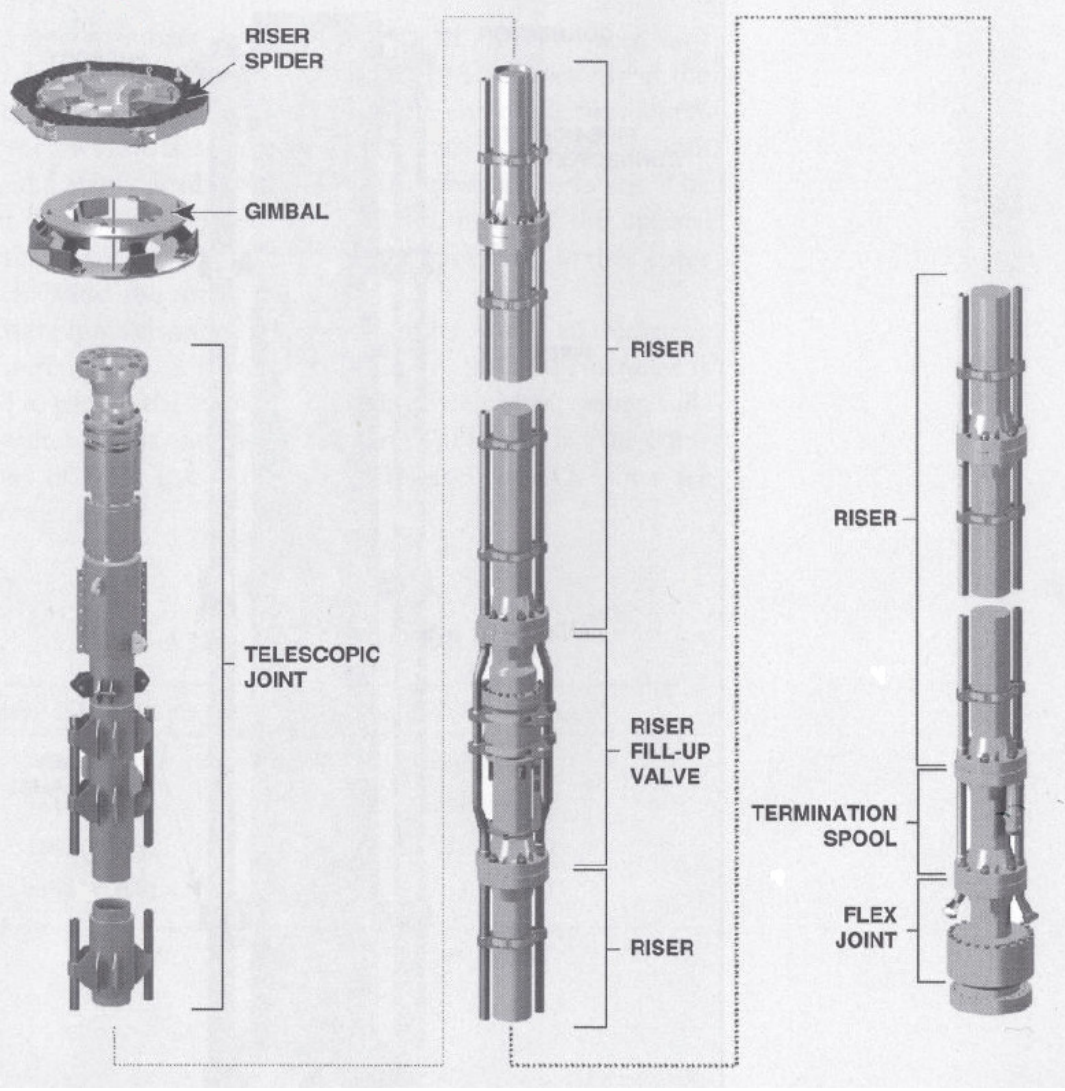

Figure 3-1: Riser system (McCrae, 2001)

Spiders support the riser joint as the pipe is being lowered into or pulled out of the water. The spider is placed just above the rotary table. It consists of a base plate, top plate and support arms between them. As new joints are added the riser and BOP rest on the riser spider (McCrae, 2001).

The gimbal is a motion compensator for ocean induced movements as roll and pitch motions. This component is especially necessary in deep water operations. The gimbal is placed between the spider and the rotary table (Bai & Bai, 2005) (McCrae, 2001).

The spider and the gimbal are used when the riser is being built or taken apart, when it is necessary to hang of weight. The next component in the system is the diverter, which is described in chapter 2.2.2. This is connected just below the drill floor, before the telescopic joint.

The slip joint, also known as the telescopic joint, work as a motion compensator in the vertical direction. It consists of an outer and an inner barrel with a common center. These barrels can slide relative to each other and allow a vertical motion, heave, in the system. The inner barrel is connected to the rig, while the outer barrel is connected to the riser joints. This concept is also applied in tension systems when tensions cylinders are used (Bai & Bai, 2005) (McCrae, 2001).

Riser joints are the components that build the main part of the riser from the rig to the wellhead, and the joints act as a conduit for the drillstring and drilling fluid. The joints are tubular sections of seamless pipe with connectors in each end. The wall thickness of these pipes depends on the water depth of the operation. The choke and kill lines are connected to the outside of the joints. The riser will be built by stabbing one joint onto another and tightening the connector for every stabbing. The joints come in standard lengths from varying 30 to 75 ft. The length and weight of the riser increase as the drilling operation moves towards larger depths (Bai & Bai, 2005) (McCrae, 2001).

Buoyancy modules are used when reduction of top tension is required; the modules are connected to the riser joint. There are two common types of buoyancy elements; syntactic foam modules and air cans (Bai & Bai, 2005).

The connectors in each end of the joint are used to connect two riser joints together. The connectors have to withstand the loads that the system and riser joints are subjected to, and are therefore designed to withstand high tensile loading. The loads on the system will increase as the system is moved to increasing water depths (Bai & Bai, 2005).

Choke and kill lines are used to control high pressure situations that can occur in the drilling riser and they have the responsibility of transporting high pressure flow between the surface choke manifoil and the BOP on the seabed. If it is not possible to control the pressure, kill lines are used to pump down cement in the borehole (Bai & Bai, 2005).

The termination spool is a standard riser joint with a side entry for the mud booster line. This joint connects the riser to the flex joint (McCrae, 2001).

The flex joint is used to minimize the bending moment in the transition between two relative stiff components, e.g. the riser and the rigid BOP. The joint allows for a percentage offset in degrees from the vertical position (McCrae, 2001). Flex joint are also used other places in the system, e.g. between the riser and the diverter.

3.2 Riser system on Deepsea Atlantic

As mentioned in earlier chapters, the risers systems may vary from vessel to vessel. The layout of the riser system onboard Deepsea Atlantic is shown in Figure 3-2. This is the riser which will be analyzed and compared to full-scale measurements in later chapters in the report. Some of the components are not explained earlier, a short explanation will be given here. The spider and the gimbal are not shown in the figure as these are positioned above the upper construction which is the drill floor. In this specific riser it can be seen that the diverter is followed by a diverter flex joint before the slip joint is connected to the system. The tension ring shown is the connection point for the tension cylinders on the riser. A gooseneck assy is an assembly component for the lines connected to the gooseneck on the tension cylinders. The telescopic joint is followed by a series of riser joints, which may include buoyancy. The number of joints, i.e. length of the riser, will depend on the water depth of the operation site. A pup joint is a shorter riser joint used to obtain the correct overall length from the slip joint to the BOP. In the transition from the riser to the BOP there is a riser adapter and a flex joint. The adapter is a fitting device for connection between the riser joint and the flex joint. In the end the system is connected to the upper part of the BOP, the LMRP.

Table 3-1: Specifications of riser components, * external diameter is estimated (Odfjell Drilling/4subsea, 2009)

Component\Properties	Internal diameter	External diameter	Length	Weight (in air)
Diverter flex joint	0.4921 m	0.5334 m	1.92 m	2971 kg
Slip joint **-inner barrel** **-outer barrel**	 0.4921 m 0.6096 m	 0.5334 m 0.6604 m	24.38 to 43.76 m Stroke capacity: 19.07 m	33 279 kg
75" Riser joint	0.4921 m	0.5334 m	22.86 m	13 542 kg
75" Riser joint w/buoyancy	0.4921 m	1.35 m*	22.86 m	22 567 kg
Pup joint (5 to 50 ft)	0.4921 m	0.5334 m	1.52 to 15.24 m	2875 to 9745 kg
BOP (incl. LMRP, Flex joint, adapter)	-	-	14.65 m	$371.73*10^3$ kg

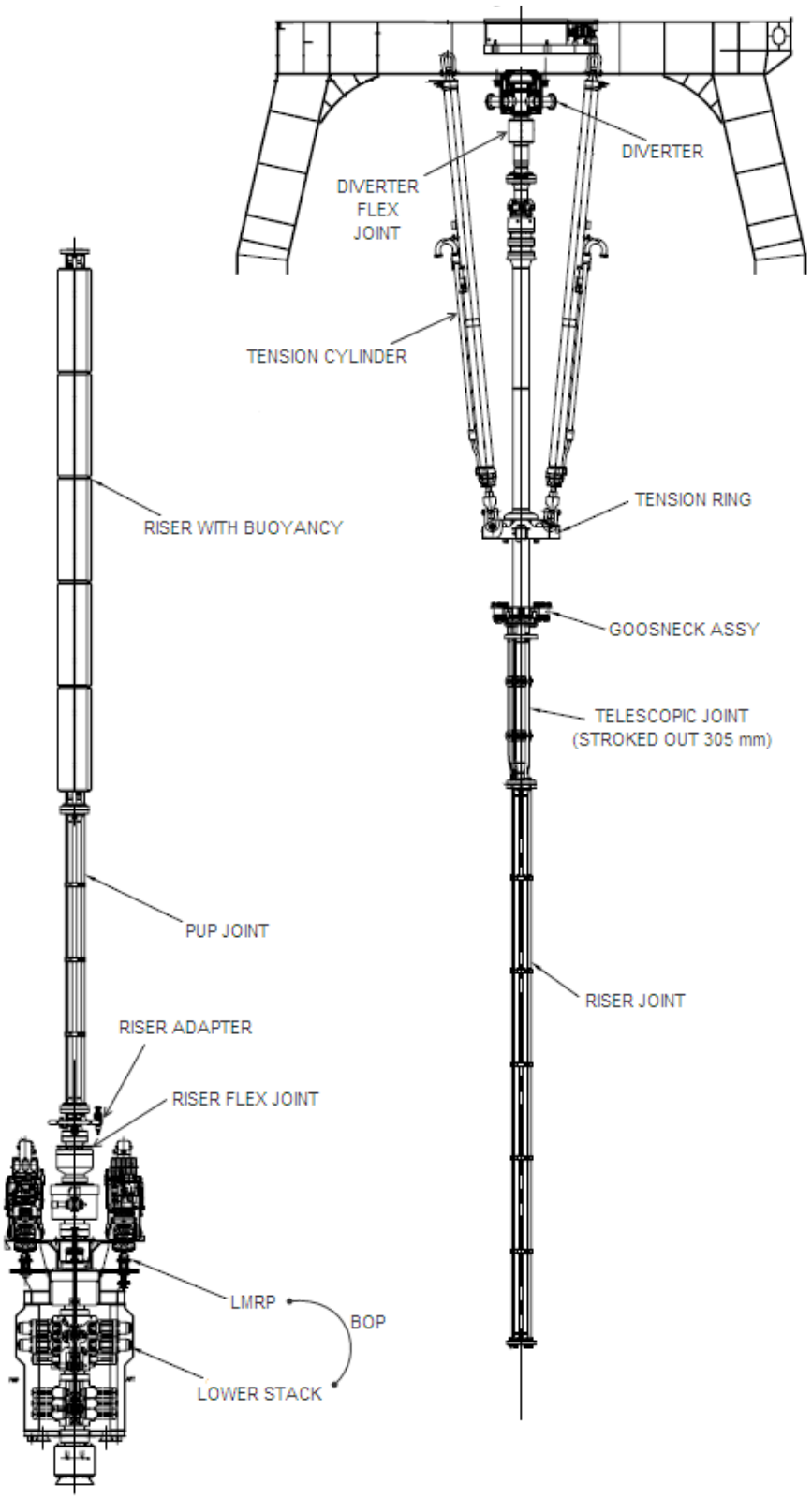

Figure 3-2: Riser system layout on DSA (Shaffer, 2009)

3.2.1 The vessel - Deepsea Atlantic (DSA)

In this report the riser explained above is connected to DSA, a sixth generation semi-submersible owned by Odfjell Invest Ltd. DSA is designed for deep water and harsh environment drilling in depths from 70 to 3000 m. The rig was commissioned and started its first drilling operation in 2009. The main dimensions and operating data of the rig are given in Table 3-2.

Table 3-2: Dimensions and operations data of DSA (Odfjell Drilling, 2009)

Main dimensions		Operating data	
Length overall	118.6 m	**Draft**	23.0 m
Width overall	100.8 m	**Displacement**	55 160 ton
Pontoon length	108.8 m	**Air gap**	13.5 m
Pontoon height	10.2 m	**Drilling depth**	11 500 m
Pontoon width	16.0 m	**Design temperature**	-20 to 40 °C
Number of columns	4	**Variable deck load**	7 500 ton
Columns dimensions	16.8x14.4 m^2	**Water depth**	70 to 3 000 m

Figure 3-3: Deepsea Atlantic (Odfjell Drilling, 2009)

4 Marine riser mechanics

A mathematical model of a physical phenomenon can be very good, but rarely perfect. This is often due to assumptions and simplifications made in the calculations. To understand the results from a riser analysis these assumptions and simplifications have to be taken into consideration. In this chapter an overview of the physics and the mathematical aspects of riser theory will be presented. This is necessary background for the analysis that will be performed in later chapters.

This chapter is in large extent written according to C.M. Larsen (2008), C.P. Sparks (2007) and ISO 13624.

4.1 Tension, pressure and weight

A riser is connected to the seabed and stretches up past the sea surface to the vessel where it is connected to a tension system. To avoid buckling and riser failure several factors has to be considered, i.e. tension, pressure, weight etc. In the following sub-chapters factors that are related to the calculation of the top tension are explained.

4.1.1 Geometric stiffness

The drilling riser is supported by top tension to increase the lateral stiffness of the riser. The riser will without the top tension experience large displacements when it is exposed to lateral forces, i.e. waves and currents, because of its long and slender structure with low elastic bending stiffness (EI). The stiffness increases because the lateral components of the tension counteract the lateral forces the riser is subjected to. This is illustrated in Figure 4-1. The additional lateral stiffness that occurs is called geometric stiffness.

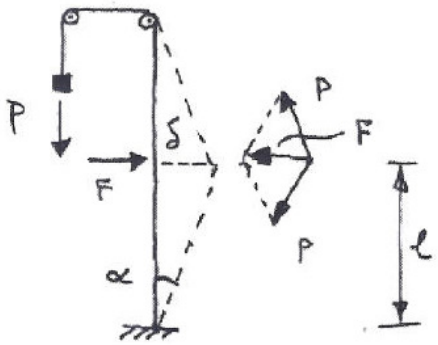

Figure 4-1: Illustration of tension effect on a slender beam (Larsen C. M., 2008).

With basis in Figure 4-1, an expression for the geometric stiffness can be found. Force equilibrium is assumed, which gives (Larsen C. M., 2008);

$$F = P_x^1 + P_x^2 = P\sin\alpha + P\sin\alpha = 2P\sin\alpha \qquad (P^1 = P^2 = P) \qquad (4\text{-}1)$$

Where F is the resulting lateral force, P is the top tension, P_x is the lateral force component of the top tension and α is the deflection angle. Further, small angles are assumed and the following expressions can be derived;

$$F \approx 2P\alpha \quad , \quad \alpha = \frac{\delta}{l} \tag{4-2}$$

Where δ is the displacement and l is the length from the bottom to the center of the resulting force. This leads us to the geometric stiffness k_G;

$$F \approx 2P\alpha = 2P\frac{\delta}{l} = \frac{2P}{l}\delta = k_G\delta \quad \Longrightarrow \quad k_G = \frac{2P}{l} \tag{4-3}$$

4.1.2 Effective tension and apparent weight

The top tension supports the weight of the riser. To obtain correct support the subject of buoyancy has to be discussed. From basic physics Archimedes law states: An object fully or partially submerged in a fluid experiences a force, buoyancy, which equals the weight of the fluid displaced by the object. This force occurs as a resultant of the closed pressure field in the displaced fluid and will act vertically in the center of the object. When adopting Archimedes law to risers it is important to be aware of the following:

- The law is only valid for completely closed pressure fields. For objects in the water surface where the pressure is zero, the field can be considered closed.
- The law does not regard internal stresses and forces.

When calculation of unknown internal forces in a submerged object is performed, the case of not closed pressure field occurs. Figure 4-2 shows a segment of a submerged object with external and internal forces. Superposition is used to find the internal forces. The external pressure field is unknown, and is complicated to calculate. To avoid a complicated calculation Archimedes law is used.

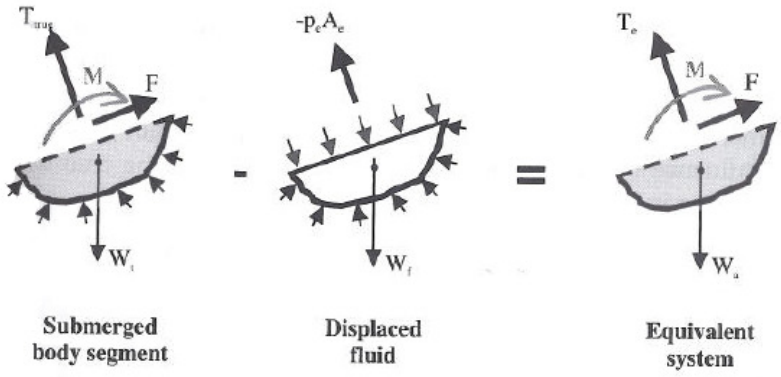

Figure 4-2: Internal forces on a segment of a submerged object (Sparks, 2007).

To be able to apply Archimedes an imaginary closed pressure field around the displaced fluid is created, see the middle drawing in Figure 4-2. It is done by adding pressure on the top part of the displaced fluid. The total pressure field is then subtracted from the forces on the body segment, i.e. the unknown pressure field below the object becomes zero. To account for the part of the pressure field that has been added an equal sized, but counteracting, force $p_e A_e$ is included in the force equilibrium. Were p_e is the pressure from the external fluid over the external cross-section A_e, The resulting forces and moments on

the segment are shown to the right in Figure 4-2. The shear force F, and the moment M are the same for the segment as for the resulting equilibrium. The resulting tension, also known as effective tension T_e, is related to the true tension, T_{true}, internal in the segment (Sparks, 2007);

$$T_e = T_{true} - (-p_e A_e) = T_{true} + p_e A_e \quad (4\text{-}4)$$

The apparent weight, w_a, of the segment is the difference between the weight of the segment, w_t, and the displaced fluid, w_e, given by (Sparks, 2007);

$$w_a = w_t - w_e \quad (4\text{-}5)$$

Two methods can be used to find equilibrium of a riser or a segment of a riser; i.e. use of effective tension and apparent weight or use of real weight, pressure and axial stress resultant. Both methods are valid and correct, but use of effective tension is more convenient and causes no loss in accuracy. Effective tension is used in computer programs for static and dynamic analysis of marine risers, as well as for calculation of buckling load and geometric stiffness due to tension in a slender beam (Larsen C. M., 2008).

An installed riser has no contact with fluid in the ends, i.e. Archimedes condition of closed pressure field is not fulfilled. In the upper end there is no problem because the atmospheric pressure at the surface is zero. The lower end demands more investigation. To find the weight and tension in the riser the principles presented can be transferred to analyze a curved segment of a pipe/riser, see Figure 4-3. The figure shows a riser/pipe section subjected to both internal and external pressure, in form of fluid pressure. Moments and shear forces have been neglected to make the example easier. The total forces are split into three contributions, the forces acting on respectively the pipe segment itself, the internal and the external fluid (Sparks, 2007).

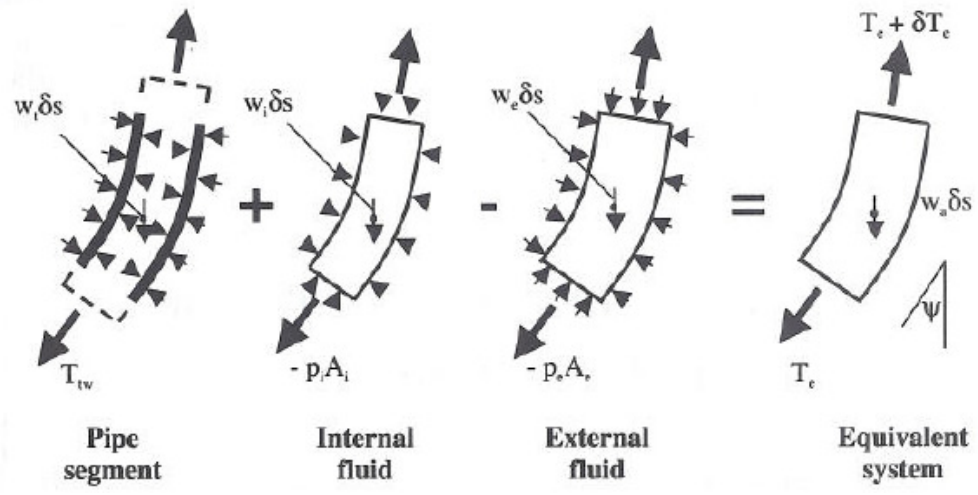

Figure 4-3: Equilibrium of pipe segment exposed to both internal and external fluids (Sparks, 2007)

The pressure fields acting on both the internal and external fluid are closed, by adding pressure on the fluids in the axial direction. Corrective pressure resultants are superimposed to the equation because of this extra pressure in the axial direction. The force system acting on the internal fluid is added to the force system acting on the pipe section, and then the force system on the external/displaced fluid is subtracted to find the resulting force. The lateral forces in the three contributions cancel each other out. The following equations give the resulting tension in the axial direction, the effective tension, and the apparent weight (Sparks, 2007);

$$T_e = T_{tw} + (-p_i A_i) - (-p_e A_e) \qquad w_a = w_t + w_i - w_e \tag{4-6}$$

Where T_{tw} is the true wall tension (axial tension) in the pipe section, p_i is the pressure in the internal fluid, A_i is the internal cross-sectional area, p_e is the pressure in the external fluid, A_e is the external cross-sectional area, w_i is the internal fluid weight and w_e is the displaced fluid weight. Notice that the effective tension is not the same as the axial tension. To find the stresses in the pipe wall the wall tension has to be known and it can be found from the equation above as long as the effective tension is known. Figure 4-3 gives the relationship between the effective tension and the apparent weight can be derived. The segment length is δs and all angles, ψ, are assumed to be small (Sparks, 2007);

$$\frac{dT_e}{ds} = w_a \cos\psi \approx w_a \tag{4-7}$$

The approach used in the previous section can be transformed to a more general definition and applied to more complex pipe/riser-systems. The presented equations are only limited by the condition of static equilibrium for the system. In other words there has been set no limiting conditions regarding the cross-section, density of the material or size of deflections of the pipe/riser, i.e. the equations have general validity. This leads to the following equations and physical description for the effective tension and apparent weight (Sparks, 2007);

$$T_e = \sum T_{tw} + \sum(-p_i A_i) - \sum(-p_e A_e) \qquad w_a = \sum w_t + \sum w_i - \sum w_e \tag{4-8}$$

"Effective tension is the total axial force in the pipe/riser column, including internal fluid columns, less the axial force in the displaced fluid column (tension positive)"

This makes it possible to calculate the effective tension in systems with; irregular shape, several pipes together, pipes in pipes, pipes with internal fluid in motion etc. The definition gives that the effective tension in any point will be the sum of forces in all pipe walls and all internal fluids less the forced in the displaced fluid column (Larsen C. M., 2008).

In the case of a drilling riser it can be of relevance to incorporate the specific effect of internal flow. The flow is incorporated in the effective tension by change of momentum; see the last term in the following equation, where ρ_i is the density of the internal fluid, and u_i is the internal fluid velocity (Sparks, 2007);

$$T_e = T_{tw} - p_i A_i + p_e A_e - \rho_i A_i u_i^2 \tag{4-9}$$

4.2 Stresses

A riser exposed to external and internal pressure and tension experience stresses in the structure. In the following the different types of stresses that will occur in a riser subjected to these loads are presented. It is assumed that the riser is a circular cylindrical pipe made from isotropic elastic material, i.e. not a flexible riser which will have a more complex material. The distribution of the stresses depends on the material; for risers made from isotropic elastic materials the distribution is governed by mechanical principles (Sparks, 2007).

4.2.1 Circumferential and radial stresses

Figure 4-4 shows the internal stresses in a cross-section of an elastic riser/pipe exposed to internal and external pressure as well as tension. The stress acting tangentially to the pipe is called the circumferential stress, denoted σ_c, and the stress acting normal to the pipe wall is the radial stress, denoted σ_r. These stresses vary in the pipe as a function of the radial distance from the axis, but the sum of them is constant over the cross-section and equals the end effect stress, σ_p, (Larsen C. M., 2008);

$$\frac{\sigma_c+\sigma_r}{2} = constant = \sigma_p \qquad (4\text{-}10)$$

The end effect stress is due to the internal and external pressure acting on the cross-sectional area of the pipe;

$$\sigma_p = \frac{p_i A_i - p_e A_e}{A_e - A_i} \qquad (4\text{-}11)$$

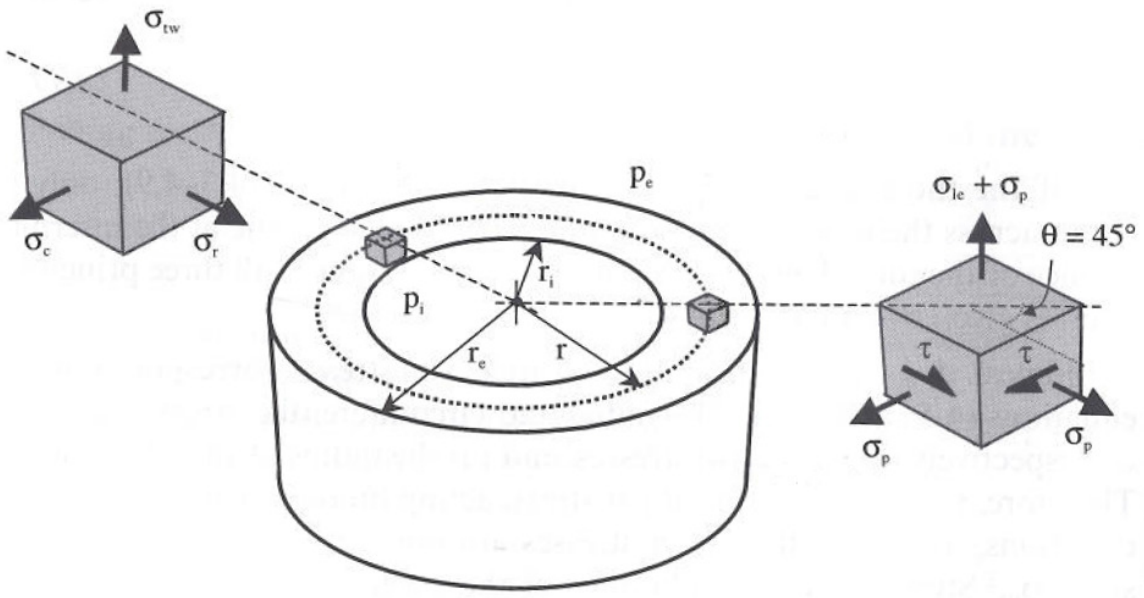

Figure 4-4: Stresses in the riser wall, two equivalent systems are shown (Sparks, 2007)

The circumferential and radial stresses can be expressed as functions of shear and end-effect stress:

$$\sigma_c = \sigma_p + \tau \qquad \sigma_r = \sigma_p - \tau \qquad (4\text{-}12)$$

Where $$\tau = \frac{(p_i - p_e)A_i A_e}{(A_e - A_i)A_r} \quad (4\text{-}13)$$

A_r is the area of a circle with radius equal to the point in the pipe wall under consideration. The axial stresses in the figure will be discussed in the next sub-chapter.

4.2.2 Axial and bending stress

The stress acting vertically in the left box in Figure 4-4 is the axial stress, σ_{tw}, caused by the axial tension, i.e. the true wall tension T_{tw}. The axial stress in a pipe is given by the axial load, here axial tension, divided by the area of the cross-section the load is acting on (Irgens, 1999). The correlation between the stress and the tension in Figure 4-4 is then given by the following equation:

$$\sigma_{tw} = \frac{T_{tw}}{A_e - A_i} \quad (4\text{-}14)$$

The axial stress can be decomposed into a sum of the end effect stress and the effective stress, σ_{le}, in the pipe. This can be seen by rephrasing the expression of effective tension found in chapter 4.1.2, equation (4-6), and combining it with equation (4-14);

$$\sigma_{tw} = \frac{p_i A_i - p_e A_e}{A_e - A_i} + \frac{T_e}{A_e - A_i} = \sigma_p + \sigma_{le} \quad (4\text{-}15)$$

This relation makes it possible to find the effective tension and axial stress in a pipe as long as the geometry, pressure loads and axial tension are known. The effective stress has a physical significance and can be described as the part of the axial stress that exceeds the in-wall hydrostatic pressure, i.e. the end effect stresses (Larsen C. M., 2008). A riser will in reality also be subjected to a bending moment, M, and stresses caused by this bending have to be taken into consideration as well. The bending stress, σ_b, for a structure with constant cross-section exposed to pure bending is assumed to be linearly distributed and given as (Irgens, 1999):

$$\sigma_b = \frac{M}{I} y \quad (4\text{-}16)$$

Where I is the second moment of area, y is the distance to the center axis in the pipe. Superposing the effect of the tensile load and the bending moment according to Navier's formula gives us the total axial stress σ_{ab};

$$\sigma_{ab} = \sigma_b + \sigma_{tw} \quad (4\text{-}17)$$

Assuming that the material is linear elastic, when yield is present the superposing will no longer be valid (Irgens, 1999).

4.2.3 Von Mises' equivalent stress – limit stress

Combination of stresses cause yielding and is therefore of great importance to check in the calculation of stresses in the material of a riser. For many years Tresca's maximum stress criteria was used for this purpose. Today most codes of practice require that the maximum distortional energy criterion,

represented by the Von Mises' equivalent stress, is checked. This is considered to be the most accurate criterion for ductile materials. The von Mises' equivalent stress for the general case of triaxial stress is given by (Sparks, 2007);

$$2\sigma_{vm}^2 = (\sigma_1 - \sigma_2)^2 + (\sigma_2 - \sigma_3)^2 + (\sigma_3 - \sigma_1)^2 + 6(\tau_{12}^2 + \tau_{23}^2 + \tau_{31}^2) \qquad (4\text{-}18)$$

Where σ_{vm} is the equivalent Von Mises' stress, σ_1, σ_2 and σ_3 is the axial stresses in the tree directions, the τ_{12}, τ_{23} and τ_{31} is the shear stresses. Yielding will occur when this stress equals the yield stress of the material. This equivalent stress can also be expressed with the effective axial stress, σ_{le}, and the shear stress, τ, see equation below (Sparks, 2007).

$$\sigma_{vm}^2 = \sigma_{le}^2 + 3\tau^2 \qquad (4\text{-}19)$$

When the riser is subjected to bending this also has to be taken into the evaluation of the stress. The Von Mises' stress must be checked at both the inner surface, where the shear stress is at its maximum, and at the outer surface, where the bending stress is at its maximum. Equation (4-19) can then be rewritten to include the bending stress, σ_b, (Sparks, 2007);

$$\sigma_{vm}^2 = (\sigma_{le} + \sigma_b)^2 + 3\tau^2 \qquad (4\text{-}20)$$

4.3 Strains

Strains will affect a riser in different ways. The interaction between riser and kill/choke lines can be influenced, the required stroke of the riser tesioner and the riser profile can change to mention some of the effects. Calculation of strains is defined by the material in the pipe; isotropic or anisotropic. In this report the strain theory for anisotropic pipes will not be presented, as this is more relevant for high-performance composites. The steel pipes in focus in this report are isotropic (Sparks, 2007).

In general stresses are related to strains by the Young's modulus E and Poisson's ratio v. This is also the case for elastic isotropic pipes. The axial strain, ε_a, can be calculated with the basis in several stresses. In the expression below the axial strain is given by the true wall axial stress, the circumferential stress and the radial stress (Sparks, 2007);

$$\varepsilon_a = \frac{1}{E}(\sigma_{tw} - \nu\sigma_c - \nu\sigma_r) \qquad (4\text{-}21)$$

All the stresses mentioned in this section have been defined in the previous chapter. The circumferential and radial stresses are separately not constant over the pipe wall. When this equation is used the mean of the circumferential stress and the mean of the radial stress should be used when a thick walled pipe is evaluated (Sparks, 2007).

The mean of sum of the circumferential and radial stress on the other hand is constant and equals the end effect stress, see chapter 4.2.1. When this is implemented into the equation for the axial stress the following equally exact in term is achieved;

$$\varepsilon_a = \frac{1}{E}\left(\sigma_{tw} - 2\nu\sigma_p\right) \quad (4\text{-}22)$$

The effective stress can also be used to express the axial strain equally exact, by use of equation (4-15) rewriting and substituting;

$$\varepsilon_a = \frac{1}{E}\left[\sigma_{le} + (1-2\nu)\sigma_p\right] \quad (4\text{-}23)$$

The in-wall shear stresses produce no axial strain and will therefore not appear as a factor in the equations. The axial strain can also be rewritten to be expressed by true wall tension or effective tension by substitution, respectively the first and second equation in the following;

$$\varepsilon_a = \frac{1}{E(A_e - A_i)}\left(T_{tw} - 2\nu p_i A_i + 2\nu p_e A_e\right) \quad (4\text{-}24)$$

$$\varepsilon_a = \frac{1}{E(A_e - A_i)}\left[T_e + (1-2\nu)p_i A_i - (1-2\nu)p_e A_e\right] \quad (4\text{-}25)$$

4.4 Rules and regulations

Design and operation of offshore equipment has to be in line with the rules and regulations specified. For design, selection, operation and maintenance of marine drilling riser systems a recommended practice and an international standard, respectively API RP 16Q and ISO 13624 are established. As the operational conditions for the marine drilling riser change, e.g. exploration moving towards deeper water, the rules and regulations have to be adapted for this. The API RP 16Q exists in different revisions and this recommended practice has, with additions, been used as the basis for the ISO 13624 standard (Kavanagh, Dib, Balch, & Stanton, 2002). ISO 13624 – *"Petroleum and natural gas industries – Drilling and production equipment"* – consist of two parts (ISO 13624-1, 2009):

- Part 1 (ISO 13624-1) – *"Design and operation of marine drilling riser equipment "*: This part describes the equipment used to build up the riser system and the conditions and limitations that have to be fulfilled for a marine riser system.
- Part 2 (ISO 13624-2) – *"Deepwater drilling riser methodologies, operations and integrity technical report"*: This part is a supplement to part one, and consist of methodologies, examples and supplementary material for the riser analysis.

The application of ISO 13624 is limited to operations with a subsea BOP stack deployed on the seafloor. ISO 13624-1 gives the recommended design practice for the operating modes that are encountered during offshore drilling operations; see Table 4-1. The modes can be divided into three; drilling, non-drilling and riser disconnected. They all depend on the environmental conditions and the loads on the system. In this thesis normal operation is the main focus, i.e. the drilling mode (ISO 13624-1, 2009).

In Table 4-1 the maximum allowed stress is given by two methods, method A for most water depths and method B for deep water, respectively 40% and 67% of yield stress for the drilling mode. These limitations are set to make sure that the riser is strong enough to support the maximum design loads, while keeping the maximum stresses below the allowable stress. A minimum tension is also required to

make sure that the riser is stable. This tension should be of a size that prevents buckling and that ensures that the effective tension in the riser is positive at all times in all parts of the riser, even if a tensioner should fail. Limitations for the flex joint angle are also given to prevent wear and damage on the joint and the riser (ISO 13624-1, 2009).

Table 4-1: Marine drilling risers, maximum design guidelines for exploratory drilling (ISO 13624-1, 2009).

Design parameter	Riser connected		Riser disconnected
	Drilling	Non-drilling	
Mean upper flex/ball jt. angle [a]	1° to 1,5°	N/A	N/A
Max. upper flex/ball jt. angle [a]	5,0°	90 % available (or contact with moonpool structure)	90 % available (or contact with moonpool structure)
Mean lower flex jt. angle [b]	2,0°	N/A	N/A
Max. lower flex jt. angle [b]	5,0°	90 % available	N/A
Stress criteria: [c,d]			
– Method "A" - allowable stress [e]	0,40 σ_y [f]	0,67 σ_y [f]	0,67 σ_y [f]
– Method "B" - allowable stress [e]	0,67 σ_y [f]	0,67 σ_y [f]	0,67 σ_y [f]
– Sign. dyn. stress range [e]			
@ SAF $\leqslant$ 1,5 [g]	69 MPa (10 ksi)	N/A	N/A
@ SAF > 1,5 [g]	15/F_{SA}	N/A	N/A
Minimum top tension [h]	T_{min}	T_{min}	N/A
Dynamic tension limit [i]	F_{DTL}	F_{DTL}	N/A
Maximum tension setting	90 % F_{DTL}	90 % F_{DTL}	N/A

A riser analysis is used for two purposes, to establish design specifications when ordering a new riser or as preparation for operations with an existing riser on a new site. The object of the analysis is to determine necessary top tension and operation limits for the environmental conditions and loads the riser is exposed to.

To perform a riser analysis a mathematical model of the riser has to be created. The riser is a tensioned beam which is approximately vertical at all times, only small angles of deviation occur. For these small deviation angles the Bernoulli-Euler beam equation can be used to describe the response of the riser. By examination of a differential element and the forces acting on the element, a beam equation for the riser can be developed. The equilibrium equations for the differential element combined with simple beam theory will give the equation of motion that represents the behavior of the riser (ISO 13624-1, 2009):

$$f_y = M\ddot{y} + EIy'''' - \Delta T y' - T_e y'' \qquad (4\text{-}26)$$

Where

EI bending stiffness

f_y the distributed hydrodynamic force acting in the y-direction

M total mass

T_e Effective tension

ΔT variation of effective tension

ÿ $\frac{d^2y}{dt}$

y' $\frac{\partial y}{\partial x}$

y'' $\frac{\partial^2 y}{\partial x^2}$

y'''' $\frac{\partial^2}{\partial x^2}\frac{\partial^2}{\partial x^2}$

The modeling of the riser interaction with the soil can be done by either coupled or decoupled analysis methodology. In the coupled analysis the modeling of the riser and the soil is done in one model, but for decoupled analysis the riser and the BOP is modeled separately (ISO 13624-1, 2009).

The riser is built up of several component and materials. There exist several design codes for riser design, depending on type of riser, area of use and material used. Some of the other codes that can be mentioned for riser design are (Bai & Bai, 2005):

- API 2RD for risers attached to floating systems, this is a stress based code using von-Mises yield criterion for yield strength checks.
- API 17B and 17J for flexible pipes
- ISO13628-5 for steel tube umbilical's

5 Riser analysis

An analysis of the riser is important to ensure the environment, general safety for the workers and economy for the company. The riser has to withstand the static and dynamic forces it is exposed to. It is therefore important to have reliable methods for the analysis which can give safe construction and operation of the riser (Larsen C. M., 2008). An analysis of marine risers will normally implement the finite element method and consist of a static and a dynamic analysis part (Larsen C. M., 1990). In the following sub-chapters theory for element formulation, static and dynamic analysis is presented.

This chapter is in large extent written according to C.M. Larsen (1990) and C.M. Larsen (2008).

5.1 Element formulation

A tensioned riser, like the drilling riser, has a statically determined initial configuration. The axial stresses and strains, node positions and effective tension can be calculated by direct inspection of vertical equilibrium. The finite element model can then be established for the riser. The finite element method is a general and efficient tool that can be applied to numerous structural applications and is therefore often used in the analysis of a marine riser (Larsen C. M., 1990). In the finite element analysis beam elements of either two or three dimensions with lengths L are used to build up the entire length of the riser. Figure 5-1 shows a 2D beam element with six degrees of freedom.

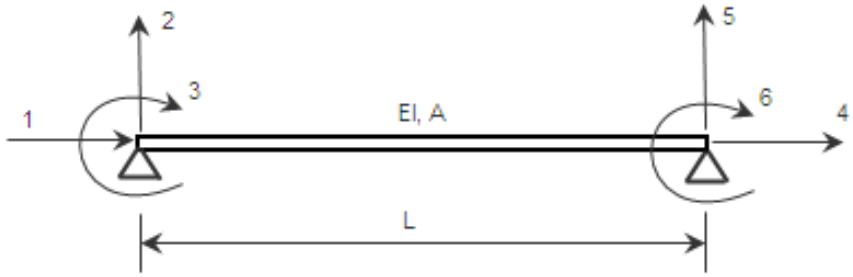

Figure 5-1: 2D beam element

The stiffness of this element has contributions from the elements stiffness itself and the stiffness that occurs when there is change in geometry (lateral displacements) because of external forces. The geometric stiffness matrix gives the contribution to the bending moment from the axial force when change in geometry occurs. The stiffness matrix can be found from considering second order strains in the beam. The total stiffness matrix, **k**, for the element is found as the sum of the beam stiffness matrix, $\mathbf{k}_E$, and the geometric stiffness matrix, $\mathbf{k}_G$ (Larsen C. M., 1990):

$$\boldsymbol{k} = \boldsymbol{k}_E + \boldsymbol{k}_G \tag{5-1}$$

This element stiffness can be transformed to the global system by use of a transformation matrix. For situations where large rotations and displacements occur a beam element with no displacement limitations is needed, hence the use of 3D elements with 12 degrees of freedom. The matrix for a 3D

element can be found in the same matter as for the 2D element, but the large rotations and the stress calculation has to be handled with awareness (Larsen C. M., 1990).

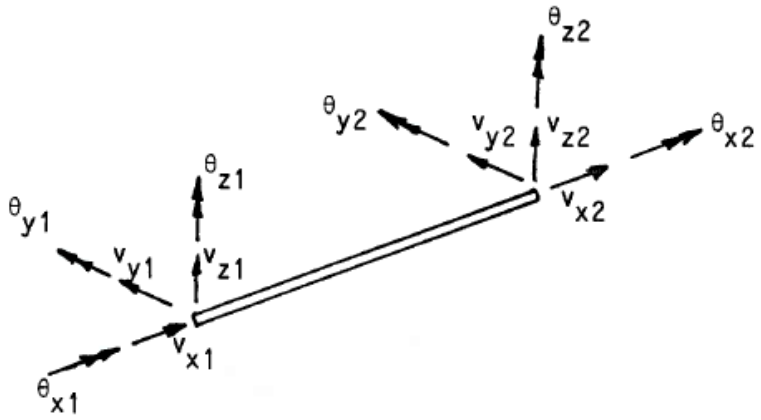

Figure 5-2: 3D beam element (Larsen C. M., 1990)

5.2 Static analysis

The objective of the static analysis is to find the equilibrium of the system under the loads it is exposed to. The first step in a static analysis is to find the axial forces in all elements that build the riser. This axial force is found by adding vertical forces from weight, buoyancy and specified loads to the tension at the top. Then the next step will be to find the total stiffness matrix, **K**, for the entire system. This total stiffness matrix is given from the stiffness in individual elements, $\mathbf{k}_j$, trough the following relation (Larsen C. M., 2008):

$$\boldsymbol{K} = \sum_j \boldsymbol{a}_j^T \boldsymbol{k}_j \boldsymbol{a}_j \qquad (5\text{-}2)$$

Where $\mathbf{a}_j$ is a transformation matrix. The total stiffness can express the equilibrium of the system with the total system load, **R**, and system displacements, **r**, of the system. From this system displacements can be found (Larsen C. M., 2008):

$$\boldsymbol{Kr} = \boldsymbol{R} \;\rightarrow\; \boldsymbol{r} = \boldsymbol{K}^{-1}\boldsymbol{R} \qquad (5\text{-}3)$$

The load matrix **R** will only contain the external forces, i.e. current and possibly offset at upper end, as the effect of top tension and structural weight are included in the geometrical stiffness. Further, the displacements **r** can be used to find the local displacements in each element by use of a transformation matrix (Larsen C. M., 2008).

If the stiffness matrix **K** and the external load **R** are independent of the displacements the problem will be classified as linear. This is only the case for small displacements. When the displacements become large compared to the geometric properties of the structure, the problem is nonlinear. This can be of importance when a riser is exposed to large currents or a large offset. The static equilibrium in nonlinear problems is found by performing an incremental loading procedure. This is an iteration process where the stiffness matrix and forces are recalculated between each loading step. This method does not give

the exact solution to the nonlinear problem, but for practical purposes a slightly nonlinear problem gives sufficient accuracy (Larsen C. M., 2008).

5.3 Dynamic analysis

In dynamic analysis the objective is to obtain information of how a structure responds and behaves when exposed to loads varying over time. The loads in the static analysis are constant. In the dynamic analysis the equation for dynamic equilibrium is given by the equation of motion for all the degrees of freedom that are included in the system:

$$\boldsymbol{M\ddot{r} + C\dot{r} + Kr = R}(t) \qquad (5\text{-}4)$$

Where **M** is the mass matrix, **C** is the damping matrix, **K** is the global stiffness matrix, **R** is the vector of external loads and **r**, $\dot{\boldsymbol{r}}$ and $\ddot{\boldsymbol{r}}$ is the vectors for displacements, velocities and accelerations. Form the equation it can be stated that the inertia, damping and restoring forces balance the external forces (Larsen C. M., 1990).

The mass matrix includes both contribution from the structures own mass and the added mass from the sounding water. The added mass can be found by inspecting the inertia forces on an accelerated structure in accelerated fluid. The largest contribution for damping in a riser structure is hydrodynamic damping. This damping is created by the relative velocity between the riser and the surrounding water. The damping included in the **C** matrix is structural damping, which can be proportional to **K** and **M**. The stiffness matrix **K** is calculated in the static analysis (Larsen C. M., 2008).

The dynamic equilibrium can be solved in several ways. Here for the finite element method two alternatives for the dynamic analysis is presented, respectively the time domain and the frequency domain analysis.

5.3.1 Frequency domain

The frequency domain method solves the dynamic equilibrium in the frequency domain. The method is linear and especially well suited for stochastic analysis, e.g. fatigue life calculation. For problems with many degrees of freedom subjected to stochastic loads this method is easy to use and it is particularly compatible with phase angle problems. For stochastic problems this method should be used. The method can be used on both fixed structures as well as risers. Frequency dependent factors, mass, damping and stiffness, are easily handled in this type of analysis. Awareness has to be directed at problems where non-linear drag is relevant, here stochastic linearization of the drag has to be performed and this induces uncertainties (Larsen C. M., 1990).

5.3.2 Time domain

Several methods can be used to solve the dynamic equilibrium in the time domain, e.g. time integration, convolution, Duhamel integration, application of Hamilton's principle etc. As methods based on time integration are widely used, that method will be in focus here. The basic principle in the time integration method is to perform discretization in time and then calculate equilibrium at given points in time. The size of the time increments is problem dependent. When the equilibrium of displacements, velocities

and acceleration in one time increment is found, the equilibrium in the next time increment can be found. There are several integration methods and they are based on the same set of basic equations, but the assumption of acceleration time history differs in the methods. When choosing the method for the time integration it is important to assess the stability, damping and period error of the method. For a system with linear dynamic, the procedure for the dynamic analysis (assuming use of coupled equations and that a static analysis is performed) is as follows (Larsen C. M., 1990):

1) The matrixes for mass, damping and stiffness have to be calculated, and the time history of the load vector has to be established.

2) Next the efficient stiffness matrix, $\widehat{\boldsymbol{K}}$, is calculated:

$$\widehat{\boldsymbol{K}} = \boldsymbol{K} + a_1\boldsymbol{C} + a_2\boldsymbol{M} \tag{5-5}$$

Where a_1 and a_2 are constants. This matrix is constant trough out the analysis.

3) For every time step the effective load, $\widehat{\boldsymbol{R}}$, is calculated from the true loads and system parameters:

$$\widehat{\boldsymbol{R}} = \boldsymbol{R}(t) + f(\boldsymbol{C}, \boldsymbol{M}, \dot{\boldsymbol{r}}) \tag{5-6}$$

4) By using the new stiffness and load the effective displacement, $\hat{\boldsymbol{r}}$, can be calculated:

$$\widehat{\boldsymbol{K}}\hat{\boldsymbol{r}} = \widehat{\boldsymbol{R}} \quad \rightarrow \quad \hat{\boldsymbol{r}} = \widehat{\boldsymbol{K}}^{-1}\widehat{\boldsymbol{R}} \tag{5-7}$$

The effective displacement is used in combination with the known displacements, velocities and accelerations in a set of equations to find the new respective values for the displacements, velocities and accelerations. An example of a equation set that can be used is given in the following:

$$\begin{aligned} r_{k+1} &= r_k + g_1(\hat{r}_k, r_k, \dot{r}_k, \ddot{r}_k) \\ \dot{r}_{k+1} &= \dot{r}_k + g_2(\hat{r}_k, r_k, \dot{r}_k, \ddot{r}_k) \\ \ddot{r}_{k+1} &= \ddot{r}_k + g_3(\hat{r}_k, r_k, \dot{r}_k, \ddot{r}_k) \end{aligned} \tag{5-8}$$

These new values will again be used in the next time step as the process is repeated. The functions f, g_1, g_2 and g_3 are algebraic functions (Larsen C. M., 2008).

This process is repeated trough the time simulation. Compared to the frequency domain some of the advantages that of the time integration procedure are that transient loads can be found, the quadratic drag term can be included in the load vector, it can be extended to include nonlinear effects, arbitrary damping models can be included and the method is simple to program and understand. The disadvantages are that the simulation takes time and large data storage is necessary, in addition if there are transient effects these may disturb the solution (Larsen C. M., 1990).

5.4 Eigenvalue analysis

The eigenfrequencies and mode shapes are factors that are important for the understanding of the dynamics of a structure. To obtain this information the free vibration equation, where damping and external force is set to zero, is used (Larsen C. M., 2008):

$$\boldsymbol{M}\ddot{\boldsymbol{r}} + \boldsymbol{K}\boldsymbol{r} = 0 \tag{5-9}$$

Assuming that the solution has of the following form

$$\boldsymbol{r} = \hat{\boldsymbol{r}} \sin \omega t \tag{5-10}$$

Where $\hat{\boldsymbol{r}}$ is the eigenvector, ω is the eigenfrequency and t is time. The free vibration equation can then be transformed to an eigenvalue equation:

$$(\boldsymbol{K} - \omega^2 \boldsymbol{M})\hat{\boldsymbol{r}} = 0 \tag{5-11}$$

For a system of N degrees of freedom the solution has N eigenvalues (ω_1^2, ω_2^2,…., ω_N^2) and corresponding N eigenvectors ($\hat{r}_1$, $\hat{r}_2$,…., $\hat{r}_N$). These represent the frequencies and mode shapes for free vibration. The eigenfrequencies of a system should not be equal or close to the frequencies of external loads. For a marine riser this means that the eigenfrequencies of the riser should not be in the range where wave frequencies with significant energy occur, if that happens large motions will be induced (Larsen C. M., 2008).

6 Analysis tools - OrcaFlex

The computer software used in riser analysis is special purpose programs. There are several programs that can be used to analyze and design flexible risers; some that can be mentioned are OrcaFlex, Riflex and Flexcom. In this thesis OrcaFlex is used to perform the riser analysis and in this chapter the theory used in the calculations in the program will be presented. OrcaFlex is a program used for static and dynamic analysis of several marine applications, including marine risers. It is a 3D non-linear time domain finite element program, which uses lumped mass element to simplify the mathematical formulation and make the calculation efficient. This chapter is in large extent written according to the user manual in OrcaFlex (2009).

In OrcaFlex the model of the riser is build up from lines, buoys and springs by use of the graphical user interface in the program. A more detailed description of the model will be given in chapter 7. The process of the analysis can be divided in specific parts. First a model of the riser is created. Next environment must be chosen, i.e. waves and current have to be established. Than the analysis wanted have to be chosen. When this is established the simulation can be run and results can be collected for post-processing. In the following the element formulation, static and dynamic analysis used by OrcaFlex is presented, while theory about the subjects mentioned can be found in chapter 5.

6.1 Element formulation of line

In OrcaFlex the transfer of the physical riser into a line model that can be used in calculations is done by dividing the actual riser into segments. Each segment is then modeled individually by massless segments with the same length and a node in each end, as illustrated in Figure 6-1.

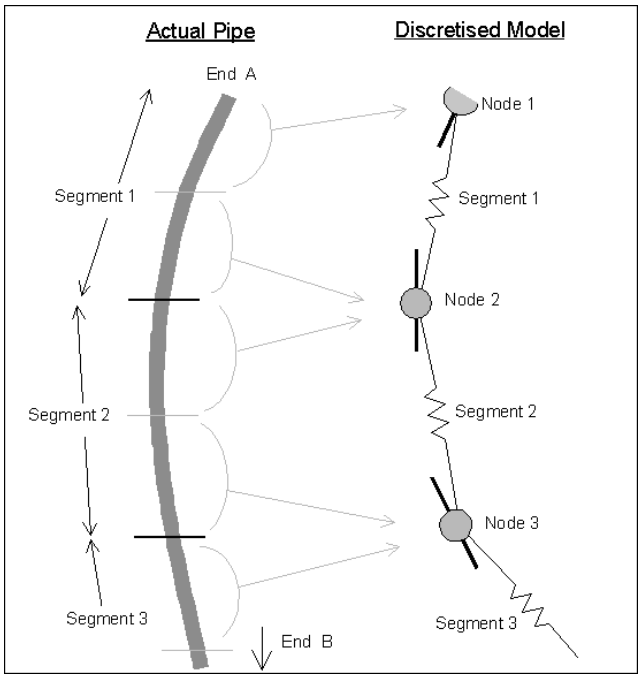

Figure 6-1: OrcaFlex line model (Orcina, 2009).

6.1.1 Node

The nodes model the mass, weight, buoyancy and drag properties of the actual line segments. These properties of the nodes are defined by half of the segment length next to the node. See illustration with arrows in Figure 6-1. The node in each end is in itself modeled as a short rod that represents the combination of the properties of the half segment on each side of the node. Forces and moments are applied at the nodes (Orcina, 2009).

6.1.2 Segment

The segments in the model give the axial and torsional properties of the physical segment. The segment can be illustrated, see Figure 6-2, as two rods with coinciding axial centers that are connected with an axial and a torsional spring/damper-system. The axial spring/damper system is placed in the center of each segment in the model, and applies an equal and opposite effective tension to the nodes at each end of the segment. The torsional spring/damper system applies equal and opposite torque moments to the nodes at each end of the segment, this system is as the axial system also positioned at the center of each segment. The inclusion of torsion in the analysis is optional, but if it is not included in the analysis the torsional spring/damper system is not included in the model and the segment is free to twist relative to each other.

In addition to the two mentioned systems a rotational spring/damper-system is positioned in the ends of each segment to maintain the bending properties assigned to the segments. This can also be seen in Figure 6-2, between the segment and the node. This system makes it possible to have different bending stiffness over the length of the model (Orcina, 2009).

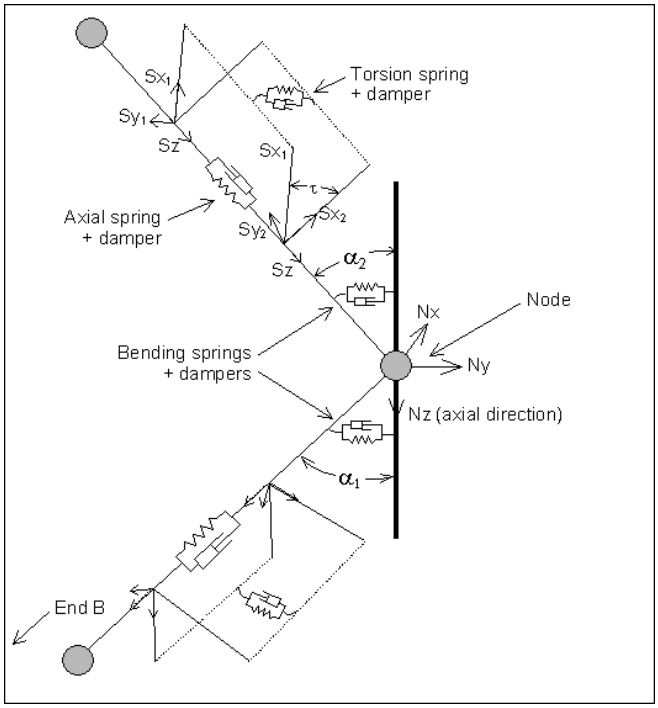

Figure 6-2: Detailed representation of the OrcaFlex line model (Orcina, 2009)

6.2 Static and Dynamic analysis

The calculation of forces and moments in the line is a large part of the calculation in the analysis of the whole system. This calculation is performed in five stages, respectively in the following order: tension forces, bending moments, shear forces, torsion moments (if included) and finally total load. When the model is constructed and the correct input for environment is applied the analysis, where the calculations of the riser are performed, can be run. The analysis is divided into two parts, a static and a dynamic part.

6.2.1 Static analysis

A static analysis is performed to determine the equilibrium position of the riser system under loads from the system itself, i.e. weight, buoyancy, drag etc. This position is calculated by iteration from the initial position of the system that is given by the input. The equilibrium configuration for each line is calculated with the assumption that the line ends are fixed. From this the out of balance force acting from the line is calculated. This is used to calculate a new position of the whole system. This is repeated until the out of balance force is zero. The position of equilibrium is further used as the starting configuration of the dynamic analysis (Orcina, 2009).

OrcaFlex performs the static analysis for each line in the model. The calculation can be divided into two steps where the first is mandatory and the second is optional. The first step is to calculate a configuration of the line. The second step calculates the true equilibrium; in this step all the forces that are modeled are included. OrcaFlex offers several other options for the calculation, if it should be computed for all degrees of freedom or none, to include buoys, free bodies and vessel or not etc. This should be adapted to the specific case that is analysed and the choices can help the model to converge (Orcina, 2009).

6.2.2 Dynamic analysis

A dynamic analysis is performed to simulate the motions of the system in the given environment over a time period that is specified. These motions can further give the displacements, forces and moments occurring in the system with the given load. Before the main motion simulation there is a build-up stage where the wave and vessel motions are ramped from zero to the full size. This is done to smooth the transition from static to full dynamic motion. In OrcaFlex it is possible to leave out this time period in the results, as it is not representative for the full loads that affect the system.

The calculation performed in the dynamic analysis is done by solving the equation of motion for the given system. The equation of motion that OrcaFlex solves is (Orcina, 2009):

$$M(p,a) + C(p,v) + K(p) = F(p,v,t) \qquad (6\text{-}1)$$

Where

M (p, a) is the system inertia load

C (p, v) is the system damping load

K (p)	is the system stiffness load
F (p, v, t)	is the external load
p	position vector
v	velocity vector
a	acceleration vector
t	simulation time

In OrcaFlex the calculation of the dynamics can be performed by two methods. Both methods compute the new system geometry for each time step, i.e. the simulation takes full account for all geometric nonlinearity. The explicit method uses forward Euler with a constant time. Statics give the initial positions. The forces and moments acting on each free body and node in the system are calculated and then used to form the individual local equation of motion for every free body and node in the system (Orcina, 2009):

$$M(p)a = F(p,v,t) - C(p,v) + K(p) \qquad (6\text{-}2)$$

This equation is solved for the acceleration at the beginning of the time step. Then integration using Euler forward integration gives the position and orientation of the nodes and the free bodies at the end of the time step. This process is repeated trough out the time of the simulation.

For the other method, the implicit method, the calculations of forces, moments, damping, mass etc. are done in the same way as for the explicit method. The integration is done by use of the Generalized -α integration. And the equation of motion of the system is then solved at the end of the time step (Orcina, 2009).

The forces and moments that are considered in the calculation of the motion equation vary with the given model, but weight, buoyancy, hydrodynamic and aerodynamic drag, hydrodynamic added mass effects, tension and shear, bending, contact forces with other objects are highly relevant in modeling a drilling riser. The choice of time step in the analysis is a balance between stable integration, accuracy in calculations and efficiency in computational time.

6.3 Loads

The loads on the system may include functional, environmental, accidental loads etc. To model the reality it is important to be aware of the loads affecting the system. Increasing water depths can introduce new concepts and material in the structure, which again can give new load combinations and failure modes. The loads that affect a marine riser and that are important to take into consideration in an anlysis include the following:

- Weight of the structure itself including flanges, internal fluid and buoyancy modules or other type of external add-on equipment
- Hydrodynamic loads from waves and current including both drag and inertia forces, possibly aerodynamic loads from wind
- Hydrostatic forces from the water surrounding the riser
- Forces occuring because of forced motion, e.g. forces from vessel on riser because of motion and offset.
- Top tension to avoid buckling in the riser and to minimize the load on the LMRP

The weight forces mentioned in the first point has been intoduced in chapter 4 in the calculation of effective tesion. These forces are included in the static analysis when the static equilibrium is calculated. Top tension is also determined from the weight of the structure and the effective tension in the riser. The forces from the vessel depends on the RAO of the vessel which again is dependent on the waves acting on the vessel. In the following the theory and implementation of loads in OrcaFlex will be presented.

Dynamic waves and currents acting on a riser over a long period of time generate fatigue stresses and fatigue is a parameter that has to be considered when the riser is designed. However, fatigue is not in focus here, as the environment for the analysis is given. The damage to the wellhead seen for DSA occurs immediate and is assumed not to be a result of fatigue.

This chapter is in large extent written according to C.P. Sparks (2007) and the user manual in OrcaFlex (2009).

6.3.1 Hydrostatic pressure

A riser is exposed to pressure from the surrounding water. The effect of this pressure on the riser is included in the calculation of the tension in the system, either wall tension or effective tension, and they are all related to each other through the following expression which is used in OrcaFlex (Orcina, 2009):

$$T_{tw} = C_1(T_e + p_i A_i - p_e A_e) \qquad (6\text{-}3)$$

Rearranging of the expression leads to the equation (4-6) for the effective tension presented in chapter 4.1.2. C_1 is a stress loading factor used by OrcaFlex to specify the proportion of the loads used in the tension calculation. The internal pressure, p_i, is calculated from contents pressure. The pressure from surrounding water, the external pressure p_e, is assumed to be zero at and above the mean water level. The internal and external cross-section areas, A_i and A_e, are both calculated from the respective stress diameters. The stress diameters are the diameters of the load bearing cylinder, i.e. effects of the kill and choke lines can be neglected and consideration is only given to the main pipe when this input is given to OrcaFlex.

6.3.2 Implementation of waves

In the dynamic analysis the model is subjected to waves. OrcaFlex gives several options for the implementation of these waves in the model; they can be regular waves, random waves or specified by a

time history. For the regular wave modeling the following choices are available: long-crested linear Airy wave or nonlinear waves using Dean, Stokes' 5th or Cnoidal wave. The waves are specified by input values for wave height, wave period and direction of propagation (Orcina, 2009).

For random waves the program creates a wave history from the linear waves decided by the user by various input values. The wave components are chosen by use of an equal energy approach and the phase of the waves is given by a random number generator. For random waves the user has to specify the frequency spectra to model the random wave. The specter shows how the energy distributes over the frequency occurring in the sea. The choices for spectrum are: JONSWAP, ISSC, Ochi-Hubble, Torsethaugen and Gaussian Swell (Orcina, 2009). The respective spectra need different input values. According to NORSOK standard N-003 Torsethaugen or JONSWAP spectra is suited to represent the design sea state in the Norwegian Sea and the North Sea (NORSOK, 2007).

JONSWAP (Joint North Sea Wave Project) is a wave specter which is created on the basis of the Pierson-Moskowitz spectrum and measured data from south-east parts of the North Sea. The specter is a good model for wind generated sea in the JONSWAP area (Myrhaug, 2007). Input values required for OrcaFlex for this spectrum is the wave height, wave period and direction of propagation.

Torsethaugen is a double peak spectral model for ocean waves originally established by fitting two JONSWAP shaped models to average measured spectra from the Norwegian Continental Shelf (Torsethaugen & Haver, 2004). This spectrum can represent sea states including both remotely generated swell and local wind generated waves. Input values required for OrcaFlex for this spectrum is the wave height and wave period.

6.3.3 Hydrodynamic loads – Morison's equation

For slender structures with circular cross-section like the marine drilling riser the the Morison's equation can be applied for calculation of the hydrodynamic forces. The equation has been considered controversial for many years, but it has been the main method for calculation of hydrdynamic forces for almost 50 years because it calculates the forces with resonable accuracy. It is considered controversial because the drag term in the equation is nonlinear. The equation is applied to the riser by strip theory to calculate the hydrodynamic force, f_H, per unit length, dz, in two dimensions. The force given by this equation can be considered as the resultant of dynamic and static pressure fields acting on the riser. The force is built up form two contributions, respectively a drag force, f_D, and an inertia force, f_I (Sparks, 2007):

$$f_H = f_D + f_I \tag{6-4}$$

The drag force is a result of the velocity of the flow that passes the riser, while the inertia force is a result of the acceleration of the flow.

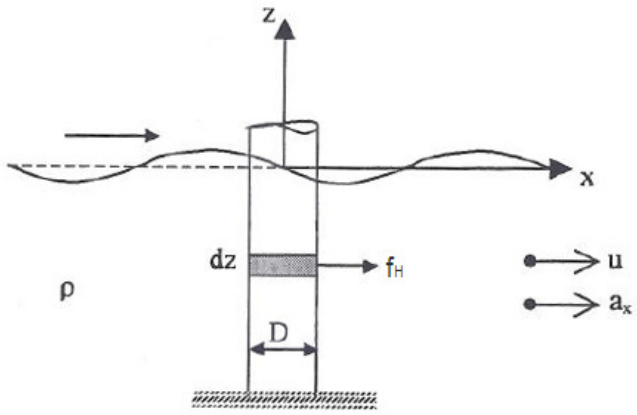

Figure 6-3: Illustration of strip division and the sizes in Morison's equation (Pettersen, 2004).

6.3.3.1 Drag force

Testing in laboratories with steady flow has shown that the drag for a circular cylinder varies with the square of the velocity of the fluid past the body. The expression of the drag term for circular cylinders exposed to flow normal to its axis can be given as follows (Sparks, 2007):

$$f_D = \frac{1}{2}\rho C_D D u|u| \qquad (6\text{-}5)$$

Where ρ is the fluid density, C_D is the drag coefficient, D is the riser diameter and u is the instantaneous velocity (i.e. the velocity in the fluid as if the object was not present) normal to the cylinder axis. If the forces on the riser cause the riser to move laterally with a velocity v, this has to be taken into consideration in the calculation of the drag term. This is done by using the relative velocity, shown in the equation below (Sparks, 2007).

$$f_D = \frac{1}{2}\rho C_D D(u-v)|u-v| \qquad (6\text{-}6)$$

6.3.3.2 Inertia force

Testing has also been done to investigate the inertia force due to the fluid acceleration. For a stationary sphere of volume V, with a density ρ, subjected to a uniform acceleration the inertia force can be expressed as (Sparks, 2007):

$$f_I = \rho C_M V\dot{u} \qquad (6\text{-}7)$$

Where C_M is the inertia coefficient and $\dot{u}$ is the instantaneous acceleration of the fluid. The inertia force has two contributions, namely the hydrodynamic force acting on the displaced fluid in the absence of the sphere ($\rho V\dot{u}$) and an additional force due to the acceleration of the fluid relative to the sphere ($(C_M-1)\rho V\dot{u}$). The expression including the inertia coefficient (C_M-1) is often set equal to C_m and termed mass coefficient or added mass coefficient in some literature. If the sphere itself is moving with an acceleration, $\dot{v}$, the relative acceleration has to be used. This results in the following equation:

$$f_I = \rho V \dot{u} + (C_M - 1)\rho V(\dot{u} - \dot{v}) \quad (6\text{-}8)$$

Per unit length, dz, the expression can be rewritten:

$$f_I = \rho A_e \dot{u} + (C_M - 1)\rho A_e(\dot{u} - \dot{v}) \quad (6\text{-}9)$$

Where A_e is the external cross-sectional area.

The two contributions result in the hydrodynamic force and per unit length of riser it can be expressed as follows:

$$f_H = \frac{1}{2}\rho C_D D(u - v)|u - v| + \rho A_e \dot{u} + (C_M - 1)\rho A_e(\dot{u} - \dot{v}) \quad (6\text{-}10)$$

For risers with a cross-section geometry consisting of more than a bare pipe the diameter and area used in the Morison's equation has to be adjusted. This is the case for drilling risers where additional lines like kill and choke lines are connected to the main pipe. An equivalent diameter and an equivalent area corresponding to the real pipe geometry should be used in the calculation of the forces (Sparks, 2007).

The mass coefficients C_m, and drag coefficient, C_D, should be determined empirically for the specific case. The coefficient depend on many factors, some that can be mentioned are Reynolds number, Keulegan-Carpenter number, roughness number, relative current number, body form, free surface effects etc. (Faltinsen, 1990). For some familiar geometries typical values for the coefficients are known, i.e. assumptions of the values of the coefficients can be made. The inertia coefficient for a smooth cylinder at high Reynolds number has typically the value 2, i.e. the mass coefficient is 1. The drag coefficient for a smooth circular cylinder which has a small diameter compared to the length of the cylinder, and is situated in high Reynolds number, can be set to 1.2 (Pettersen, 2004).

6.3.3.3 Hydrodynamic force in OrcaFlex

In OrcaFlex the hydrodynamic loads are calculated for lines and buoys used in the model, and the Morison's equation is used to perform the calculation:

$$F_W = (\Delta a_W + C_m \Delta a_r) + \frac{1}{2}\rho V_r |V_r| C_D A \quad (6\text{-}11)$$

This is the same expression as shown in the previous sub-chapter, but it is not given per meter it is given for the whole length of the object in focus. F_W is the wave force, i.e. the hydrodynamic force f_H. The expression in the parentheses is the inertia force, where Δ is the mass of the fluid displaced by the body (volume times the density), a_w is the fluid acceleration, a_r is the fluid acceleration relative to the body. The last term in the equation is the drag force. V_r is the fluid velocity relative to the body and A is the drag area (Orcina, 2009).

The drag on the model is calculated using the cross flow principle, i.e. the fluid velocity is split into components acting normal and parallel to the line axis. The drag coefficients are also split into the respective directions, and the drag areas have to correspond to the directions as well. The drag

coefficients normal to the axis can be specified constant or to vary with Reynolds number or height above seabed.

Added mass for the line model is built up from two contributions and is calculated separately for the local x-, y- and z-directions. The two contributions are the Froude-Krylov force, the forces from the undisturbed wave, and the added mass force, as have been introduced in 6.3.3.2.

The lift on the model can also be calculated. The lift coefficients can be specified constant or to vary with Reynolds number or height above seabed. But if a symmetric cross-section is assumed there will be no lift force as there exists no pressure difference.

6.4 Coordinate system

OrcaFlex has three types of coordinate systems. GXYZ is the global coordinate system. This global reference system must be a right handed system with the Z-axis directed upwards. The position of origin is chosen by the user, in riser analysis it is often positioned in the water surface (Orcina, 2009).

Lxyz is the local coordinate system; each object has this coordinate system. This system will vary in orientation depending on the object used, but the origin is typically in a fixed point. The seabed also has a local axis and origin (Orcina, 2009).

The third system is Exyz which is the system for the line end orientation. Ez is always directed from end A to end B in a line. Definition of which end of the modeled line is A or B is a choice for the user (Orcina, 2009).

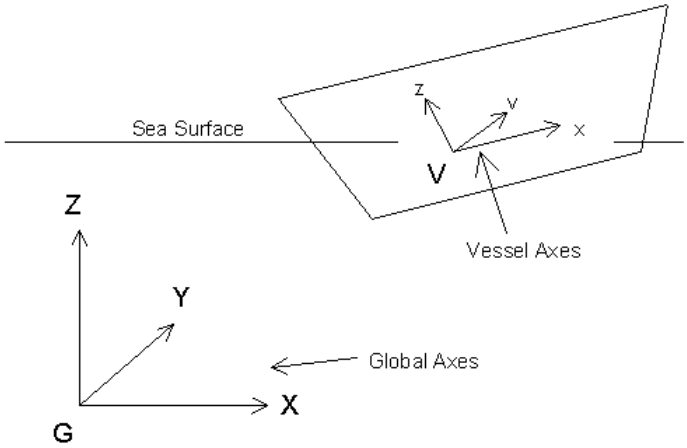

Figure 6-4: Illustration of coordinate systems in OrcaFlex, where Vxyz is the same as Lxyz for the vessel (Orcina, 2009)

7 Modeling

Riser analysis is performed with the intentions of simulating the reality as accurate as possible in a computer program. Limitations occur as the modeling demands simplifications to be able to perform calculations; this will make the model deviate from the reality. It is therefore important to keep the physical properties correct in the transition from reality to model.

The drilling riser is modeled as a vertical cable exposed to currents, from a structural point of view. The boundary conditions in the upper end of the riser are rig motions. The rig motions depend on rig design, wave and wind loads (Bai & Bai, 2005). The model created in this thesis is based on the riser used on the Troll field during the recording of the measurements. The analysis is also run with the same environment as the riser experienced during the measurements. This is done to make it possible to compare the analysis results with the measurements. In the following sub-chapters the model used in the analysis will be presented.

7.1 Methodology in ISO 13624-2

ISO 13624-2 Technical report is, as mentioned in chapter 4.4, a supplement to the first part of the standard and gives methodologies and examples of how the riser analysis should be performed. Two methodologies for the modeling of the riser are presented in the report, respectively coupled and decoupled methodology. These methodologies have been used as a basis for the choice of model in this thesis. The main area of focus here is the forces and moments acting on wellhead.

7.1.1 Coupled methodology

This is a single stage procedure where the model stretches from the conductor to the upper flex joint, see Figure 7-1. Vessel motions, waves and current loading can be applied and used to predict behavior of the riser and the displacements of the conductor in the soil. This method is appropriate to apply for analysis with focus on the response of the conductor/casing, for drift-off and weak point analysis. The reason for this is that in the coupled analysis the BOP deflects with the riser as the analysis allow for full interaction between applied vessel motions, hydrodynamics and soil behavior. This also introduces more complicity (ISO 13624-2, 2009).

7.1.2 Decoupled methodology

This is a two stage procedure. The behavior in the full riser system is predicted by two separate models. The first part of the model represents the system from the top of the LMRP to the upper flex joint (the riser). The second model represents the part from the conductor to the LMRP, see Figure 7-1. Here the vessel offset, current and wave loading are only applied to the riser part of the model; as a result of this the effect of the loads cannot be directly applied to the model of the lower part of the system. The loads found in the endpoint at the LMRP from the first model are applied to the second model in the upper point at the LMRP. This makes the model more time consuming to perform, but gives conservative results for most applications. Note should be taken for shallow water and stiff clay applications, as slightly non-conservative results may occur (ISO 13624-2, 2009).

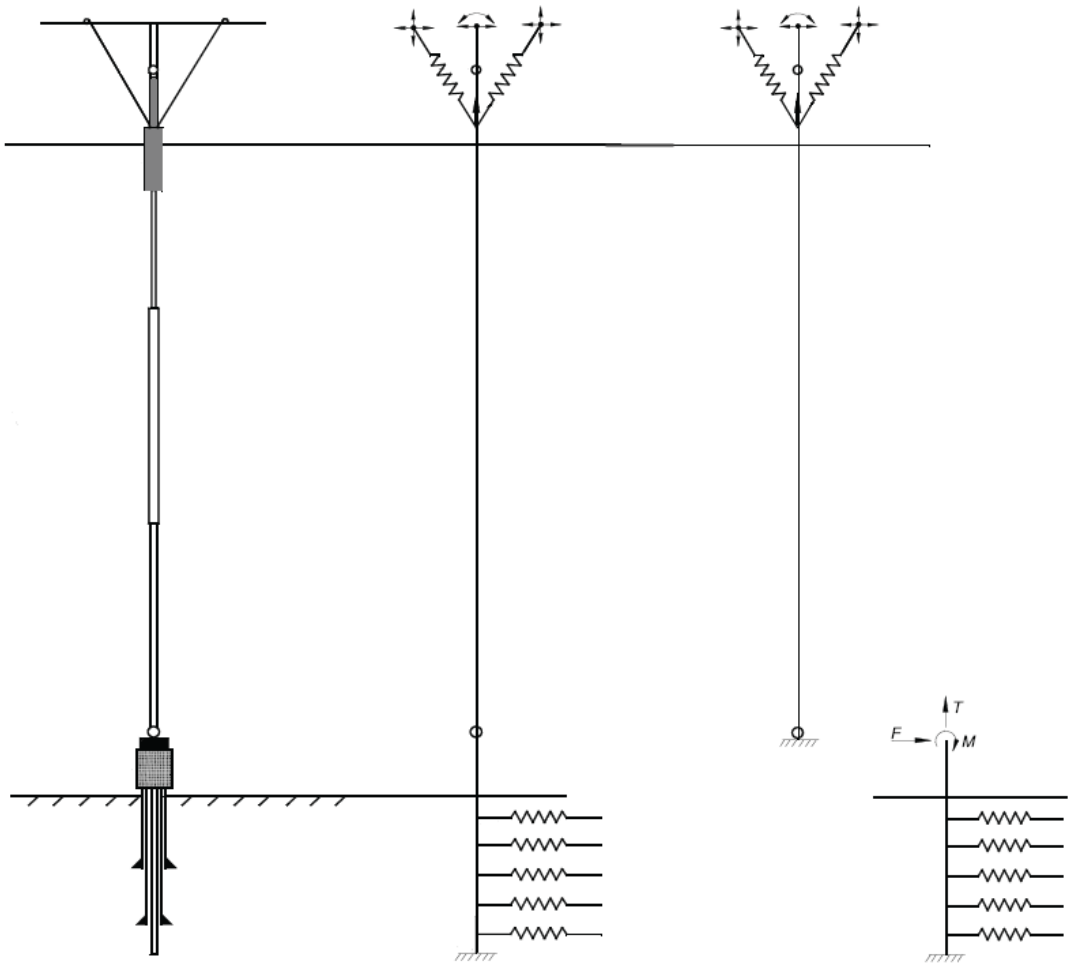

Figure 7-1: Riser system and the corresponding coupled (middle) and decoupled (right) analysis models (ISO 13624-2, 2009)

7.1.3 Choice of model

As the analysis is performed in shallow water and the response of the wellhead is in focus here, the coupled methodology is the most suited for the analysis in this thesis. As can be seen from Figure 7-1 both methodologies require soil stiffness modeled as springs with varying (increasing) stiffness downwards in the soil. The stiffness of the springs should correspond to the stiffness of the actual soil, and can be found from p-y curves for the soil in the area in question. The p-y curves relate unit soil resistance to pile deflection. The slope of a p-y curve at any represents the tangent soil stiffness at a given deflection. The p-y curves are based on the diameter for the contact between cement around the wellhead and the soil (Odfjell Drilling Technology, 2010). As these curves have not been available in this thesis, an intermediate method has to be used.

The model in this thesis stretches from the upper flex joint to the top of the wellhead, i.e. the LMRP and BOP are included, but the conductor is not. From the wellhead and down, springs are used to model the soil stiffness. The reason for this is that the soil stiffness given for the field is defined from the top of the wellhead and down (Odfjell Drilling Technology, 2010). The soil stiffness is defined as two vertical

springs, one in x-direction and another in y direction, and a rotational stiffness. In addition a vertical spring with infinity stiffness is added to the model in the same point, assuming that the BOP and LMRP will not sink into the soil after being cemented into place.

7.2 Model

The simplest model of a tensioned riser will be a straight pinned beam with tension acting as a force at the top and which is free to translate in the vertical direction at top end. The model presented in this chapter is slightly more complicated and consist of several parts. The build up for OrcaFlex and data input used for the riser system in the analysis will be presented in the following.

The different components in the riser system will be interpreted and added to the model as either a stiff mass or a flexible mass. The stiff mass will in most cases be close to rigid. It is important to calculate the components weight in both air and water and use the correct value in the analysis. Hydrodynamic coefficients used in the analysis will include the normal drag coefficient and the associated drag diameters for the bare and buoyancy joints (Bai & Bai, 2005).

7.2.1 Model components and build-up in OrcaFlex

The drilling riser stack-up is shown to the left in Figure 7-2. This is the stack up used during the measurement runs and the base for the model that will be built and analysed. The model built in OrcaFlex consists of a vessel, four lines, four buoys and nine springs. The riser line is assumed to start at the upper flex joint, where the connection to the vessel has a nonlinear stiffness and is given by the deflection angle and corresponding bending moment defined for the flex joint. OrcaFlex interpolate linearly for values between the ones given as input.

The upper flex joint is connected to the inner barrel on the slip joint and the part of the outer barrel which is positioned above the tension ring. This makes up the first line part of the riser and is connected in the lower end to the tension ring with infinity stiffness. There are also 6 tension cylinders carrying the riser weight with a top tension, these are connected to the vessel in the upper end and to the tension ring in the lower end. The tension cylinders are modeled as springs with stiffness and damping equalizing the stiffness and damping given by the hydraulic pressure in the tension cylinders.

The tension ring is modeled as a body with six degrees of freedom, i.e. moment and translation effects can be transferred to and from the body to the connected lines. The body used is called a 6D buoy in OrcaFlex, but it does not necessarily act as a buoy, this depends on the input properties given. The important thing is that the physical properties are maintained, and the buoy is the best choice for modeling a body that have to transfer motions and forces to connected lines. The only function of the body is to be a connection point for the tension cylinders as springs cannot be connected to nodes on a line, only end points.

The next line piece is connected to the tension ring with infinity stiffness as well, i.e. the displacement is transferred from the first line part, to the tension ring and then to the top of the second line part. Components that make up this line are the part of the slip joint below the tension ring, a 30 ft pup joint,

ten 75 ft slick riser joints, three 75 ft riser joints with buoyancy modules attached, a 10 ft pup joint, the riser adapter and the lower flex joint. The lower end is connected to the LMRP with a nonlinear stiffness given by the deflection angle and corresponding bending moment defined for the flex joint.

The LMRP and the lower stack are modeled as 6D buoys as the tension ring. This means that the components are modeled as bodies with six degrees of freedom, and hydrodynamic forces are calculated using Morison's equation as for lines (Orcina, 2009). These two bodies also function as connection points and have no stiffness properties, only mass and geometry.

Translations and moments are transferred from the second line to the LMRP. These properties are further transferred to the lower stack by a connection line from the center of the LMRP to the center of the lower stack; the connection line also applies stiffness to the bodies. This stiffness is assumed to be large, as the large components are very stiff in real life. A similar connection line is also stretched from the lower stack to the wellhead.

The wellhead is modeled as a buoy with three degrees of freedom; translations. Rotations are not included as the rotational stiffness in the system is added in the lower end of the connection line, which equals the rotational stiffness of the soil. The wellhead also exists as a connection point; the springs that model the vertical and horizontal soil stiffness are connected to this buoy. These springs have been chosen to be long in extent to minimize rotational angles in the anchored end for the springs experiencing translations with the wellhead connections.

The data not used are either set to blank, zero or very small. The latter case occur where OrcaFlex require values to be stated.

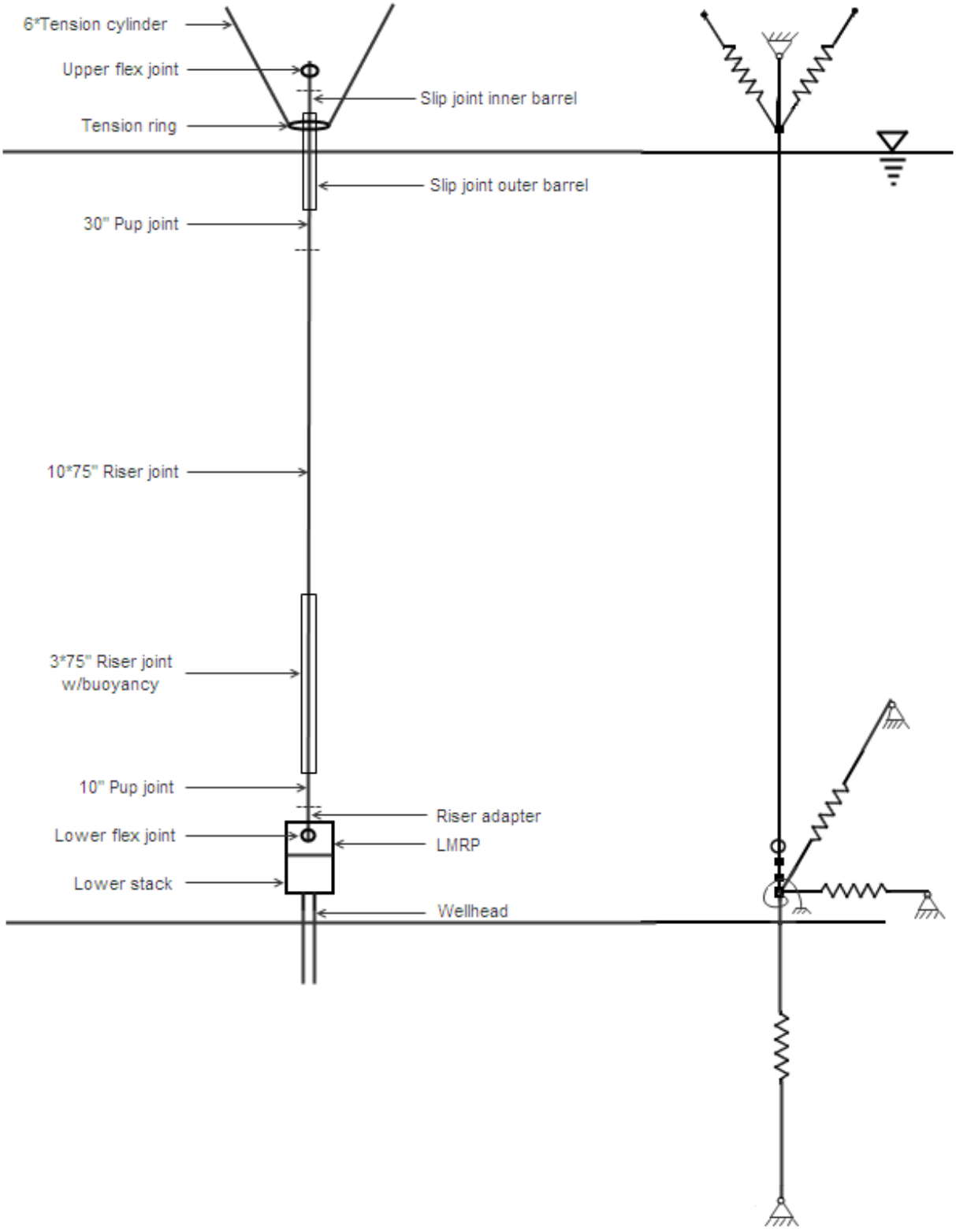

Figure 7-2: Riser stack-up on the left and the model crated in program on the right

7.2.2 Data for input and calculation

The data input is presented as it is required to be given in OrcaFlex, and the choices for analysis parameters will be presented. The variable input, significant wave height, wave period and over pull at LMRP, i.e. top tension, is given in the specific cases that will be analysed. These are presented in a later chapter.

7.2.2.1 Environmental data

Data used in calculations and as input for the environment in OrcaFlex is presented in Table 7-1. It is assumed that the rig is kept in position by anchoring and drift-off is neglected.

Table 7-1: Environmental data for the troll field

Environmental data for the Troll field		
Density air	1	[kg/m^3]
Density water	1025	[kg/m^3]
Kinematic viscosity[1)]	1.35E-6	[m^2/s]
Water temperature[2)]	7.75	[°C]
Water depth[3)]	334	[m]
Current[4)]	Variable with depth	-
Wave	Random	-
Frequency spectrum	Torsethaugen	-
Direction[5)]	180	deg

1) Using the default value in OrcaFlex
2) Temperature is an average over the depth in January, taken from the Metocean report for the Troll Field (StatoilHydro, 2009)
3) (Odfjell Drilling Technology, 2010)
4) Variable data used as input, see Appendix A, is taken from the Metocean report for the Troll Field (StatoilHydro, 2009)
5) Assumed direction of the waves and current

The environment used in the model should be as similar to the conditions during the measurements, and the waves and current applied to the model should therefore be taken from the measurements. Because of lack of measurements for the current during the test run, these have to be taken from the Metocean Design Basis for the Troll Field. The data for the current may not correspond with the environmental situation present during the test runs and may induce conservative or non-conservative results. This all

depends on how the current correlates with other loads. A smaller constant current can also be applied, e.g. 0.2 m/s over the water depth. Tidal variations are assumed to be included in the current applied.

During the operations on Troll the waves came in a few degrees port of head sea. No exact number is given; the direction of the waves and current is therefore assumed to be 180 degrees, i.e. the waves and current act in the negative x-direction, incoming in the front of the rig (ref nick). This is a simplification of the complex reality, the current may act in another direction than the waves and may change direction trough the water depth.

7.2.2.2 Component data

Geometry and mass

Data used in calculations for the components and as input in OrcaFlex for geometry and mass is given in Table 7-2. Some parts of the risers are bare pipes and some are pipes with auxiliary lines, i.e. kill/choke, hydraulic and mud lines. In OrcaFlex only simple cylinders are modeled, therefore equivalent diameters had to be calculated and applied for the pipes with auxiliary lines, hence equivalent internal diameter ID_{eq} and equivalent external diameter OD_{eq}. This is done to preserve the physical properties, e.g. weight and buoyancy. See excel sheets for input calculation on DVD in Appendix E for the calculation of the properties. The data for input and calculations are found in drawings of the individual components or in Rig Data Requirements, a document collecting the dimensions and important parameters for the equipment on the rig. During the measurements the fluid contents in the riser system is sea water.

The connection line between the LMRP and lower stack and between the lower stack and wellhead has been chosen to have a small diameter as it is the connection and stiffness in the line which is of importance. Dimensions affecting the geometry, mass and drag are given in the buoy properties.

The input for the vessel can be found in Table 3-2. The vessel is not included in static analysis, i.e. the position defined by input is the position given as input for the dynamic analysis. The motions in the vessel are purely wave-generated and the responses in the vessel due to the incoming waves are given by the displacement RAOs for the vessel in the specific draft.

Table 7-2: Geometry and weight input for OrcaFlex

Component	ID_{eq} [m]	OD_{eq} [m]	Weight in air [kg]	Length [m]
Upper flex joint	0.4921	0.7019	2 971	1.922
Slip joint inner barrel	0.4921	0.5334	7 000	9.864
Slip joint – outer barrel	0.6096	0.7261	15 905	16.56
Slip joint – outer barrel w/ aux. lines	0.6495	0.8235	10 374	6.556
75” Riser joint	0.5409	0.6232	13 542	22.86
75” Riser joint w/buoyancy	0.5409	1.2769	22 567	22.86
30” Pup joint	0.5409	0.6412	6 702	9.144
10” Pup joint	0.5409	0.6966	3 629	3.048
Riser adapter	0.5264	0.9008	3 692	1.119
Lower flex joint	0.4763	0.8267	3 850	1.366
LMRP	-	-	133 765	4.303
Lower stack	-	-	230 420	8.81

Stress and drag

OrcaFlex also require input data for stress and drag calculation, this input is given in Table 7-3. The diameters used for stress calculations are the dimensions of the load bearing cylinder, i.e. the main pipe. The drag diameter used in this model is the bolt circle plus the outer radius of the kill line times two (the kill and choke lines have the same diameter dimensions). The calculation of drag diameter can be done in several ways, see Appendix B. The broadest length in the transverse dimensions is used as the drag input. This is also the case for calculation of the drag input for the LMRP and lower stack drag area. In addition to the drag area the drag coefficient is needed as input for the drag calculations. The drag coefficient is assumed to be 1.2 for the whole model, see chapter 6.3.3.2.

Input and calculation data for the LMRP and lower stack, i.e. mass, moments of inertia, drag area, drag moment of area, hydrodynamic mass and inertia together with added mass coefficients, is presented in the excel file for calculation of input data on the DVD in Appendix E. Appendix D in the recommended practice DNV-RP-C205 has been used for calculation of added mass coefficients.

Table 7-3: Values for diameter input for stress and drag in OrcaFlex

Component	ID_{stress} [m]	OD_{stress} [m]	D_{drag} [m]
Upper flex joint	0.4921	0.5334	1.006
Slip joint inner barrel	0.4921	0.5334	0.533
Slip joint – outer barrel	0.6096	0.6604	0.660
Slip joint – outer barrel w/ aux. lines	0.6096	0.6604	1.143
75" Riser joint	0.4921	0.5334	1.016
75" Riser joint w/buoyancy	0.4921	0.5334	1.372
30" Pup joint	0.4921	0.5334	1.016
10" Pup joint	0.4921	0.5334	1.016
Riser adapter	0.4763	0.5334	1.156
Lower flex joint	0.4763	0.5334	0.533

Stiffness

Bending and axial stiffness is also calculated for each line component and given as input to the model. These input values are given in Appendix A and the equations for the calculation is given in Appendix B, the calculation itself is included in the excel files for calculation of input on the DVD in Appendix E. To include the vertical movement in the slip joint the axial stiffness in the inner barrel of the slip joint is assumed to be very low and equal to 1 kN. For the connection lines between the LMRP, lower stack and wellhead the stiffness is assumed to be large and has been based on earlier models (Odfjell Drilling Technology, 2010).

The size of torsional stiffness is also assumed, based on earlier models (Odfjell Drilling Technology, 2010). Torsional stiffness is assumed only to occur in the lower part of the model and is therefore only included in the connection lines in the model. In the connections for the flex joints nonlinear stiffness is used as input. This stiffness is given by the manufacturer of the component. The input values are given in Appendix A.

The six tension cylinders in the model is as mentioned earlier modeled as springs with stiffness and damping. The tension varies with the overpull on the LMRP. Overpull is the extra top tension that is applied to the system to ensure successful emergency disconnection if this should be necessary. This is explained closer in chapter 7.3.

The soil is modeled by four springs, two horizontal, one vertical and one rotational, where the three first are connected to the wellhead and the rotational stiffness is included in the connection point between the wellhead and lower stack. Translation will be transferred to the spring from the wellhead body and further to the horizontal and vertical springs, but the rotational stiffness in the wellhead body absorbs the rotations. The vertical spring is assumed to be very stiff and is given an assumed large size. Damping is not included in this spring. The properties of the three other springs are given as displacements and rotations calculated from the soil properties, see file on DVD in Appendix E. The stiffness and damping in the horizontal springs are nonlinear and is calculated from the given displacements. The rotational stiffness is calculated form given rotations. See calculation in excel sheet for calculation of input data on DVD in Appendix E.

In most deep water fields loose clay is the common seabed characteristic. This has an effect on the riser and has to be taken into account in the riser analysis. The stiffness in the clay can make the top-hole drilling complicated for the top tensioned/drilling riser. The interaction between the soil and the riser is often modeled with friction coefficients and linear springs. It is important to model the interaction between the riser and the soil as correct as possible to reproduce the correct real life situation (Bai & Bai, 2005). It is assumed that this is done for the data given in this report, i.e. that the four springs used will correspond to a model with stiffness modeled from p-y-curves for the soil. This will be the model recommended from ISO for coupled analysis.

7.2.2.3 Analysis parameters

In addition to the model input computational parameters have to be decided to run the analysis. In this sub-chapter the parameters applied in the analysis will be given.

Segmentation

The riser is built up by components and for the calculation performed in the program, these components are divided into segments. The segments represent the actual line with a beam element and two nodes, see chapter 6.1. Static and dynamic calculations are performed for each segment. In turn that means that increasing number of segments increases the calculation, i.e. increased analysis time. The numbers of segments, i.e. the size of the segments, also determines the accuracy of the calculations. In areas with large changes per calculation (time step) demand a finer division of the components, e.g. the areas close to the connection points need more segments than the middle of a line and components like the flex joint where a flexible part meets a less flexible part need more attention. In OrcaFlex a target segment length is chosen and the number of segments adding up to the total length is calculated, and OrcaFlex uses the closest size to the one targeted. The choices for the segmentation in this model are shown in Table 7-4. Here it can be seen that for the upper flex joint the target segment length is 0.3 m and the actual segment length is the total length divided by the number of segments, i.e. 0.32 m.

Table 7-4: Segmentation of the components in the model

Segmentation of line			
Component	**Total length [m]**	**Target segment length [m]**	**No. of segments**
Upper flex joint	1.922	0.3	6
Slip joint inner barrel	9.864	9.864	1
Slip joint – outer barrel	16.56	0.5	33
Slip joint – outer barrel w/ aux. lines	6.556	1	7
75” Riser joint	228.600	3	76
75” Riser joint w/buoyancy	68.580	2	34
30” Pup joint	9.144	2	5
10” Pup joint	3.048	0.5	6
Riser adapter	1.119	0.25	4
Lower flex joint	1.366	0.25	5
LMRP connection line	6.556	6.556	1
Lower stack connection line	4.405	4.405	1

The target segment length is decided by a combination of evaluation, convergence of model and try and fail. The desired division is chosen and run. If there is a problem with the conversion of the model, a finer division may have to be chosen. The division is chosen small enough to get good results, but as large as possible to save simulation time.

Choices for analysis; integration method, time step and simulation time

The static analysis is run for the whole system, excluding the vessel and the wellhead. These are avoided to make the model convergence. For the integration, the implicit method is chosen. The other choice of method, explicit, demands very mall time steps, i.e. long simulation time. The time step is chosen to be variable with a maximum of 0.25 seconds. When this is chosen to be variable the program uses larger steps for areas with small variations and simple calculations and smaller steps for difficult areas. The tolerance is the limit for the error accepted in the calculations. The numbers for these analysis variables are chosen with experience, try and fail to make the model converge.

Table 7-5: Analysis specifications

Specifications for analysis		
Integration method	Implicit	-
Maximum time step	0.25	s
Maximum no. of iterations	20	-
Tolerance	25E-6	-

To run a complete 3 hour (10 800s) analysis is time demanding. A simplified method is chosen here to save time. The simulation time set is with a 30 second build up period. To ensure that the expected maximum wave is included in the simulation period, a check of the wave development for the chosen sea state is done in OrcaFlex. The full three hour wave development can give the maximum wave as a rise and a fall. To include these maxima in the analysis, it is chosen that the wave loads starts approximately 150 s before the maximum fall/rise occur and is run until approximately 150 s after the maximum rise/fall. This allows the model to create a motion pattern for the loads acting on it. The time step will then vary in length depending on when the wave profile has its maximum fall and rise (Orcina , 2008). The minimum total simulation time is 300 s.

7.3 Analysis cases

The analyses will among other things determine the vessel excursions, installation and operation limits. The riser has to be flexible enough to tolerate large motions in the vessel and the arrangement of it has to correspond with acceptable limits for the external loading it is subjected to. For a riser different type of analysis will be performed, e.g. running and retrieving, operability, weak point, drift-off, VIV, wave fatigue, hang-off, dual operation interface, contact wear and recoil analysis. All of the analysis has to have results/limits in accordance with the governing rules and regulations (Bai & Bai, 2005). In this report the main focus is to perform an analysis that is as similar to the actual situation during measurements as possible. This is a condition for the comparison between the measurements and the analysis results, i.e. the wave height, wave period and the tension input should be the same in the analysis as it was during the measurement runs. These factors vary over time and in this chapter different cases are presented for analysis. The measurements were performed in three runs which were divided into a number of sequences. Time logs make it possible to correlate the sequences against measured waves. The choice of cases is based on several factors; stable measurements, existing measurements, available information on tension settings etc.

The wave heights and periods should ideally be given from measurements. Unfortunately these data has not been available in a format that can be processed by the author, but during the sequence logging, the wave heights and wave periods were read of the rigs own measurement equipment for each sequence.

In addition, the wave height and period from Statoil's Metocean service on Troll A were registered in the log. From these values for the wave heights and periods over the measurement time, a plot have been made by DNV in a report investigating load levels and foundation capacity for the same full-scale testing that the focus in this thesis, see Figure 7-3.

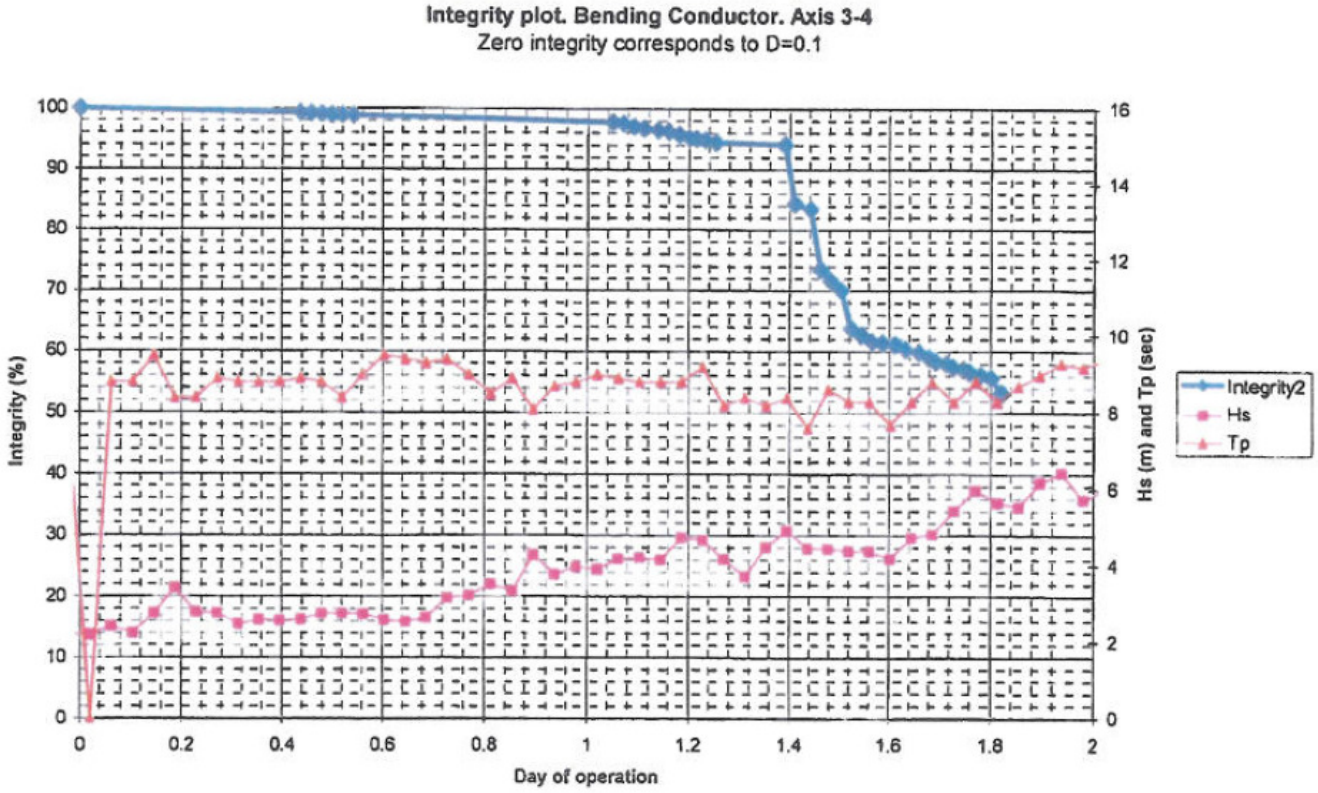

Figure 7-3: Integrity plot from DNV report. Wave height and period plotted from manually logged measurements (DNV, 2010)

In the figure, time is given with reference to the total time for which the measurements in test run 2 and 3 are performed. A sequence in the test run is chosen, thereafter the wave height and period is taken from the plot above. The cases were chosen from the sequences where all the desired information was given. Cases with their corresponding values are given in the following sub-chapters.

For design analysis the tension is calculated from design practice rules, but the tension implemented in the model for analysis is the tension used during the measurement sequences. The tension in the tension cylinders vary for the different sequences. For each sequence the overpull at LMRP is registered in the log. The necessary top tension for the specific sequences is calculated from the total weight of the system and the overpull at LMRP, excel sheet for calculation of input data on DVD in Appendix E. Known cylinder tension-stroke correlations for system set tensions, see graph given in Appendix B, are used to extrapolate values for the stiffness needed in the springs, modeling the tension cylinders. See the case specific input values in Appendix A.

The results from the analysis of the cases will be presented in chapter 10.

7.3.1 Variable input for Case 1 and Case 2

Table 7-6 gives the input for the variable data in Case 1 and Case 2. The same model is used in the two cases, but the data given in Table 7-6 will be the difference in the analysis run for the two cases. The table also states which measurement log (test run and sequence) results from the analyses should be compared to.

Motions of the wellhead were observed at day of operation equal 0.75 (DNV, 2010), see Figure 7-3. To have a correct model as possible input values were chosen where stabile weather had been registered and before the motions in the wellhead occurred. The reason for this is that fewer uncertainties will be included in the comparison if the most accurate values available are used. For later analysis and improvement of the model a broader selection of sea states can be implemented in the analysis.

OrcaFlex model files and simulation files for both cases are given on the DVD in Appendix E.

Table 7-6: Variable input data for analysis Case 1 and Case2

Variable input for the analysis				
	Case 1		Case 2	
Test run[1)]	2	-	2	-
Sequence[1)]	6	-	01d	-
Day of operation[2)]	0.05	-	0.25	-
Significant wave height, Hs[3)]	2.3	[m]	2.9	[m]
Wave period, Ts[3)]	8.5	[s]	8.5	[s]
Overpull at LMRP[1)]	80 000	[kg]	196 800	[kg]
Simulation time[4)]	1200	s	300	s

1) (Odfjell Drilling AS, 2010)
2) Referring to time axis in Figure 7-3
3) (DNV, 2010)
4) Including both maximum fall and rise wave

8 Full scale measurements

Comparing measurements and analysis results is very challenging. To have valid and good basis of comparison it is important to obtain the correct and accurate environmental conditions and working conditions for the riser during the measurements. Vital parameters that can be mentioned are tension in pipe, weight of system, internal fluid weight, current, position, wave height and period etc.

The intention in this thesis was that data for all the important parameters were measured. In the end this is not the case here. Good measurements have been obtained for the strains in the riser and wellhead, but current and wave measurements have not been obtained. A comparison will be performed, but lack of data can be a cause of possible deviations in the results.

In the following the measurement set-up is presented. The measurement data received for the riser and wellhead are given in strains, moments and forces. In the comparison the given forces and bending moments are used, but a suggested method of conversion of the measured data is also given in the following.

The theory for the conversion of data is in great deal taken from the pre-project performed by the author prior to this thesis. The topic in the pre-project was analysis of measurement data from the Hywind pilot. This has no direct correlation to the subject in this thesis, but the theory for conversion of measurements in strain for circular cylinders can be transferred. References are given to the original sources used.

8.1 Measurement set-up

During the testing several measurements were performed. The measurements of interest for this thesis are the strains measured on the lower part of the riser and on the wellhead. Strain sensors from GeoDrive Technology BV, see Figure 8-1, were placed on the wellhead and on the 10 ft pup joint. The same type of sensor was used in all positions.

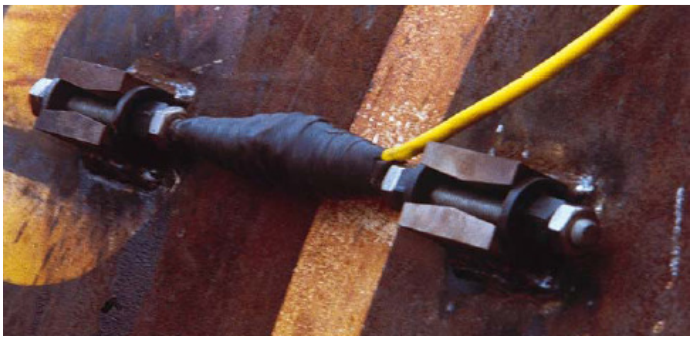

Figure 8-1: Strain sensor used on the riser and wellhead (GeoDrive Technology BV, 2009)

Four strain sensors are mounted at the same height on the system component with 90 degrees separation between them. With the four strains measured, bending moments and axial forces in the component can be calculated (GeoDrive Technology BV, 2009). Figure 8-2 shows the position of the sensors on the 10 ft pup joint. In the cross-sectional figure it is showed that the sensors are positioned

with 90 degrees interval, numbered from 1 to 4, but the sensors are not necessarily positioned on the axis. This has to be taken into consideration when the conversion calculations and comparison is performed.

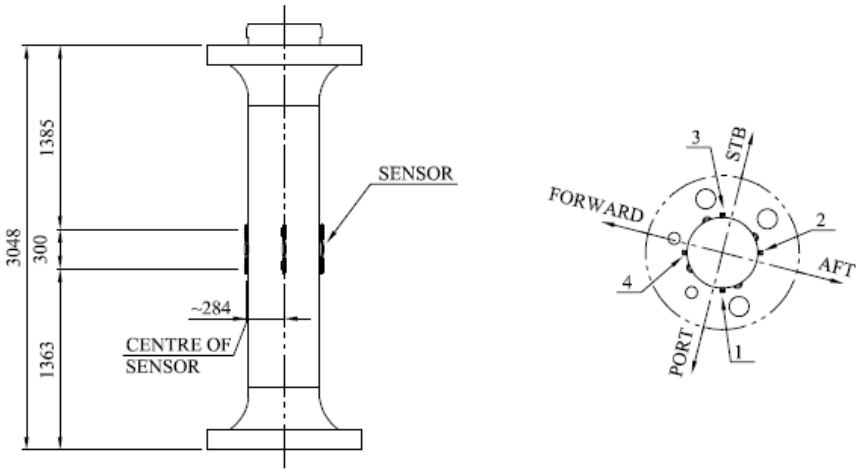

Figure 8-2: Position of strain sensors on 10 ft pup joint (Odfjell Drilling AS, 2010)

Figure 8-3 shows the position of the sensors on the wellhead. The sensors are in reality located on the conductor, but it will be referred to as the wellhead in this report. The figure also shows that the wellhead stretches a length of almost four meters above the seabed. Normally this height for the wellhead will be lower, but because of the sensors positioned on the conductor pipe it could not be fully lowered into the seabed. Position of the sensors in the cross-section is on the axis directions, as showed with numbers 1 to 4 in the figure.

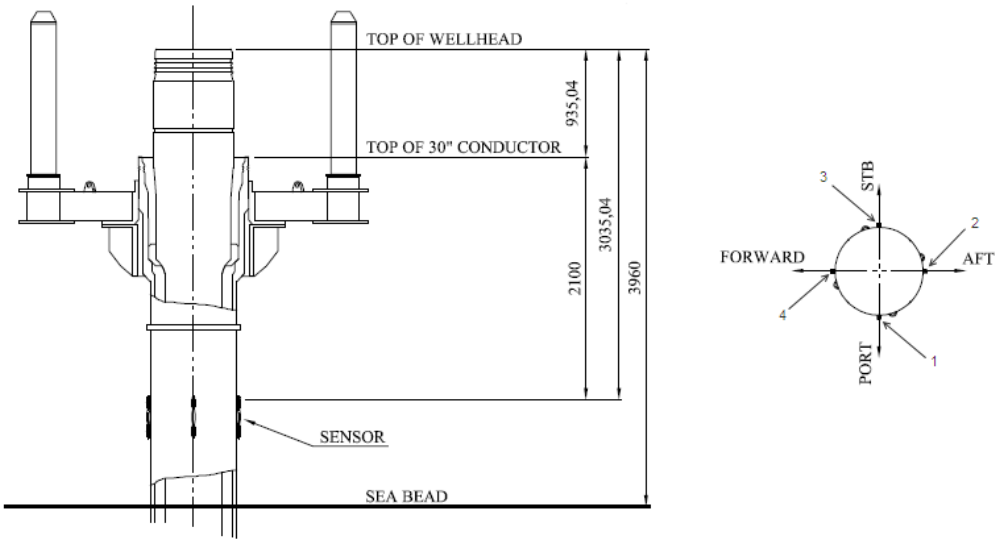

Figure 8-3: Position of strain sensors on wellhead (Odfjell Drilling AS, 2010)

8.2 Conversion of data

The measurement data from the wellhead and pup joint are given in strains, bending moment and axial forces by the supplier of the sensors, i.e. the calculation from the strain measurement to moment and force have been performed by GeoDrive Technologies BV. It can be relevant to perform a control check of the extraction of moments and forces from the strains measured. In this chapter, theory for conversion from strains to bending moments and axial forces will be presented.

8.2.1 From strain to bending moment and axial force

When a structure is exposed to loads, stresses occur in the material. These stresses can be linked to the strains in the material. In the theory, two types of material are mentioned when calculation of stresses is performed (Irgens, 1999):

- Linear elastic material
- Linear elastic - ideal plastic material

These are both materials that are defined by assumptions which are not identical to the reality, but the theory can give an insight to connections that are important to understand. According to the standards for calculation of steel structures like NS-3472, calculations for a structure in bending can be designed after the theory of either one of the materials mentioned (Irgens, 1999).

A linear elastic material is defined by a connection between the normal stress σ, strain ε and elastic modulus E of the material. This connection is called Hooke's law:

$$\sigma = E\varepsilon \tag{8-1}$$

Linear elastic - ideal plastic material will follow Hooke's law as long the stresses that occur in the structure is lower than the yield stress, which will be assumed here. Further, if it is assumed that the material response is linear and isotropic, the following equations can be used to calculate the coordinate stresses in the surface where strain is measured with strain sensors (Irgens, 1999):

$$\begin{aligned}
\sigma_x &= \frac{E}{(1+\nu)(1-2\nu)}[(1-\nu)\varepsilon_x + \nu(\varepsilon_y + \varepsilon_z)] \\
\sigma_y &= \frac{E}{(1+\nu)(1-2\nu)}[(1-\nu)\varepsilon_y + \nu(\varepsilon_z + \varepsilon_x)] \\
\sigma_z &= \frac{E}{(1+\nu)(1-2\nu)}[(1-\nu)\varepsilon_z + \nu(\varepsilon_x + \varepsilon_y)] \\
\tau_{xy} &= G\gamma_{xy}, \tau_{yz} = G\gamma_{yz}, \tau_{zx} = G\gamma_{zx}
\end{aligned}
\quad \rightarrow \text{Plane tension} \quad
\begin{aligned}
\sigma_x &= \frac{E}{1-\nu^2}(\varepsilon_x + \nu\varepsilon_y) \\
\sigma_y &= \frac{E}{1-\nu^2}(\varepsilon_y + \nu\varepsilon_x) \\
\tau_{xy} &= G\gamma_{xy}
\end{aligned}
\tag{8-2}$$

Where ε is linear coordinate strain in the given directions, γ is coordinate shear strain, σ is the coordinate stresses, τ is the coordinate shear stresses, ν is the Poisson ratio and G is the shear modulus. The effect of temperature variations on the stress and strains are neglected. The equations assume that it is the

coordinate strains that are known and that we have plane stress. The principal stresses and principal stress directions can be derived from the following formulas (Irgens, 1999):

$$\sigma_1 = \frac{\sigma_x + \sigma_y}{2} + \sqrt{\left[\frac{\sigma_x - \sigma_y}{2}\right]^2 + \tau_{xy}^2}$$
$$\sigma_2 = \frac{\sigma_x + \sigma_y}{2} - \sqrt{\left[\frac{\sigma_x - \sigma_y}{2}\right]^2 + \tau_{xy}^2} \qquad (8\text{-}3)$$
$$\phi_1 = \arctan\left(\frac{\sigma_1 - \sigma_x}{\tau_{xy}}\right), \phi_2 = \phi_1 + \frac{\pi}{2}$$

Another approach to find the stresses is to calculate the principal strains from the equations below and thereafter use the formula-set (8-2) to find the principal stresses (Irgens, 1999):

$$\varepsilon_1 = \frac{\varepsilon_x + \varepsilon_y}{2} + \sqrt{\left[\frac{\varepsilon_x - \varepsilon_y}{2}\right]^2 + \left(\frac{\gamma_{xy}}{2}\right)^2}$$
$$\varepsilon_1 = \frac{\varepsilon_x + \varepsilon_y}{2} - \sqrt{\left[\frac{\varepsilon_x - \varepsilon_y}{2}\right]^2 + \left(\frac{\gamma_{xy}}{2}\right)^2} \qquad (8\text{-}4)$$
$$\phi_1 = \arctan\left(\frac{(\varepsilon_1 - \varepsilon_x)}{\gamma_{xy}}\right), \phi_2 = \phi_1 + \frac{\pi}{2}$$

If it is assumed that one axial strain is received from each sensor per time, conversion as explained above is therefore not necessary to perform as this is already performed by the measurement instrumentation on the riser. The strain data can therefore be utilized directly in Hooke's law when the stress in the measurement points is to be calculated.

The riser will be exposed to loads of different nature, but if it is assumed that only bending moment is affecting the structure an isotopic material and no shear force can be assumed. The assumptions can be valid because in an isotropic material the cross-section shear stresses can be neglected and shear stresses caused by shear forces are usually small compared to stresses caused by bending moments. When the structure is exposed to pure bending and a constant cross-section is assumed, a relation between tension, σ, and bending moment, M, is given as (Irgens, 1999):

$$\sigma = \frac{M}{I} y \qquad (8\text{-}5)$$

Where y is the distance from the centre of the element and I is the moment of inertia. For a circular cylinder with inner radius r_i and outer radius r_e the moment of inertia can be expressed as (Irgens F. , 1999):

$$I = \frac{\pi(r_e^4 - r_i^4)}{4} \quad (8\text{-}6)$$

If axial force is to be taken into consideration in addition to the bending moment, then superposing of the two load contributions is possible as long as the material is linear elastic. Then the total stress will be expressed with Navier's formula, where N is the axial force and A is the area the force acts on. In addition bending in two planes can be considered, than the following can be expressed (Irgens, 1999):

$$\sigma = \frac{N}{A} + \frac{M_z}{I_z} y + \frac{M_y}{I_y} z \quad (8\text{-}7)$$

I_z and I_y is the moment of inertia about respectively the z-axis and the y-axis. Nonlinear stress-strain relationships are neglected here, but if they should be of interest for further work the Ramberg-Osgood model can be implemented (Chan & Chui, 2000). It is assumed that the linear Hooke's law, (8-1), and the linear connection between moments, force and stress, (8-7), can be used and therefore indirectly that the accompanying assumptions for the material are fulfilled. As one principal strain value is given from each sensor the bending moments and forces in a point of measurement can be found by the following correlation:

$$E\varepsilon = \frac{N}{A} + \frac{M_z}{I_z} y + \frac{M_y}{I_y} z \quad (8\text{-}8)$$

The presented formulas may indicate how the conversion from strains to wanted sizes can be done for a control check. But the calculation above may deviate from the reality as there are many assumptions performed. It is important that the correct cross-section is used, i.e. calculations of the cross-section at the position of measurement sensors should be used. In addition, it is important take into consideration the position of the sensors relative to the axes. The control check will not be performed in this thesis, as the measurements are given in bending moments and axial forces, but it can be a subject for further work. It is assumed that the noise in the measurements is filtered out in the time series used as a base for the calculations here.

9 Presentation of data

Most of the theory in this chapter is taken from the pre-project performed by the author prior to this thesis. References are given to the original sources used.

The strains are measured several places in the riser over time. For presentation and interpretation of data it is interesting to see how the bending moments and axial force varies over time; this can be done by plotting a time history of the respective sizes. The plot should have time as the first axis and moment or force in one point on the second axis. This is interesting to see from both the measurements and the analysis results. Plots for the same point in the riser system can be created form measurements and analysis and comparison between the analysis results and the bending moments and forces occurring in the riser can be done.

9.1 Energy spectrum

In combination with the bending moment and other variables it can be interesting to look into which wind and sea states that are acting on the structure. Statistical parameters of the bending moment and forces are of interest to present, as they can give us typical and maximum values of interest. If the most typical sea state is found from a distribution function, the affect it has on the structure can be found. This is possible because a time register for the waves in the test period can be correlated with the time series for the bending moment. The following equation can describe a realization of a variable, x(t), bending moment for instance. This variable is dependent on amplitude x_i, time t, frequency of the response component ω_i and a random phase angle ε_i (Larsen C. M., 2007):

$$x(t) = \sum_{n=1}^{\infty} x_i \sin(\omega_i t + \varepsilon_i) \qquad (9\text{-}1)$$

Present results are independent of time. A spectrum is a method of presenting a Gaussian process independent of time as it gives the energy of the process as a function of the frequency. The spectrum will give a description of the statistical properties, standard deviation, zero-up-crossing and extreme values, of the Gaussian process. The expression for the spectrum, $S_x(\omega_i)$, has the following general form (Larsen C. M., 2007):

$$\frac{1}{2} x_i^2 = S_x(\omega_i) \Delta\omega_i \qquad (9\text{-}2)$$

Where $S_x(\omega_i)$ is the spectrum depending on the frequency and $\Delta\omega$ is the frequency interval corresponding to the realization. The measurements that in turn give the bending moments in the structure over time are realizations of the underlying stochastic process. An energy spectrum should be created for the bending moment in the riser by utilizing the equations given above. It is then important to be aware of permanent moments acting in the structure; these will be shown in the spectrum and create a different form than what is expected, often in the area of low frequencies. To remove this effect, de-trend procedure should be implemented.

The measurements from the riser are time domain representations of the statistic process and the spectrum will be in the frequency plane. By Fourier-transformation the energy spectrum for a set of

measurements can be transferred to the frequency plane. The spectrum is then an estimate for the real spectrum because of the finite time of the series in the measurements. For long time series it is time demanding for a computer to solve the Fourier transformation, for this purpose Fast Fourier Transformation (FFT) can be utilized. FFT is a special numerical technique developed to perform Fourier transformations for long time series, and it is used in large extent for treatment of measurement data and response analysis (Larsen C. M., 2007).

Spectrum can also be created for the waves acting on the structure; the amplitude will be the wave amplitude. If this is done, the transfer function, $H_x^2(\omega)$, for the structure can be expressed by the following relationship (Larsen C. M., 2007):

$$S_x(\omega) = H_x^2(\omega)S_\zeta(\omega) \rightarrow H_x^2(\omega) = \frac{S_x(\omega)}{S_\zeta(\omega)} \qquad (9\text{-}3)$$

Where $S_x(\omega)$ is the response spectrum, here bending moment, and $S_\zeta(\omega)$ is the wave spectrum. The transfer function is a function of the frequency and independent of time. It shows how large the bending moment amplitude is at a given frequency relative to the wave amplitude of the incoming wave at the same frequency. It is assumed that linear superposition applies and that the load is given as a harmonic function. If these assumptions are not applied then the calculations cannot be performed in the frequency plane, and time domain has to be utilized in the non-linear case. The latter will be the case if the drag force is dominating (Larsen C. M., 2007).

9.2 Statistical parameters and distribution

The distribution function of different variables, e.g. waves, wind, bending moment etc., should be found because the theoretical calculations are based on given statistical distributions. It will be of interest to see how good these correlate. When the response spectrum is found for the response variable x, the statistical properties of the response are defined by the spectrum moments, m_{xn}. The n^{th}-order of moments of the response can be expressed (Larsen C. M., 2007):

$$m_{xn} = \int_0^\omega \omega^n S(\omega) d\omega \qquad (9\text{-}4)$$

For n equals zero the moment gives the standard deviation, σ_{ST}, which can be found by the following (Larsen C. M., 2007):

$$\sigma_{ST} = \sqrt{m_{x0}} \qquad \left(m_{x0} = \int_0^\omega S(\omega) d\omega\right) \qquad (9\text{-}5)$$

And the zero-up-crossing period, T_{xz}, can be found with n equal to zero and two by the following equation (Larsen C. M., 2007):

$$T_{xz} = 2\pi\sqrt{\frac{m_{x0}}{m_{x2}}} \qquad (9\text{-}6)$$

As the standard deviation is known, the Rayleigh distribution of the variable x, $F_X(x)$, is given (Larsen C. M., 2007):

$$F_X(x) = 1 - exp\left(-\frac{1}{2}\left(\frac{x}{\sigma_{ST}}\right)^2\right) \quad (9\text{-}7)$$

For the Rayleigh distribution to be applicable, linearity and narrow banded process has to be assumed. This distribution can be used for all the variables that are of interest and where a standard deviation can be obtained. It is not necessary to find the spectrum to express the distribution because the standard deviation also can be found from the time series of the measurements (Larsen C. M., 2007).

The Rayleigh distribution is the distribution of all the maxima in a narrow banded time series. It is used in parts of the fatigue calculations. In addition it can be of interest to look at the distribution of the largest out of the maxima obtained in a series; this is when extreme value distribution is utilized. This is especially interesting for ULS design.

9.3 Routine used for spectrum generation

For the presentation of measurements a MATLAB routine is used for plotting of time series and creation of energy spectrum for parameters of interest. The routine used to generate the power spectrum from time series in this report, SPEGEN_T.m, is found in a previous master thesis. It is made by previous Professor II Finn Gunnar Nielsen (Statoil) and with approval from him it is used in this thesis. The routine is given on DVD in Appendix E. OrcaFlex provides the corresponding time series, spectrum and statistical values for parameters of choice in the model analysis.

The theory for energy spectrum described previously in this chapter is implemented in MATLAB to establish the energy spectrum and statistical values. The routine used, SPEGEN_T.m, generates power spectrum from a time history. The spectrum generated is a function of frequency and it s estimated by splitting the time history into blocks. An FFT is applied for each block and the results are averaged. Each block is smoothed by a cosine function to obtain a smooth and even spectre. Increasing number of blocks increases the smoothing of the spectrum. Input variables for the routine is the time history, number of blocks and the sampling interval in the time history. In addition to the spectrum the routine also calculate estimates of statistical parameters for the time history.

The choice of number of blocks will have a large effect on the spectrum and can be s source of error in the results as it is decided by try and fail. De-trend procedures are not implemented so permanent moments may occur in the spectrums generated. Spectrums are only created for the measurements used, i.e. bending moment and force, not for sea states as data for these are not used here.

10 Results and processed measurements

In this chapter the results from the dynamic analysis and the processed measurement data are presented. These can be used to evaluate the goodness of the model. The main focus in this analysis is on the wellhead, but results for the 10ft pup joint positioned above the riser adapter is also presented to provide a wider evaluation basis. The model has been run for two cases, as described in 7.3, corresponding to two measurement sequences. A comparison between model and reality, for wellhead and pup joint, in both cases are presented in the end of this chapter.

10.1 Analysis results

OrcaFlex can provide numerous result formats; here the bending moments and axial forces in the points where measurements have been performed are of interest. In the following the results found in OrcaFlex are presented. For the pup joint the measurements are performed in a point equivalent to node 134 in the line between tension ring and LMRP in the model, i.e. values can be exacted directly from the model for the point of interest. For the results on the wellhead this is not the case as the riser is only modeled to the wellhead datum (top of the wellhead) and the measurements are performed in the lower part of the wellhead.

Wave spectrums for the waves applied in the OrcaFlex model in the two cases run is given in Appendix C.

10.1.1 Wellhead

Results cannot be found directly in the point of interest on the wellhead from OrcaFlex. To be able to compare the measurements with the model the forces and moments in the wellhead are calculated with base in analysis results from a point close to the wellhead. The forces and moments have here been taken from the lower end of the line between the tension ring and the LMRP, i.e. at the lower flex joint. For the moments in the point of interest equilibrium of moments has been calculated about this point. The force is found by tension and weight considerations in the point. Detailed description of approach and calculation is given in Appendix C.

10.1.1.1 Case 1

Figure 10-1 shows how the x-bending moment, y-bending moment and axial force vary over a simulation time of 1200s in the dynamic analysis performed on the model in case 1. The time history can give us statistical values, i.e. mean, standard deviation, maximum and minimum, which can be used in comparison of results.

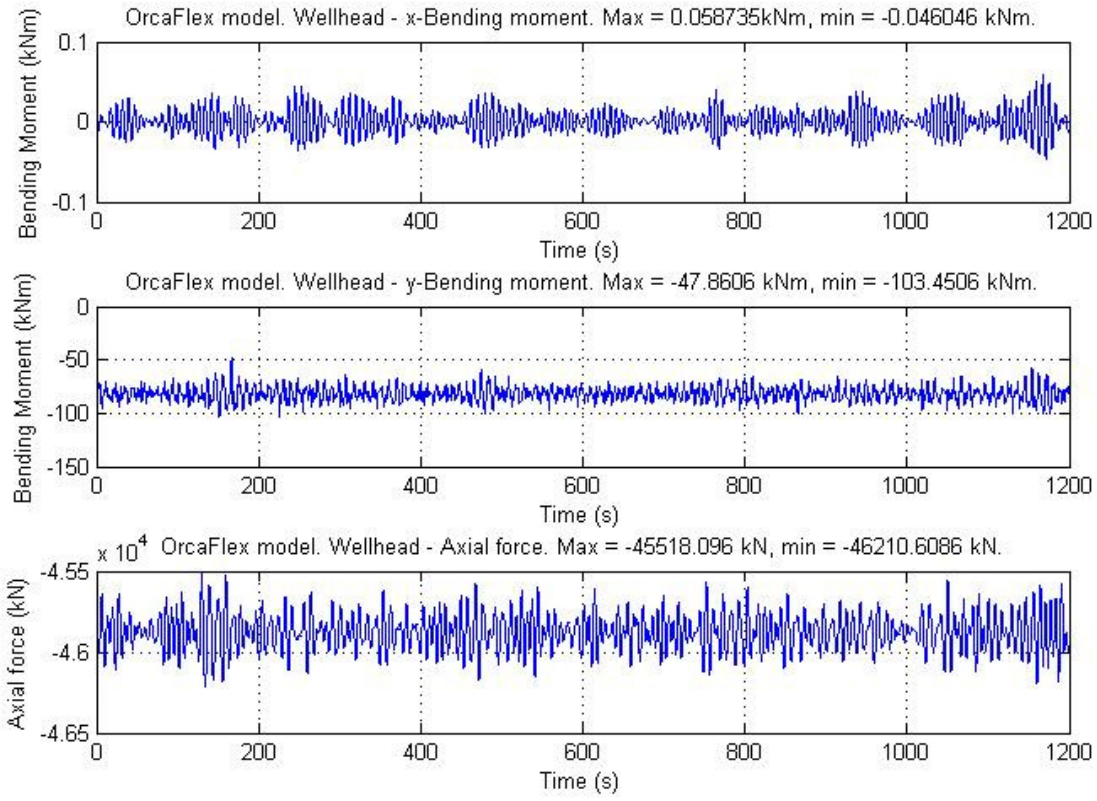

Figure 10-1: Time history plots for OrcaFlex model in wellhead, from case 1. The upper plot is the variation of x-bending moment in the wellhead and middle plot is the variation of y-bending moment. The lowest plot is the variation of the axial force in the wellhead over time.

In this case the time history shows that the x-bending moment varies around 0 kNm, and is small compared to the y-bending moment which has larger variations and varies around 80 kNm. For a longer simulation time the other results for max and min may occur, but mean values will be approx the same. Further investigation, comparison and discussion are performed in chapter 10.3.

Figure 10-2 gives the energy spectrum for x- and y-bending and Figure 10-3 gives the energy spectrum for the axial force in case 1. This energy spectrum can give information about the response of the model; this response should correspond to the real life response of the riser system. For x-bending moment the largest energy is assembled in the frequency interval from 0.1 to 0.15 Hz, i.e. a period interval of around 6.5 - 10 seconds. For y-bending the interval is from 0.08 to 0.125 Hz. The axial force has two peaks, but these are very close, i.e. larges energy is assembled from 0.075 to 0.175 Hz.

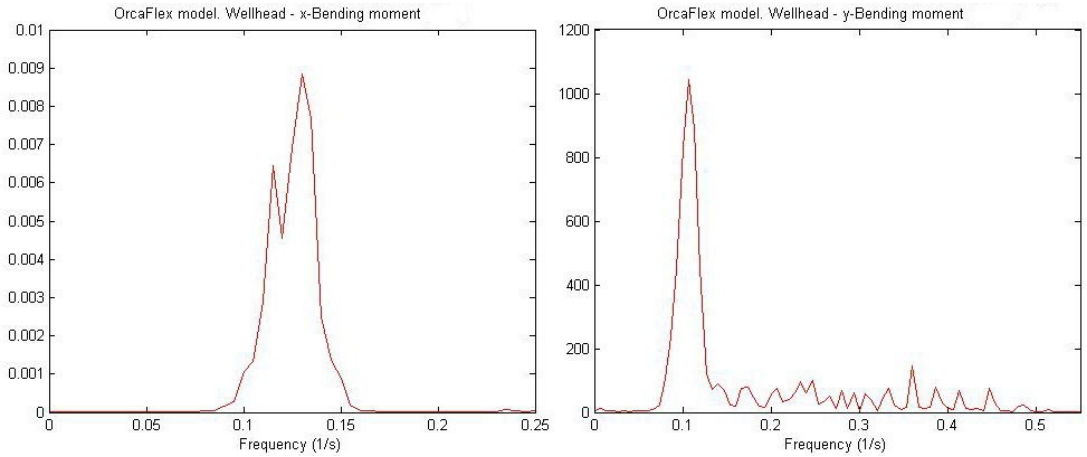

Figure 10-2: Energy spectrum for the x-bending moment (left) and the y-bending moment (right) in the wellhead for the OrcaFlex analysis case 1.

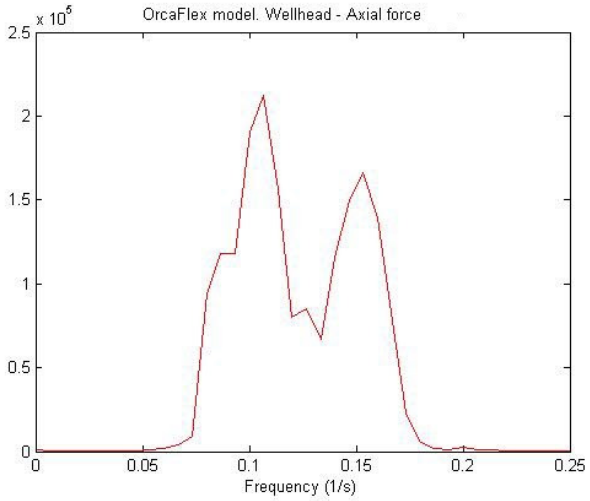

Figure 10-3: Energy spectrum for axial force in the wellhead for the OrcaFlex analysis case 1.

10.1.1.2 Case 2

The time history and spectrum plots for the moments and forces in the wellhead in case 2 are given in Appendix C. Statistical parameters and results from this case are presented and discussed further in chapter 10.3.

10.1.2 10 ft Pup joint

For the pup joint the results found in the model can be compared directly with the measurement data, no calculations are necessary. Node 134 in the line between tension ring and LMRP is approximately in the same position as the strain sensor that measured strains in the full scale riser. The value used to express the axial force in the point of interest is the wall tension. Wall tension corresponds to the axial force in a non pressurized pipe exposed to seawater on the inside and outside, as is the situation for the riser pipe model and the riser pipe in reality.

10.1.2.1 Case 1

The time history and spectrum plots for the moments and forces in the pup joint in case 1 are given in Appendix C. Statistical parameters and results from this case are presented and discussed further in chapter 10.3.

10.1.2.2 Case 2

The time history and spectrum plots for the moments and forces in the pup joint in case 2 is given in Appendix C. Statistical parameters and results from this case are presented and discussed further in chapter 10.3.

10.2 Full scale measurements results

The measurement results are plotted and presented directly from the data files given from the measurements. . It is assumed that measurement noise is removed by the supplier and that the data can be used directly. In the files strains, bending moments and forces are given, as mentioned earlier the moments and force will be used here.

10.2.1 Wellhead

The measurements in the wellhead are given as Bending Moments 1-2 S-P (starboard-port), Bending Moment 3-4 A-F (aft-forward) and Axial Force. Information about how these parameters are calculated is not given. It is assumed in this thesis that the bending moment noted 1-2 S-P is the moment about the x-axis and the bending moment 3-4 A-F is the moment about the y-axis, as forward is in positive x-direction.

10.2.1.1 Case 1

As for the analysis results in the wellhead a time history is plotted. An extract of the first 1000 seconds of the measurements data in case 1, i.e. sequence 6 in the test run2, is plotted in Figure 10-4. This shows how the variation of the moment and force over time. The total time for the measurements was 3600 seconds and the plot for the total time shows the same developing trend as the first 1000 seconds.

From the time history it can be seen that the x-bending moment in real life vary around 100 kNm, the x-bending moment vary around 400 kNm and the axial force vary around 0.65 MN. It can be noted that these values differ a great deal from the analysis result on the wellhead (case1).

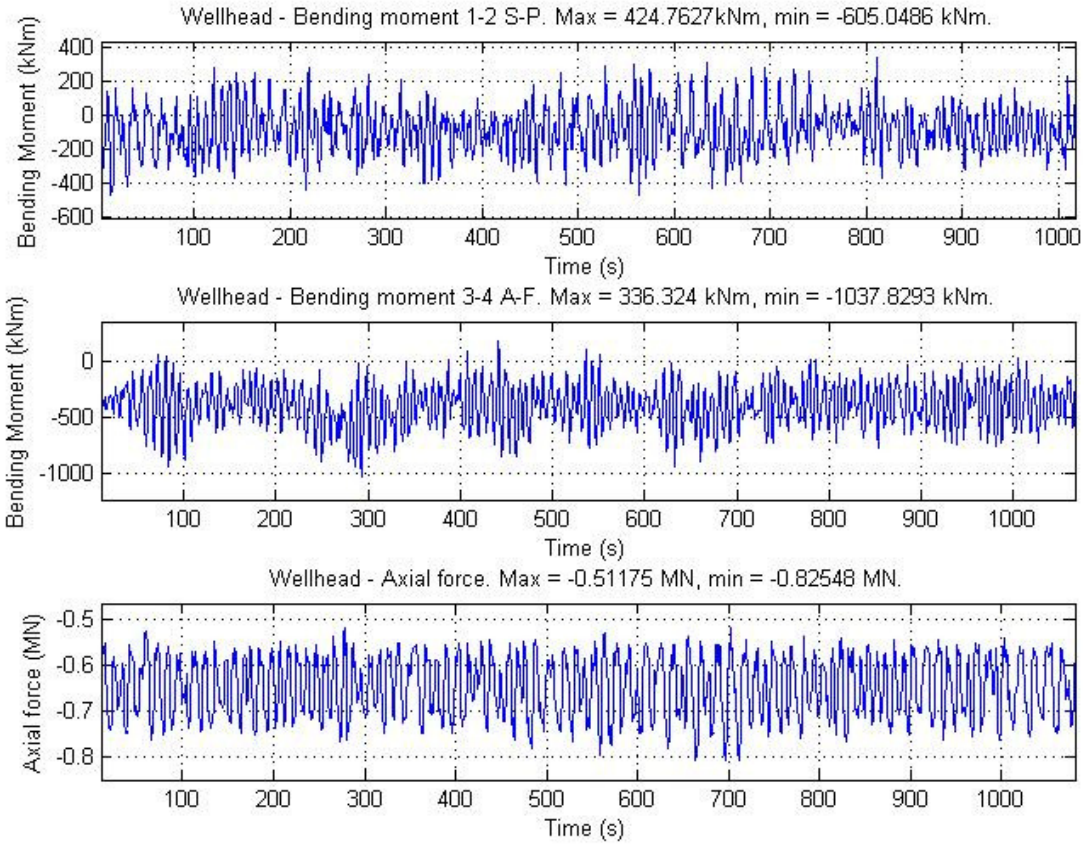

Figure 10-4: Time history plots for measurements in wellhead, from case 1. Where the plot of the bending moment 1-2 S-P (upper plot) corresponds to the moment about the x–axis and the plot of the bending moment 3-4 A-F (middle plot) corresponds to the moment about the y–axis. The lowest plot is the variation of the axial force in the wellhead over time.

The corresponding energy spectrums for the three time histories are plotted in Figure 10-5, bending moment about x- and y-axis, and Figure 10-6, axial force. These energy spectrums give the real life response of the riser system. For x-bending moment the largest energy is assembled in the frequency interval from 0.1 to 0.15 Hz, i.e. a period interval of around 6.5 - 10 seconds. For y-bending the interval is from 0.1 to 0.15 Hz. The axial force has two peaks, but these are very close, i.e. larges energy is assembled from 0.05 to 0.12 Hz. Compared to the intervals of energy peaks in the spectrum plots for the model, these are very similar, i.e. the response of the model is similar to the response of the actual riser system.

Unlike the spectrum plots for the model, the plots here also show energy peaks appearing in the area for lower frequencies. These peaks explained by permanent moments acting in the structure, assuming no de-trend procedure is implemented, or they can be caused by low frequency wave drift forces acting on the system. The wave drift forces are caused by second order wave drift forces that vary slowly (MARIN,

2009). These have not been included in the model, and therefore does not appear in the spectrum plots for the model.

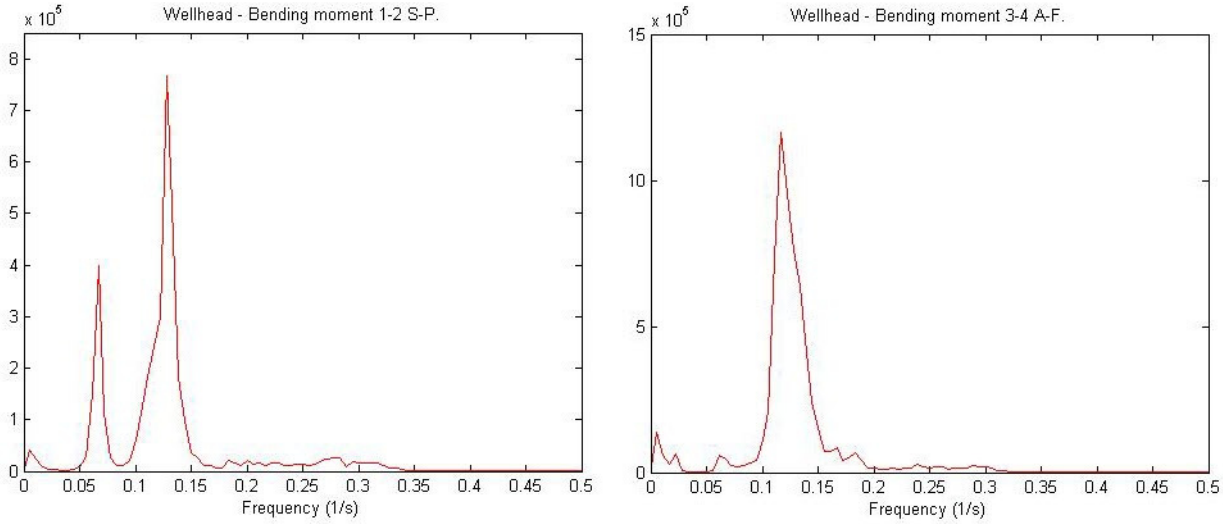

Figure 10-5: Energy spectrum for the bending moment 1-2 S-P (left) corresponding to the moment about the x–axis and the bending moment 3-4 A-F (right) corresponding to the moment about the y–axis in the wellhead for case 1 in the measurements.

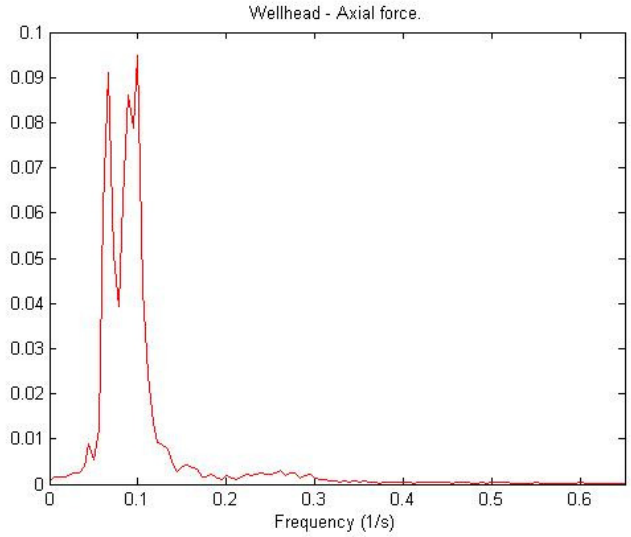

Figure 10-6: Energy spectrum for the axial force in the wellhead for case 1 in the measurements

10.2.1.2 Case 2

The time history and spectrum plots for the moments and forces from measurements in the wellhead in case 2 are given in Appendix D. Statistical parameters and results from this case are presented and discussed further in chapter 10.3.

10.2.2 10 ft Pup joint

The measurements in the pup joint are also given as Bending Moments 1-2 S-P (starboard-port), Bending Moment 3-4 A-F (aft-forward) and Axial Force. It is known that the sensors on the pup joint is not positioned exactly on the axes, because auxiliary pipes, but for further comparison it is assumed that the calculation have taken this into account and that the bending moment noted 1-2 S-P is the moment about the x-axis and the bending moment 3-4 A-F is the moment about the y-axis, as forward is in positive x-direction. The plots for the pup joint measurements for both case 1 and 2 are given in Appendix D.

10.2.2.1 Case 1

The time history and spectrum plots for the moments and forces from measurements in the pup joint in case 1 are given in Appendix D. Statistical parameters and results from this case are presented and discussed further in chapter 10.3.

10.2.2.2 Case 2

The time history and spectrum plots for the moments and forces from measurements in the pup joint in case 2 is given in Appendix D. Statistical parameters and results from this case are presented and discussed further in chapter 10.3.

10.3 Evaluation of model compared to the reality

In this chapter an evaluation of the model is performed, the model results are compared to the measured data from the real life riser system. Table 10-1 shows statistical values found for the wellhead in both cases run, while Table 10-2 shows the same values found in the pup joint. Exact numbers in the tables vary a great deal and are not of interest as these depend on simplifications performed in the model, but it is interesting to look into the order of magnitude of the absolute values and perform a percentage or proportion evaluation.

Comparison between the two cases within the model is not performed as input as well as the results are very similar to each other. It can be seen that this is the case for the measurements as well; they are very similar for the two cases.

In the tables M_x correspond to bending about x-axis (Bending moment 12 (SP) from analysis results), M_y correspond to bending about y-axis (Bending moment 34 (AF) from analysis results) and F_z correspond to axial force (wall tension). The statistical parameters given are the mean, standard deviation, maximum and minimum values. The mean shows the overall average value for the total time while the standard deviation gives the variation of the values from the mean in the time history. Low standard deviation means that there is low variation from mean in the data plotted.

Both tables show that the bending moment about the x-axes, M_x, in the model is very small in case1 as well as case 2, and they are small compared to the actual bending moment given from the measurements. This can be explained by the direction of the waves and current in the model. A direction of 180 degrees has been chosen as a simplification in the model. This will in practice mean that all the

environmental loads are implemented in the x-direction which again will mainly cause large movements about the y-axes. This is not the case in reality and this implies that the movement about the x-axes is not modeled correctly and the motion pattern of the BOP will deviate from the reality when it is not loaded correctly. The waves may have a main direction close to the one given here, but the direction of the current is most probably wrong as it changes direction trough the water depth, i.e. the effect of Coriolis has to be taken into consideration.

Table 10-1: Statistical values for model and measurements results, wellhead. Absolute values used, M_x correspond to bending moment about x-axis, M_y correspond to bending moment about y-axis and F_z correspond to the axial force.

Wellhead	**Model**			**Measurements**		
Case 1	**M_x [kNm]**	**M_y [kNm]**	**F_z [MN]**	**M_x [kNm]**	**M_y [kNm]**	**F_z [MN]**
Mean	0.00053	-81.7469	-45.8745	-88.6169	-351.6489	-0.6529
Standard deviation	0.0144	6.5774	0.1140	147.6185	199.9765	0.0681
Max.	0.0587	-47.8606	-45.5181	424.7627	336.324	-0.5118
Min.	-0.0460	-103.4506	-46.2106	-605.0486	-1037.8293	-0.8255
Case 2	**M_x [kNm]**	**M_y [kNm]**	**F_z [MN]**	**M_x [kNm]**	**M_y [kNm]**	**F_z [MN]**
Mean	0.00226	-72.2142	-41.1231	-189.1293	-292.7522	-0.7058
Standard deviation	0.0413	11.2172	0.1528	163.0721	226.8269	0.07590
Max.	0.1402	-30.8896	-40.7103	389.9642	409.8317	-0.5152
Min.	-0.0954	-103.8393	-41.5597	-698.8127	-1133.1879	-0.9169

Table 10-1 also shows large differences between the model and the measured data for both the bending about the y-axes and axial force in the wellhead. The values in the wellhead have, as explained earlier, been found from calculations performed with basis in results from another point in the model. These calculations include several sources of errors as they simplify the model even more in the lower part of the system. The calculations simplify the area between the lower flex joint to the point of interest in the wellhead to a simple beam. This will affect the bending because not all effects are taken into consideration here. For the axial force calculations the critical parameter is the buoyancy of the LMRP and the lower stack, as this is estimated to high it can be a source of error giving larger axial forces than the model would give.

A model corresponding to the proposed ISO model mentioned in chapter 7.1.2 will be better to use, i.e. a model stretching down through the seabed with a detailed soil model built from p-y curves for the soil.

This requires known soil properties. Then results can be given directly from OrcaFlex and fewer sources of errors present.

For the pup joint the results for the bending about the y-axes and axial force correspond better with the measurements. The standard deviations for moment and force in the model are slightly higher than for the measurements for case 1 and case 2. The models mean axial force gives good results compared to the measurements, the statistical parameters are of the same magnitude. In case 2 the differences are slightly higher, which can be because of the shorter simulation time implemented in the model for this case. The y-bending mean in the model is somewhat lower in both cases run respectively 50 and 75% lower; this implies a non conservative model.

Table 10-2: Statistical values for model and measurements results, pup joint. Absolute values used M_x correspond to bending moment about x-axis, M_y correspond to bending moment about y-axis and F_z correspond to the axial force.

10 ft Pup joint	Model			Measurements		
Case 1	M_x [kNm]	M_y [kNm]	F_z [MN]	M_x [kNm]	M_y [kNm]	F_z [MN]
Mean	0.0002	46.4981	2.2321	-145.7395	-96.4266	2.4723
Standard deviation	0.0051	11.9161	0.1140	5.1387	14.6432	0.0427
Max.	0.0216	87.6977	2.5887	-126.4511	-54.8618	2.5517
Min.	-0.0161	5.4829	1.8959	-165.2407	-149.7587	2.3773
Case 2	M_x [kNm]	M_y [kNm]	F_z [MN]	M_x [kNm]	M_y [kNm]	F_z [MN]
Mean	0.0006	21.8987	3.8805	-150.4113	-93.0509	2.4483
Standard deviation	0.0121	20.7667	0.1527	5.4868	17.1817	0.0489
Max.	0.0411	70.5598	4.2934	-132.1846	-40.8493	2.5746
Min.	-0.0276	-31.1712	3.444	-171.0085	-161.8825	2.321

An evaluation of the energy spectrums presented for the wellhead and pup joint for all the cases in chapter 10.2.1, 10.2.2, Appendix C and Appendix D are performed by comparing the frequency intervals for the energy peaks, as done in 10.2.1.1. The comparison shows that the energy peaks in the plots for the model occur for the approximately same frequency as for the measurement plots. For x-bending moment the largest energy is assembled in the frequency interval from 0.1 to 0.15 Hz, i.e. a period interval of 6.5 - 10 seconds. For y-bending the interval is from 0.1 to 0.15 Hz and for the axial force the interval 0.005 to 0.175 Hz. Any deviations can have been caused by choice in number of blocks in calculation of the spectrum by the MATLAB routine. The similarity indicates that the response of the model is approximately the same as the response of the real life riser system.

11 Conclusion

The main objective when creating an analysis model is to reproduce the reality. This is impossible to do exactly, but with all data available it should be possible to create a good approximation. In this thesis a model has been created, and an evaluation of this model by comparison with full-scale measurements is presented with the intention to optimize the model and to give better understanding of the forces occurring in the wellhead for specific cases.

From the comparison it is seen that at the area of interest, the wellhead, the analysis model does not provide accurate results. The forces and moments found do not correspond with the full scale measurements obtained. An investigation of the forces and moments in the wellhead is therefore not possible with the current model. The model should be extended to include the whole wellhead including the conductor going into the soil. In addition, a soil model based on p-y-curves should be obtained and implemented, where p-y curves relate unit soil resistance to pile deflection.

In addition to the comparison performed for the wellhead, an investigation of the forces and moments in the 10 ft pup joint positioned above the riser adapter is performed as good measurements were available here. This comparison shows better results than in the wellhead and the results coincide to some extent with the reality, especially the axial force and partially the y-bending moment. However the analysis results are non-conservative.

For both the wellhead and the pup joint the analysis results for bending moments about the x-axes does not correspond well with the reality, the reason for this is that waves and current were only affecting the system in one direction, and this is an assumption that does not correspond with the reality. The current will vary over the water depth, for further analysis the correct current distribution and wave heading should be implemented.

Two cases with different sea states were implemented for the comparison and analysis of both the wellhead and pup joint, these sea states was very similar and do not show much difference in the results. To obtain a broader evaluation platform a variety of sea states should be implemented in the analysis of the model, provided that measurement data are available for comparison.

The energy spectrum for both the wellhead and the riser joint is found for all cases analyzed. These all show the same trend; that the model response equals the response of the measured system. Combined with the results found for the 10 ft pup joint this implies that the model has some correct elements and is a good model down to the wellhead.

The model built in this thesis can be used as a basis for further development. The correct waves and current should be implemented from measured data; and the soil and wellhead model should be modeled in more detail, with correct stiffness for the soil.

12 Suggestions for further work

As mentioned in the last chapter, further development of the model should be performed to obtain a model that correlates better with the measurements. This can be done by implementing a more detailed soil and wellhead model, similar to the one presented for coupled analysis in ISO 13624-2 TR.

For a better comparison basis the measurements of waves should be transferred to a process able format and implemented in the analysis. In addition the implementation of current in OrcaFlex should include the variation in direction trough the water column. This should be found from measurements if possible, otherwise Metocean data have to be implemented.

Implementation of an alternative way of modeling the lower part of the riser, i.e. the LMRP and lower stack can be to assume pipes with geometry, mass, drag etc. corresponding to the properties of the true bodies can also be tested.

A broader comparison basis can be created if the analysis is run for a broader range of sea states, provided that the measurement data are available, and with full 3 hour simulations.

Control checks of the bending moments and axial force given in the measurement data can be performed by calculation from strains to bending moments and force.

Perform new comparisons with a more detailed model and then do a thorough investigation of the forces and moments in the wellhead.

Perform a theoretical decay test in OrcaFlex to find the eigenfrequency of the system and correlate to the response spectrum.

13 Bibliography

Bai, Y., & Bai, Q. (2005). *Subsea pipelines and risers.* Elsevier.

Chan, S. L., & Chui, P. P. (2000). *Non-Linear Static and Cyclic Analysis of Steel Frames with Semi-Rigid Connections.* Amsterdam: Elsevier.

DNV. (2010). *Report; Comparing load level with foundation capacity.* Høvik: Det Norske Veritas.

DNV. (2009). *Wellhead Fatigue - Method Statement Update.* Høvik: Det Norske Veritas.

Driling risers. Drilling, Mobile.

Faltinsen, O. M. (1990). *Sealoads on ships and offshore structures.* Cambridge, U.K.: Cambridge University Press.

GeoDrive Technology BV. (2009). *Conductor Moitoring at Troll Field Norway on Deepsea Atlantic.* Bussum.

Irgens, F. (1999). *Fasthetslære.* Trondheim: Tapir forlag.

Irgens, F. (1999). *Formelsamling mekanikk.* Trondheim: Tapir akademiske forlag.

ISO 13624-1. (2009). *ISO 13624-1: International standard. Design and operation of marine drilling riser equipment.* Geneva: ISO.

ISO 13624-2. (2009). *ISO/TR 13624-2, Technical report. Deepwater drilling riser methodologies, operations and integrity report.* Geneva: ISO.

Kavanagh, K., Dib, M., Balch, E., & Stanton, P. (2002). New revision of Drilling Riser Recomended Practice (API RP 16Q). *OTC 14263.* Huston: Offshore Technology Conference.

Larsen, C. M. (2008). *Aspects of Marine Riser Analysis.* Trondheim: Depertment of marine structures, NTNU.

Larsen, C. M. (2010, April). Deep water. Trondheim, Norway.

Larsen, C. M. (1990). *Response Modelling of Marine Risers and Pipelines.* Trondheim: NTNU, Division of marine structures.

Larsen, C. M. (2007). *TMR4180 Marin Dynamikk.* Trondheim: NTNU, Department of Marine Technology.

MARIN. (2009). *Low frequency motions*. Retrieved June 18, 2010, from Welcome to MARIN (Maritime Reasearch Institute Netherlands): http://www.marin.nl/web/show/id=79251

McCrae, H. (2001). *Marine riser systems and subsea blowout preventers.* Texas: Petroleum Extension Service.

Mobil Drilling . Section V - Drlling Risers . In M. Drilling. Mobile Drilling .

Myrhaug, D. (2007). *TMR4180 MARIN DYNAMIKK, Uregelmessig sjø.* Trondheim: NTNU, Department of Marine Technology .

NORSOK. (2007). *NORSOK STANDARD N-003, Action and action effects.* Lysaker: Standards Norway.

NORSOK. (2004). *NORSOK STANDARD N-004, Design of steeel structures.* Lysaker: Standards Norway.

Odfjell Drilling AS. (2010, January 19). Riser and tensioner monitoring, sensor location. Drawing number: DSA-335-070-D-XE-0001-02 . Bergen.

Odfjell Drilling AS. (2010, January 20). Run 2 - Sequence logg. Bergen.

Odfjell Drilling. (2009). *Odfjell Drilling*. Retrieved May 8, 2010, from Mobile offshore Units: http://www.odfjelldrilling.com/en/News/Image-gallery/Mobile-offshore-Units/

Odfjell Drilling. (2009). *Odfjell Drilling.* Retrieved April 19, 2010, from Odfjell Drilling: http://www.odfjelldrilling.com/en/Our-business/Mobile-offshore-units/Operated-rigs/Deepsea-Atlantic/, http://www.odfjelldrilling.com/en/News/Image-gallery/Mobile-offshore-Units/

Odfjell Drilling Technology. (2010, June 18). Input/clarification. *E-mail from Odjfell Drilling AS (Nicholas James Toynbee, Marius Stamnes)* .

Odfjell Drilling/4subsea. (2009). *Rig Data Requirements- Deepsea Atlantic.* Statoil.

Orcina . (2008, May 06). E-mail from orcina regarding: Recommended build-up time for a riser analysis.

Orcina. (2009). OrcaFlex usermanual. Cumbria, UK.

Pettersen, B. (2004). *Marin Hydrodynamikk og konstruksjonsteknikk, Grunnkurs 1.* Trondheim: Department of Marine Technology.

Rong, R. H. (2004). *Dynamisk resons av flytende vindturbin.* Trondheim: NTNU, Department of Marine Technology.

Rudi, B. R. (2008). *Design Analysis of Workover Riser.* Trondheim: NTNU - Master thesis.

Sangesland, S. (2008). Drilling and completion of subsea wells. NTNU.

Shaffer. (2009). Odfjell Riser system layout, system drawings for DSA.

Sparks, C. P. (2007). *Fundamentals of Marine Riser Mechanics: Basic Prinsiples and Simplified Analyses.* Tulsa, Oklahoma: PennWell.

StatoilHydro. (2009). *Troll Field Metocean Design Basis.* StatoilHydro.

Torsethaugen, K., & Haver, S. (2004). Simplified double peak spectral model for ocean waves. *Proceedings of The Fourteenth (2004) International Offshore and Polar Engineering Conference.* Toulon, France: The International Society of Offshore and Polar Engineers.

Appendix A Input and data for calculation

A1. Current

Measurements of the current during test runs were not obtained therefore a current is chosen. Current speed varying over water depth is given in Table A-1. The data used is the extreme values for is the one year omni-directional distributions at the Troll field taken from the Metocean report for the field (StatoilHydro, 2009). These numbers are high and may not correspond with the reality. A smaller constant current can also be applied.

Table A-1: Omni directional current speed distributed over the water depth for the Troll field, annual probability of exceedance: 10^{-1}.

Depth [m]	Velocity [m/s]
0	1.55
2	1.55
12	1.23
50	1.05
100	0.72
200	0.68
331	0.48
334	0

A2. Material properties

In calculations of input data for stiffness and geometry properties of the material is used. The following table gives these properties.

Table A-2: Material properties for steel used in calculations

Material properties		
Material	Steel	-
Density [1)]	7860	[kg/m^3]
Young's modulus, E[1)]	210E9	[N/m^2]

1) Assumed value for the steel components in this thesis (NORSOK, 2004)

A3. Bending, axial and torsional stiffness for line components

The bending stiffness and axial stiffness are calculated for each component in the excel sheet for calculation on the DVD in Appendix E, accept the stiffness properties for the connection line which is assumed to be large and are based on earlier experience. The torsional stiffness is assumed as well (Odfjell Drilling Technology, 2010). The equations used in the calculation are presented in Appendix B.

Table A-3: Input for bending, axial and torsional stiffness of line components

Component	Bending stiffness [kNm^2]	Axial stiffness [kN]	Torsional stiffness [kNm^2]
Upper flex joint	226.7E3	6.886E6	175E3
Slip joint inner barrel	226.7E3	1	175E3
Slip joint – outer barrel	529.5E3	10.489E6	409E3
Slip joint – outer barrel w/ aux. lines	529.5E3	10.489E6	409E3
75” Riser joint	226.7E3	6.886E6	175E3
75” Riser joint w/buoyancy	226.7E3	6.886E6	175E3
30” Pup joint	226.7E3	6.886E6	175E3
10” Pup joint	226.7E3	6.886E6	175E3
Riser adapter	299.8E3	9.381E6	175E3
Lower flex joint	299.8E3	9.381E6	175E3
Connection lines	977.78E6	12.752E9	10E6

A4. Nonlinear connection stiffness for the Flex joints

Input data for upper and lower flex joint (Odfjell Drilling/4subsea, 2009). OrcaFlex interpolates linearly between the points given in the input.

Table A-4: Stiffness properties of the upper and lower stress joint.

Upper flex joint		Lower flex joint	
Angle [deg]	**Bending moment [kNm]**	**Angle [deg]**	**Bending moment [kNm]**
0	0	0	0
0.1	7.27	0.1	33.94
0.5	23.12	0.5	107.99
1	38.06	1	177.82
2	62.68	2	292.76
3	83.91	3	391.9
4	103.21	4	482.01
5	121.18	5	565.93
7	154.37	6	645.25
9	184.97	7	720.92
11	213.7	8	793.6
13	241	9	863.78
15	267.14	10	931.79

A5. Stiffness and damping input for tension cylinders

The following tables give the input values for the six springs modeling the tension cylinders in the riser system. Values for Case 1 and Case 2 are given in the same table and the same input is given for the all the springs, assuming they shear the weight carried equally between them.

Table A-5: Input values for stiffness in the springs modeling the tension cylinders

Stiffness input for tension cylinders			
Case 1		Case 2	
Stroke length [m]	Tension [kN]	Stroke length [m]	Tension [kN]
18	567.11	18	758.08
21.81	621.62	21.81	812.59
25.62	676.13	25.62	867.1
29.43	730.64	29.43	921.61
33.24	785.16	33.24	976.12

Table A-6: Input values for damping in the springs modeling the tension cylinders

Damping input for tension cylinders			
Case 1		Case 2	
Velocity [m/s]	Tension [kN]	Velocity [m/s]	Tension [kN]
-1.8	-330	-1.8	-330
-1	-150	-1	-150
0	0	0	0
1	150	1	150
1.8	330	1.8	330

Appendix B Calculation of system element properties

B1. Calculation of drag diameter

The diameter used as the drag diameter in this model is the bolt circle plus the outer diameter of the kill line. The kill line and the choke line have the same diameter properties, i.e. diameter of kill line equals half the radius of the kill plus half the radius of the choke line. The broadest length in the transverse dimensions is used as drag diameter in this report.

Another approach has been presented by DNV, where the diameter of the main pipe plus the diameter of the kill and the diameter of the choke line are added to a total diameter, neglecting the space between the pipes (DNV, 2009).

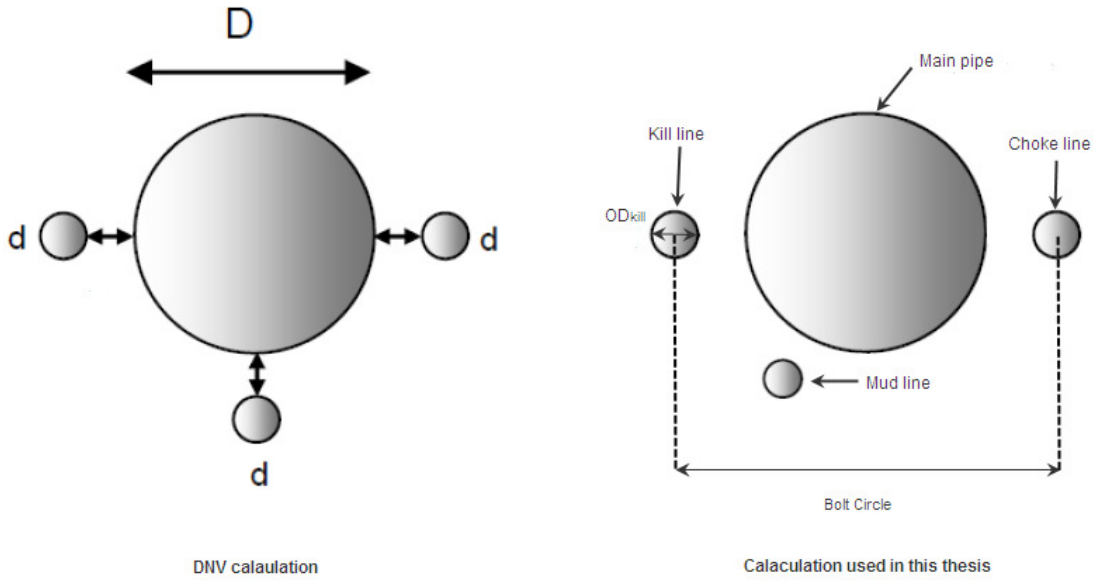

Figure B-1: Calculation approach for drag diameter, DNV method vs. method chosen in this report.

B2. Bending and axial stiffness

The calculations of bending and axial stiffness in the lines for the analysis model are calculated by employing the following equations:

Bending stiffness: $$EI = E\pi \frac{\left(\frac{OD}{2}\right)^4 - \left(\frac{ID}{2}\right)^4}{4} \quad \text{(B-1)}$$

Axial stiffness: $$EA = E\pi \left(\left(\frac{OD}{2}\right)^2 - \left(\frac{ID}{2}\right)^2\right) \quad \text{(B-2)}$$

Where OD is the outer diameter of the load bearing pipe/main pipe, ID is the respective internal diameter.

B3. Tension in tension cylinders

The tension implemented in the model for analysis is the tension used during the measurement sequences. The necessary top tension for the specific sequences is calculated from the total weight of the system and the overpull at LMRP, see excel file for input calculations on DVD in Appendix E. The calculated stroke tension correlation given for the system on DSA, see Figure B-2, is used to extrapolate a new line for the tension needed in the specific cases. The extrapolation is performed by assuming that the slope varies linearly between the lines. A new slope is found and the value for this new line gives us the stiffness in each of the cylinders. See calculation of the tension in the tension cylinders for each case in the excel sheet for calculation of input on DVD in Appendix E.

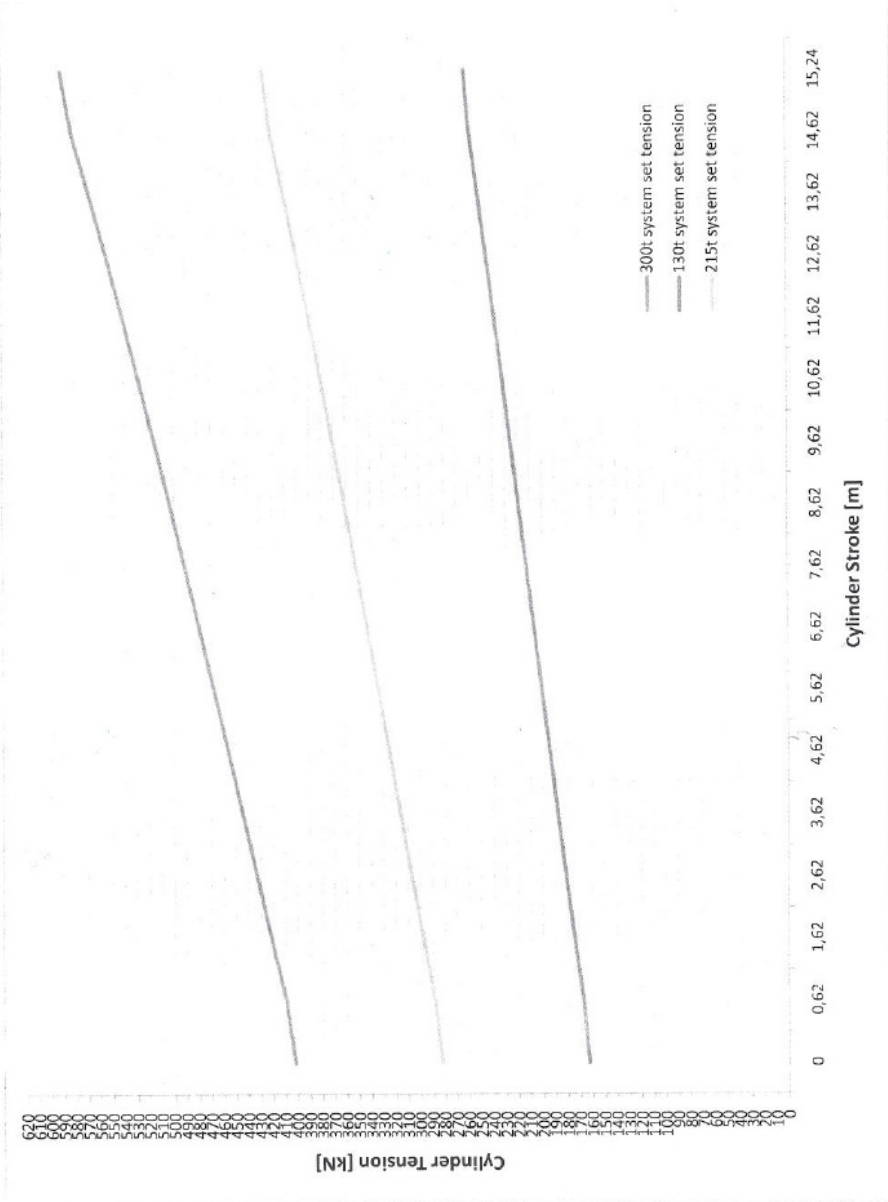

Figure B-2: Stroke tension correlation for different system set tensions for DSA.

Appendix C Calculation of results and plots from OrcaFlex model

C1. Calculation of bending moment and axial force in wellhead

The results on the wellhead have to be calculated as the measurements are given for a point on the wellhead 0.775 m above the seabed, and results can only be taken out of OrcaFlex down to the top of the wellhead.

To find the moments in the point of interest the equilibrium of moments is calculated, see equation (C-1). The shear forces in x- and y-direction and the corresponding bending moments about the y- and x-axes are found in the end of the line between tension ring and LMRP in OrcaFlex, i.e. at the lower flex joint in the system. And the moment arm is the distance from the position of the measurement sensor to the lower flex joint, see illustration in Figure C-.

$$M_{point\ of\ interest} = M_{in\ end\ of\ line} + (F_{shear\ in\ end\ of\ line} \cdot Moment\ arm) \quad \text{(C-1)}$$

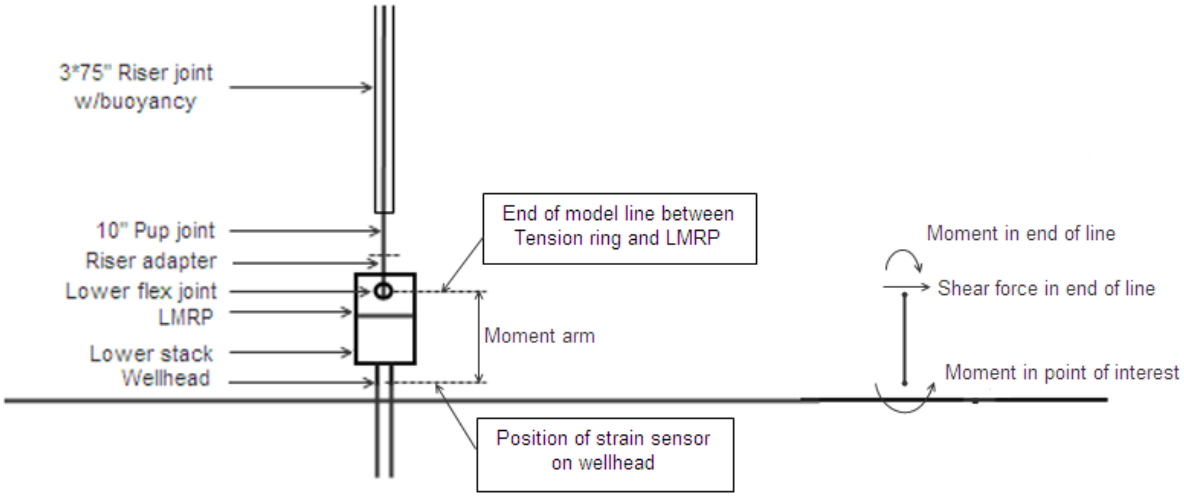

Figure C-1: Illustration of forces and moments used from OrcaFlex to calculate- and y-bending moment in wellhead.

Time histories for the shear force and bending moments in the end of the line is found from OrcaFlex and the equation above is used to create a new time history for the bending in point of interest in the wellhead. The calculation is performed in the excel file for calculation of analysis results in wellhead on DVD in Appendix E.

To find the axial force in the point of interest, i.e. the point where the strain sensor is positioned on the wellhead, the equilibrium of forces is calculated. The effective tension is found in the end of the line between tension ring and LMRP in OrcaFlex, i.e. at the lower flex joint in the system. This combined with the weight and buoyancy of the BOP, i.e. LMRP and Lower stack, and the mass of the internal fluid in the BOP is used to find the effective tension in the point of interest, see following equation:

$$T_{e,\ wellhead} = T_{e,in\ end\ of\ line} - (g \cdot m_{BOP}) + B_{buoyancy\ of\ empty\ BOP} - \left(g \cdot m_{internal\ fluid}\right) \quad \text{(C-2)}$$

This effective tension is again used to find the true wall tension in the point of interest. For a non-pressurized pipe with seawater on the inside as well as on the outside the true wall tension equals the axial force. The true wall tension in the point of interest, i.e. in the wellhead, equals the effective tension in the point plus the internal pressure minus the external pressure. Given as follows:

(C-3)

It is important to use the correct cross-section, to get the correct areas in equation (C-3). This axial force the calculation depends on unknown factors as the buoyancy of the BOP, in the excel file this is calculated by assuming that the BOP consist of only steel, which is not the case in reality where gas tanks and hydraulic fluid can be mentioned as some of the components in a BOP deviation from the assumption. This can give large errors in the calculation, and should be taken into consideration when the comparison is performed.

C2. Wave spectrums

Wave spectrum for the waves applied in the OrcaFlex Model

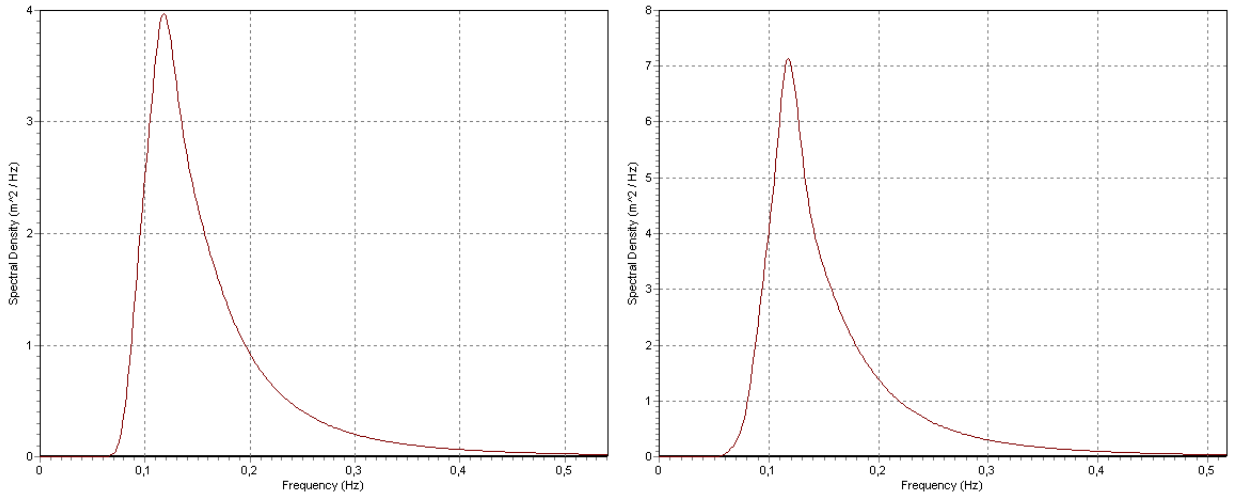

Figure C-2: Wave spectrum for waves applied in the OrcaFlex Model. On the right for case 1, Torsethaugen, sea state Hs=2.3 m and Tp=8.5 s. On the left for case 2, Torsethaugen, sea state Hs=2.9 m and Tp=8.5 s

C3. Time history and energy spectrum plots

Wellhead

The results on the wellhead are calculated as the measurements are given for a point on the wellhead 0.775 m above the seabed, and results can only be taken out of OrcaFlex down to the top of the wellhead. See the first chapter in this appendix and excel sheet for calculation of analysis results in wellhead on DVD in Appendix E. In the following the results found in the wellhead are presented.

Case 1

The results for case 1 are presented in chapter 10.1.1.1.

Case 2

The time history for the x-bending moment, y-bending moment and axial force in case 2 are given in the figure below.

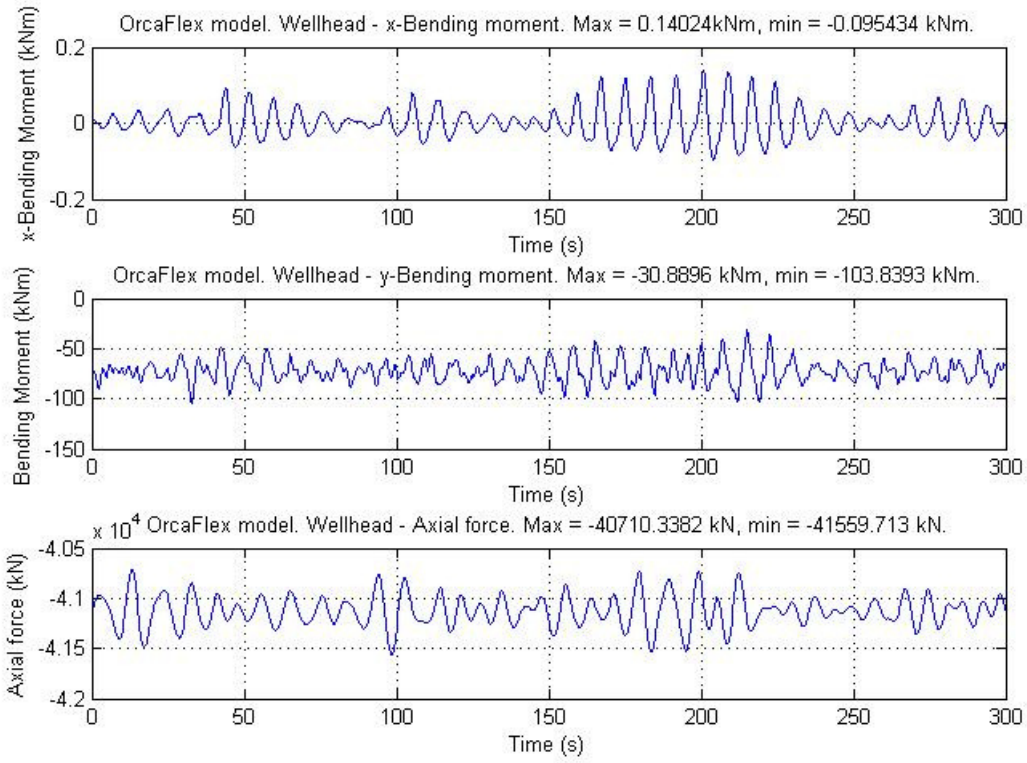

Figure C-3: Time history plots for OrcaFlex model in wellhead, from case 2. The upper plot is the variation of x-bending moment in the wellhead and middle plot is the variation of y-bending moment. The lowest plot is the variation of the axial force in the wellhead over time.

The corresponding spectrums are given in the three graphs presented in the following.

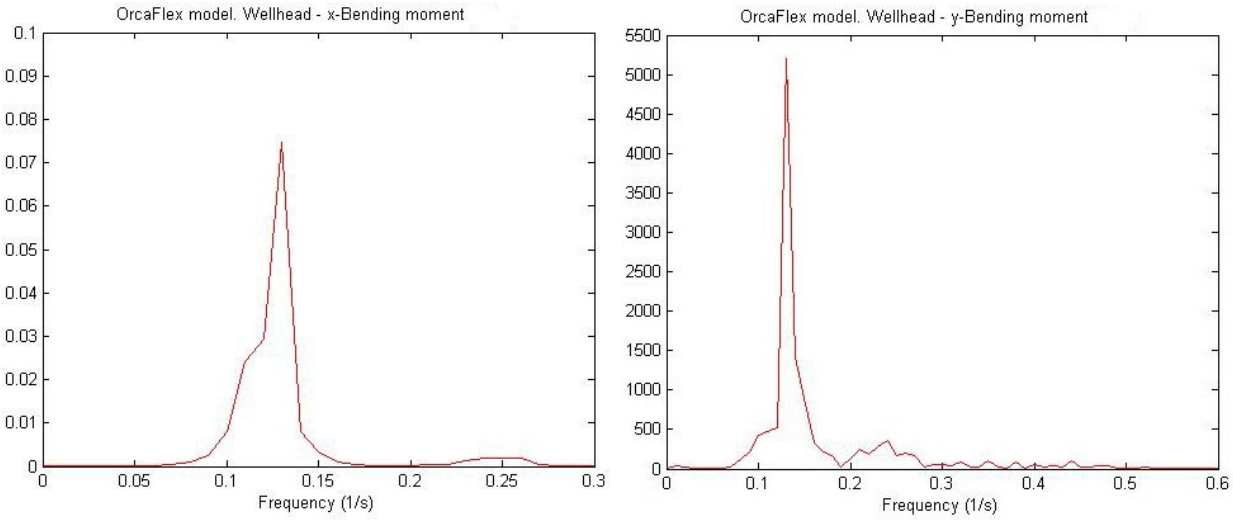

Figure C-4: Right: Energy spectrum for the x-bending moment in the wellhead for case 1. Left: Energy spectrum for the y-bending moment in the wellhead for case 1

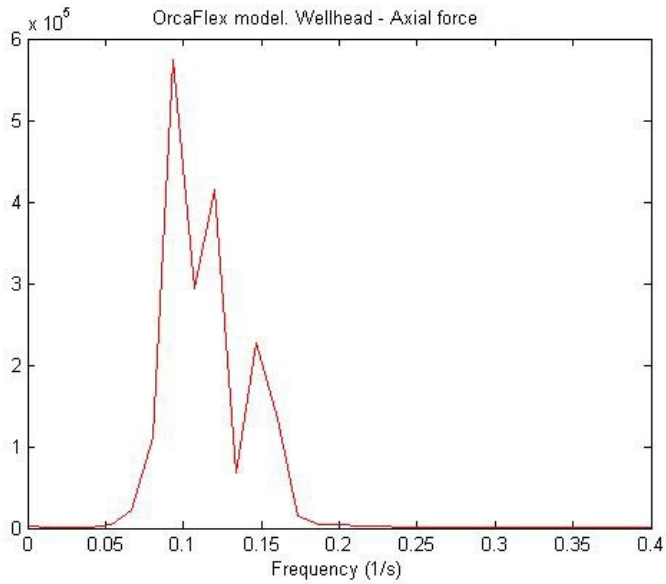

Figure C-5: Energy spectrum for the axial force in the wellhead for case 1

10 ft Pup joint

The results for the 10 ft pup joint are taken from node 134 in the line between tension ring and LMRP in the OrcaFlex model, the point correspond with the point where measurements were obtained. In the following the results found are presented.

Case 1

The time history for the x-bending moment, y-bending moment and axial force in case 1 are given in the following figures.

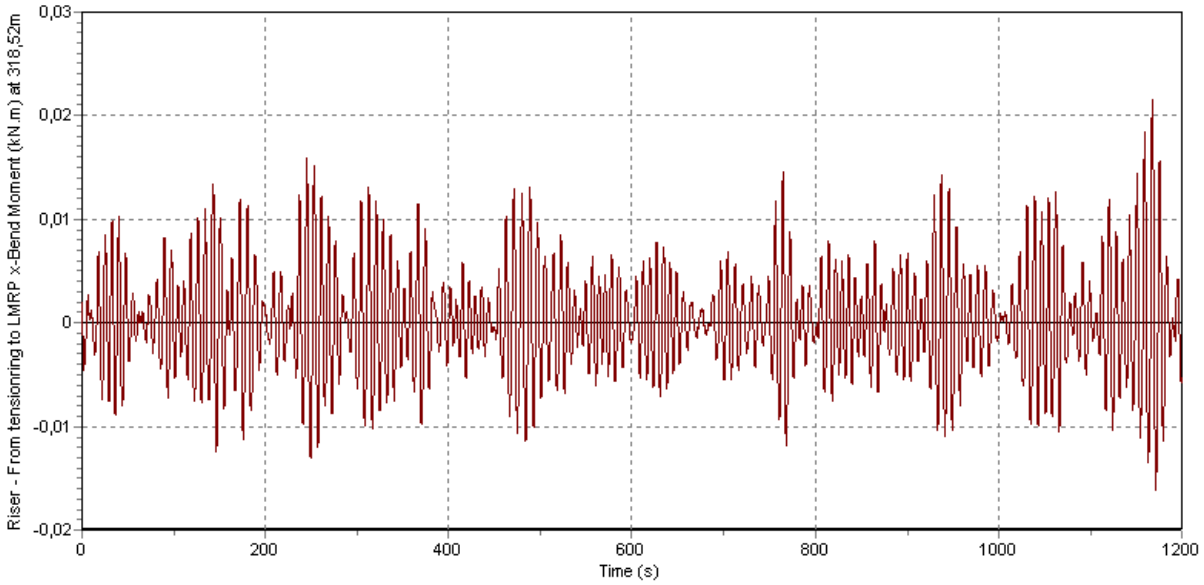

Figure C-6: Time history plot of the x–bending moment for model result in pup joint, i.e. node 134 in model, from case 1.

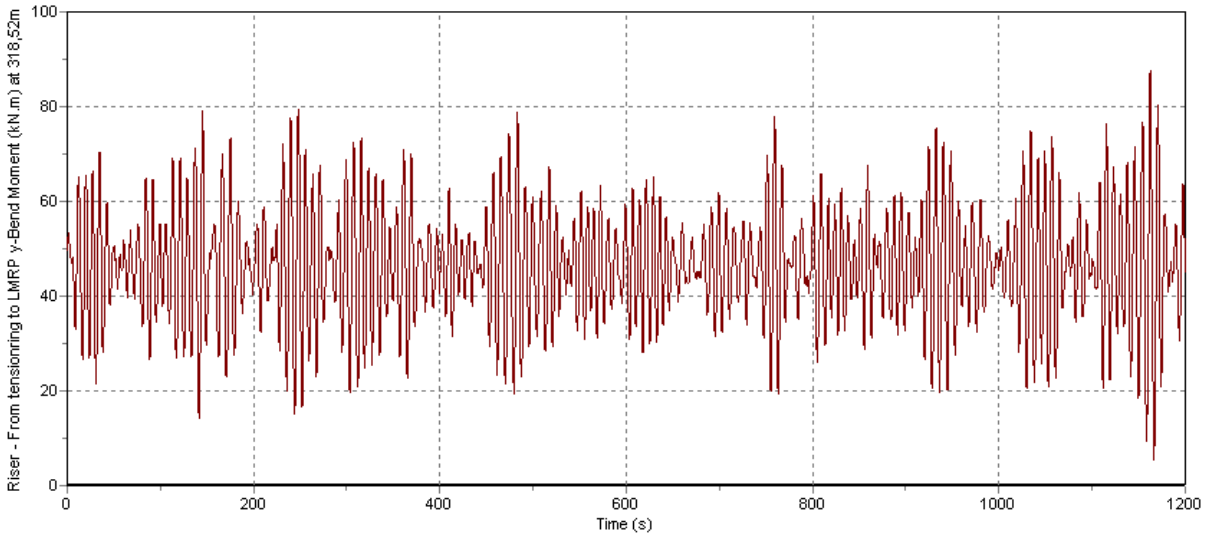

Figure C-7: Time history plot of the y–bending moment for model result in pup joint, i.e. node 134 in model, from case 1.

For a non-pressurized pipe with seawater on the inside as well as on the outside the true wall tension equals the axial force.

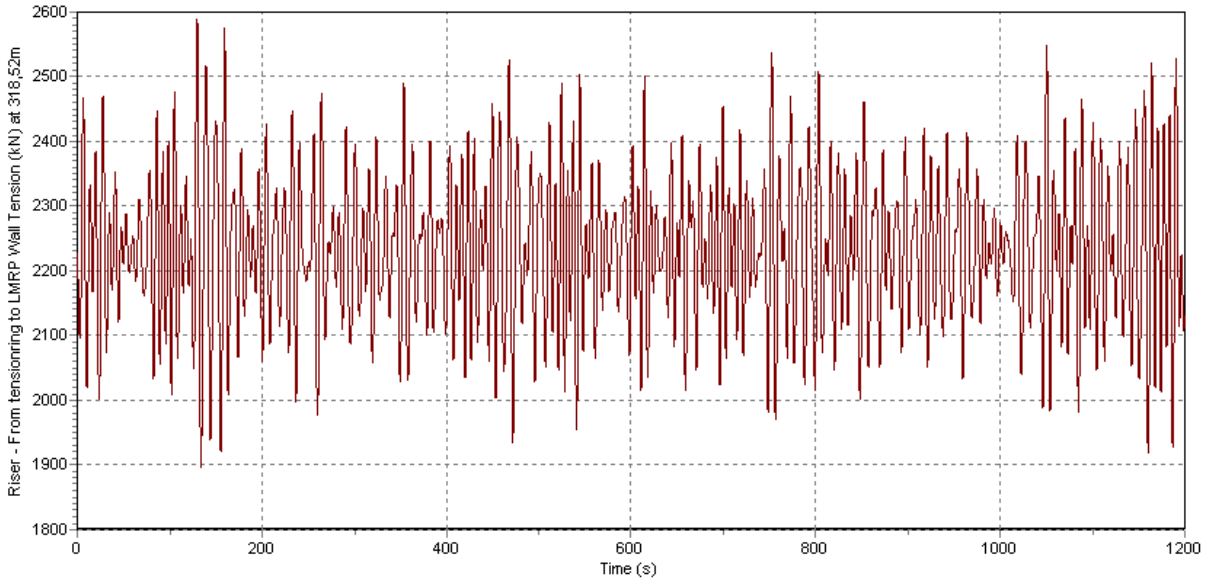

Figure C-8: Time history plot of the axial force for model result in pup joint, i.e. node 134 in model, from case 1.

The corresponding spectrums are given in the three graphs presented in the following.

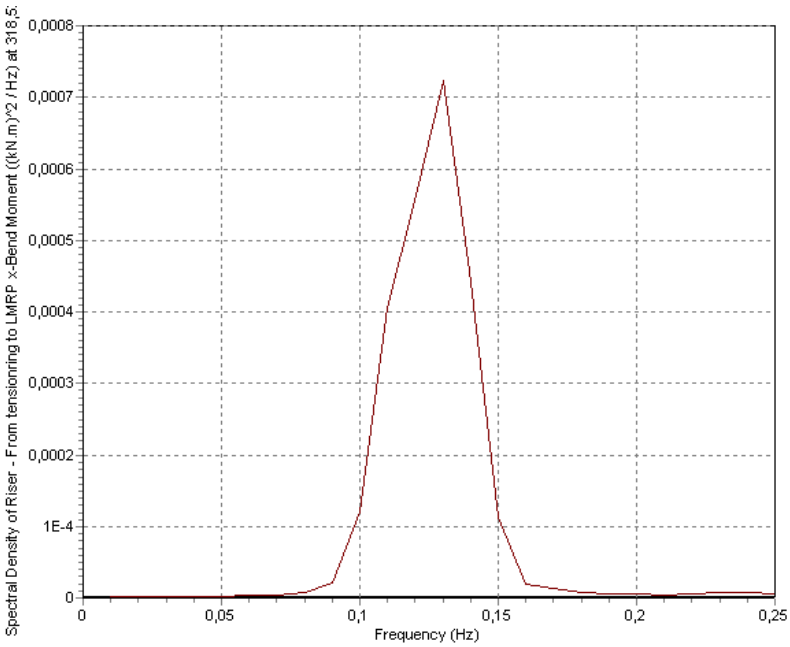

Figure C-9: Energy spectrum for the x-bending moment in the pup joint for case 1.

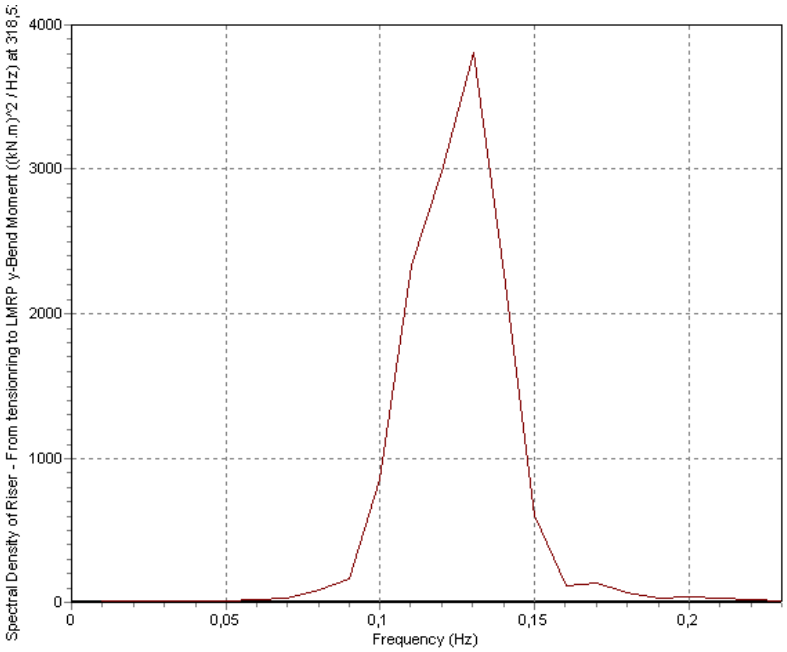

Figure C-30: Energy spectrum for the y-bending moment in the pup joint for case 1

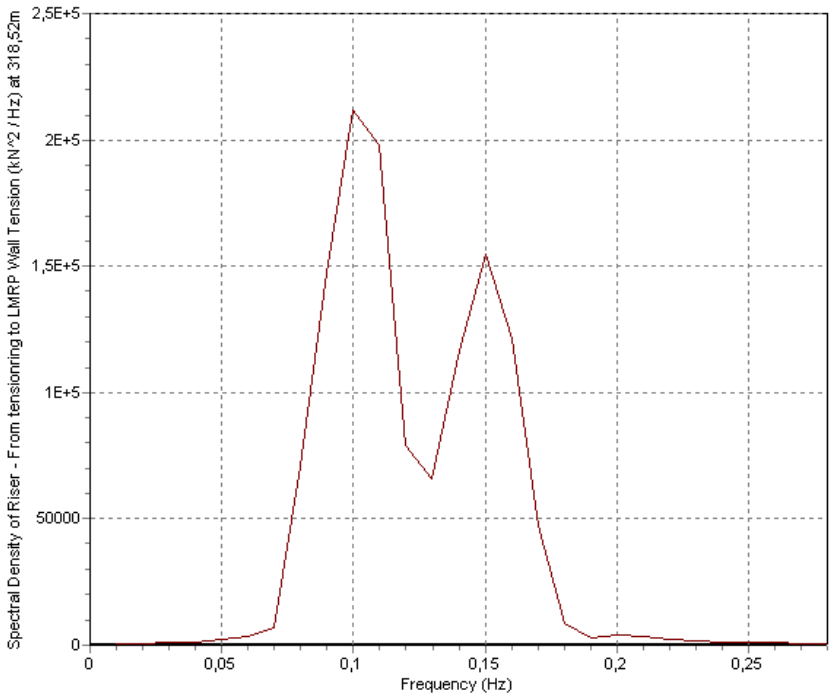

Figure C-41: Energy spectrum for the axial force in the pup joint for case 1

Case 2

The time history for the x-bending moment, y-bending moment and axial force in case 2 are given in the following figures.

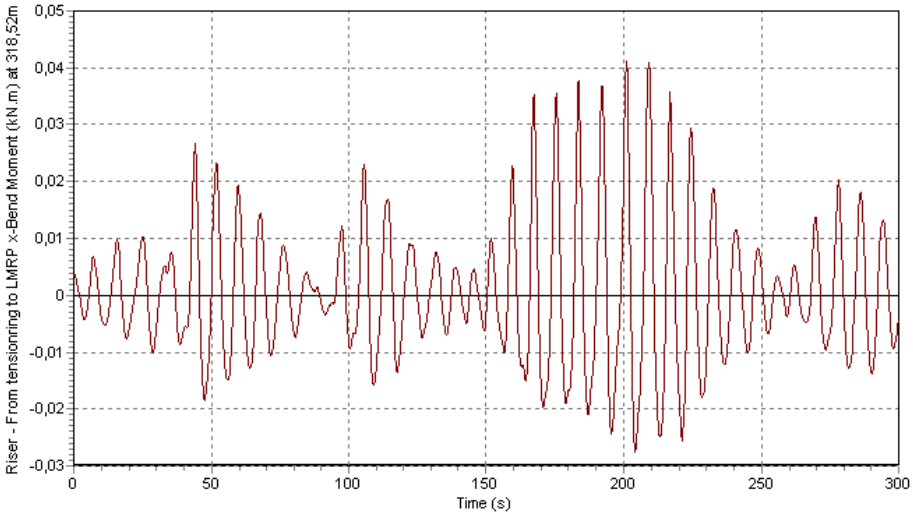

Figure C-52: : Time history plot of the x–bending moment for model result in pup joint, i.e. node 134 in model, from case 2.

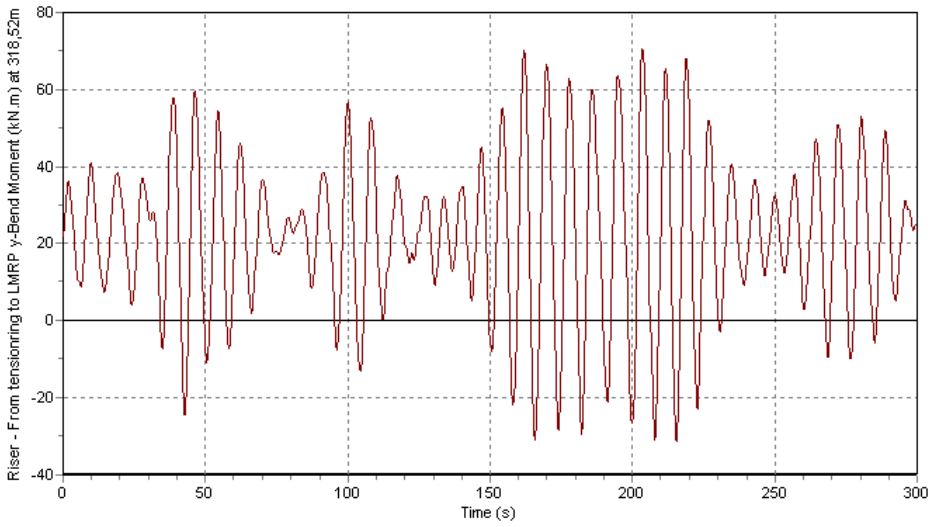

Figure C-63: Time history plot of the y–bending moment for model result in pup joint, i.e. node 134 in model, from case 2.

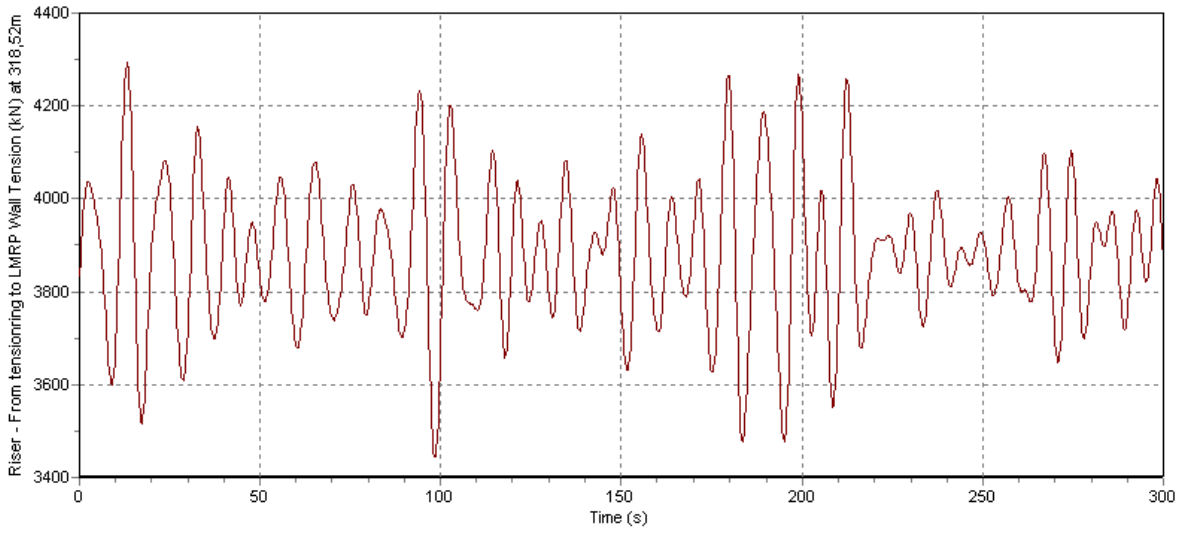

Figure C-74: : Time history plot of the axial force for model result in pup joint, i.e. node 134 in model, from case 2.

The corresponding spectrums are given in the three graphs presented in the following.

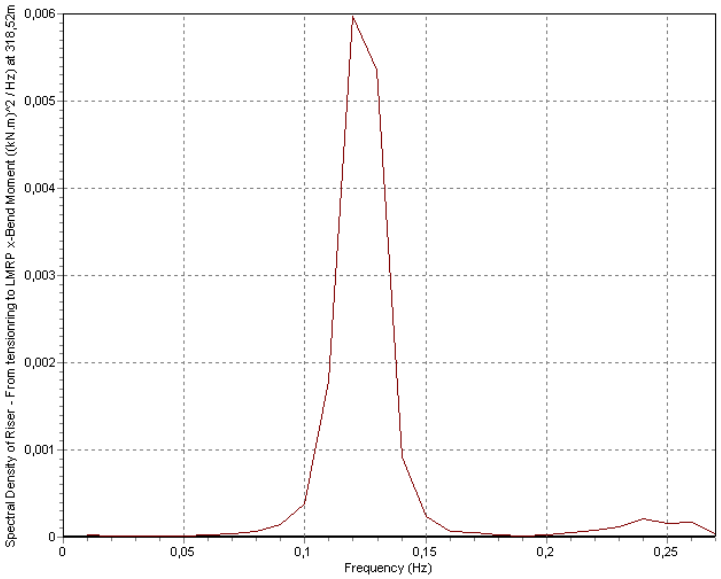

Figure C-85: Energy spectrum for the x-bending moment in the pup joint for case 2

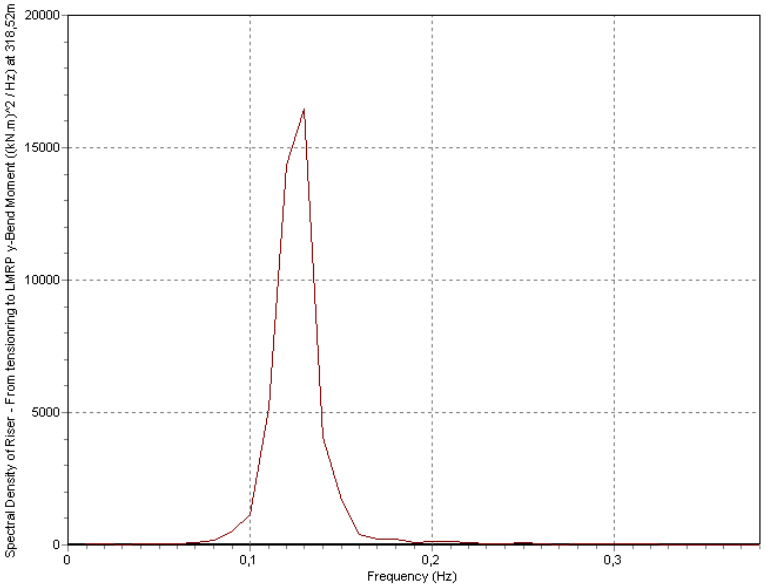

Figure C-96: Energy spectrum for the y-bending moment in the pup joint for case 2

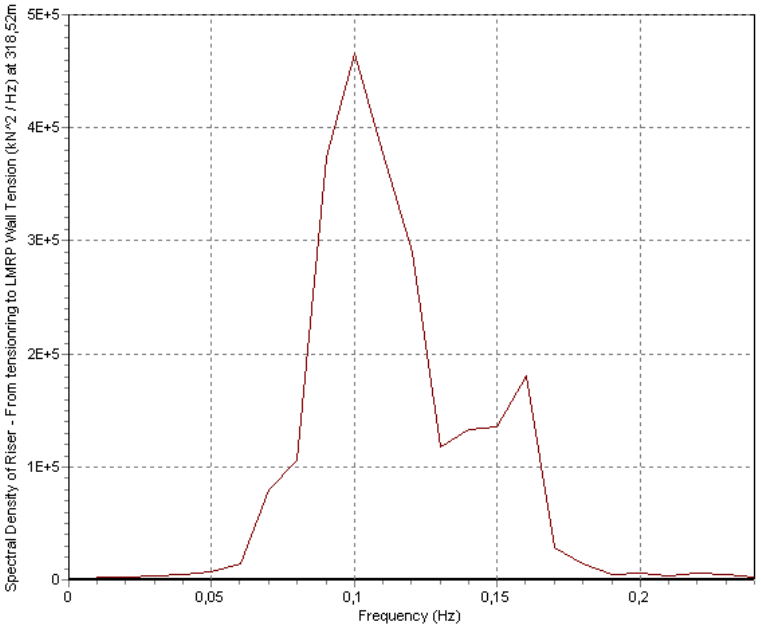

Figure C-107: Energy spectrum for the axial force in the pup joint for case 2

Appendix D Measurement result plots

D1. Wellhead

Case 1

The results for case 1 are presented in chapter 10.2.1.1.

Case 2

The time history for the x-bending moment, y-bending moment and axial force in case 2 are given in the following figures.

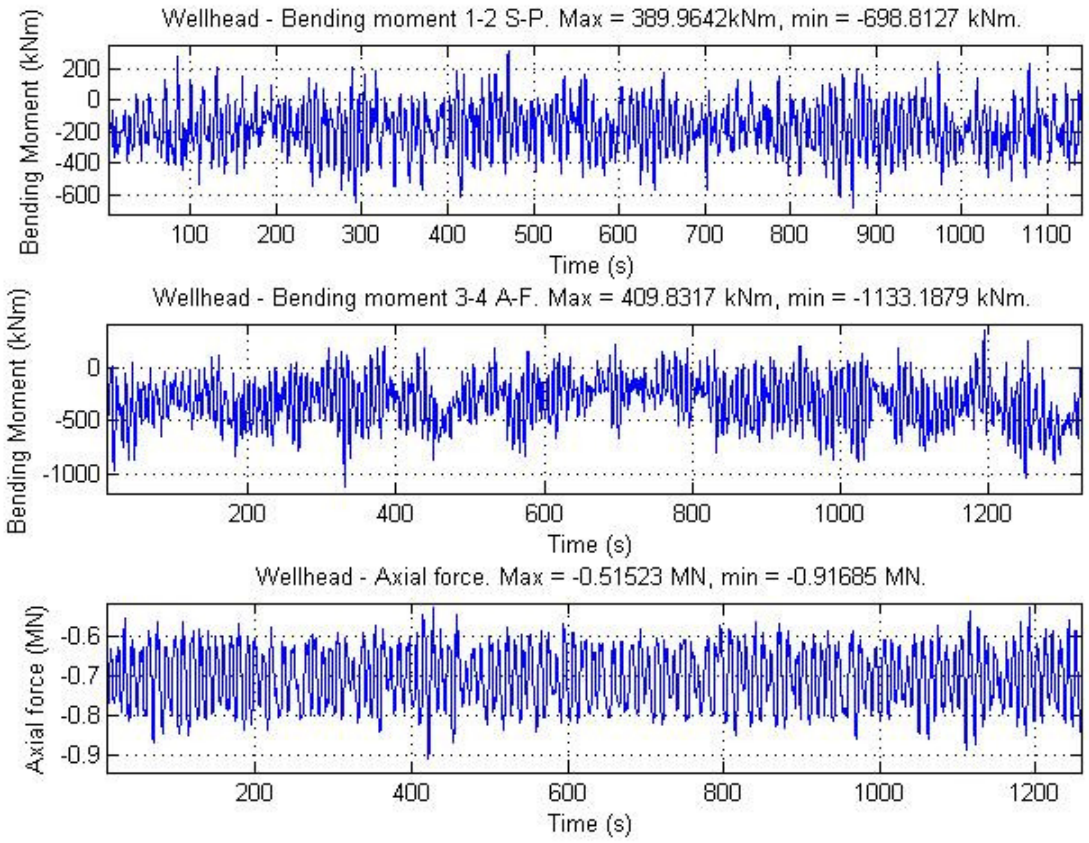

Figure D-1: Time history plots for measurements in wellhead, from case 2. Where the plot of the bending moment 1-2 S-P corresponds to the moment about the x–axis and the plot of the bending moment 3-4 A-F corresponds to the moment about the y–axis.

The corresponding spectrums are given in the three graphs presented in the following.

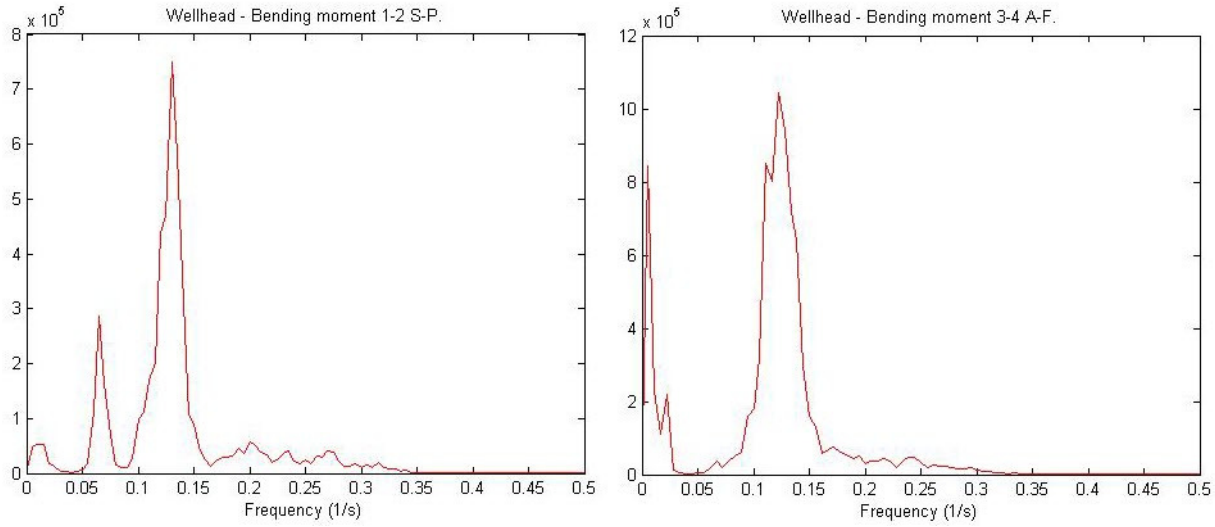

Figure D-11: Energy spectrum for the bending moment 1-2 S-P (left) corresponding to the moment about the x–axis and the bending moment 3-4 A-F (right) corresponding to the moment about the y–axis in the wellhead for case 2.

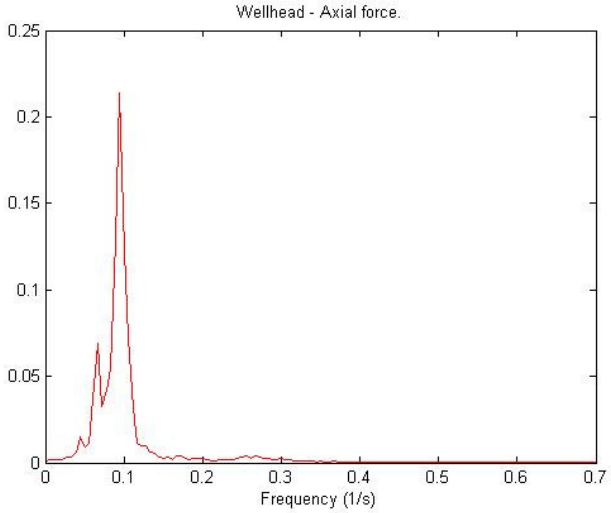

Figure D-3: Energy spectrum for the axial force in the wellhead for case 2.

D2. 10 ft Pup joint

The measurements in the pup joint are also given as Bending Moments 1-2 S-P (starboard-port), Bending Moment 3-4 A-F (aft-forward) and Axial Force. It is known that the sensors on the pup joint is not positioned exactly on the axes, but for further comparison it is assumed that the calculation have taken this into account and that the bending moment noted 1-2 S-P is the moment about the x-axis and the bending moment 3-4 A-F is the moment about the y-axis, as forward is in positive x-direction.

Case 1

The time history for the x-bending moment, y-bending moment and axial force in case 1 are given in the following figures.

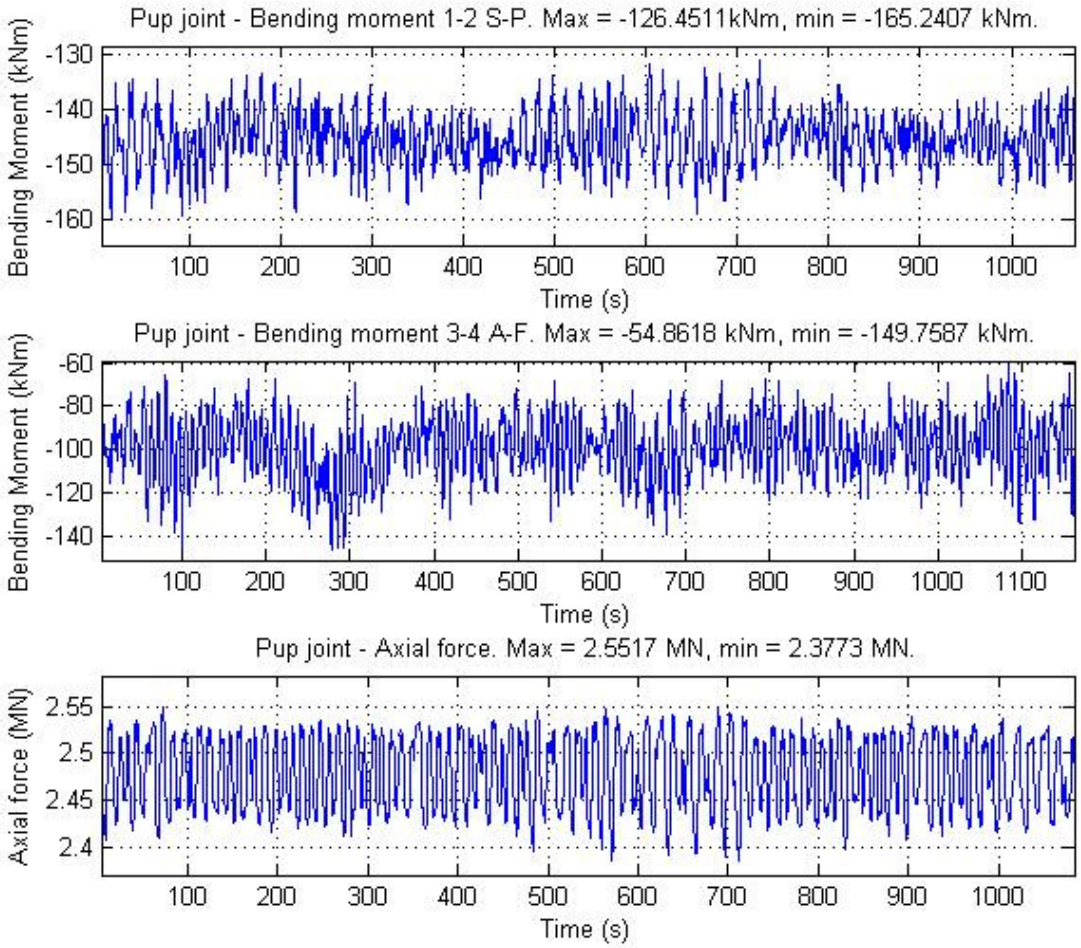

Figure D-4: Time history plots for measurements in pup joint, from case 1. Where the plot of the bending moment 1-2 S-P corresponds to the moment about the x–axis and the plot of the bending moment 3-4 A-F corresponds to the moment about the y–axis.

The corresponding spectrums are given in the three graphs presented in the following.

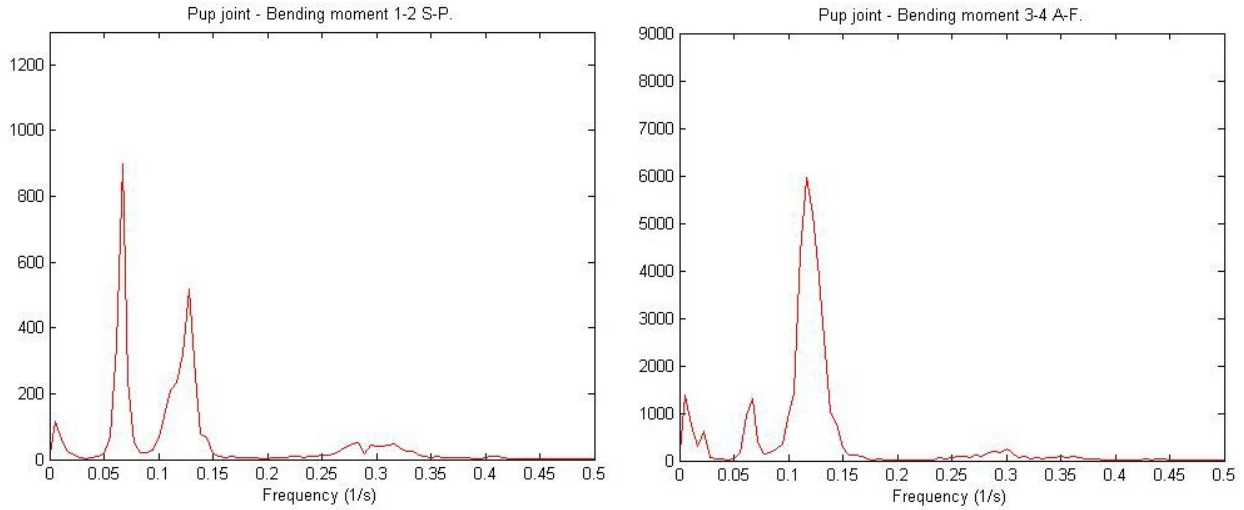

Figure D-5: Energy spectrum for the bending moment 1-2 S-P (left) corresponding to the moment about the x–axis and the bending moment 3-4 A-F (right) corresponding to the moment about the y–axis in the pup joint for case 1.

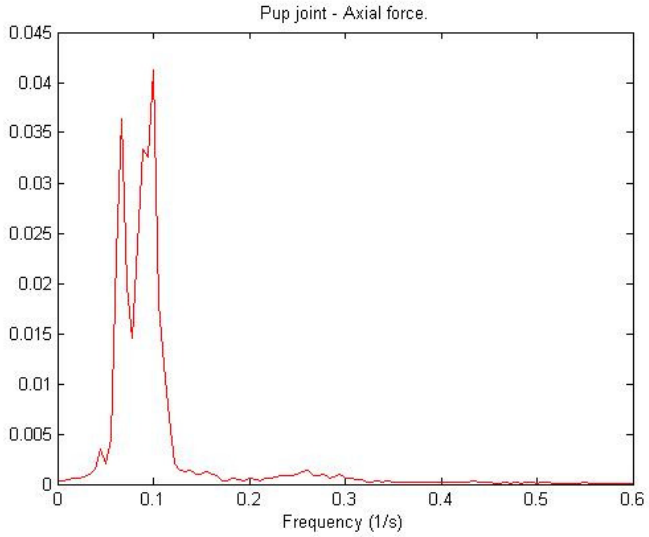

Figure D-6: Energy spectrum for the axial force in the pup joint for case 1.

Case 2

The time history for the x-bending moment, y-bending moment and axial force in case 2 are given in the following figures.

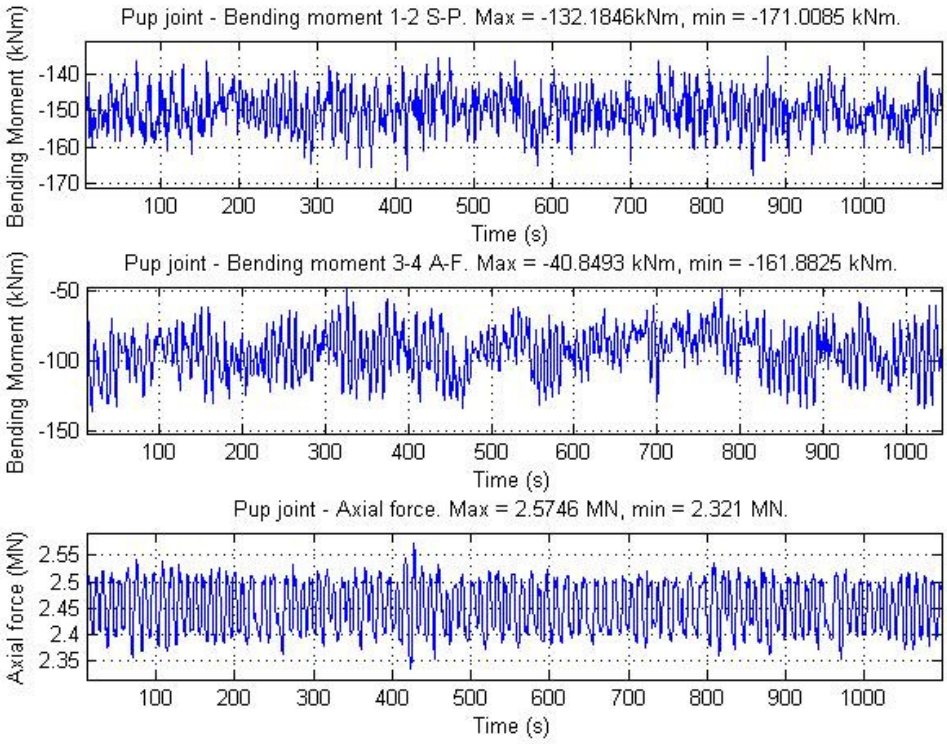

Figure D-7: Time history plots for measurements in pup joint, from case 2. Where the plot of the bending moment 1-2 S-P corresponds to the moment about the x–axis and the plot of the bending moment 3-4 A-F corresponds to the moment about the y–axis.

The corresponding spectrums are given in the three graphs presented in the following.

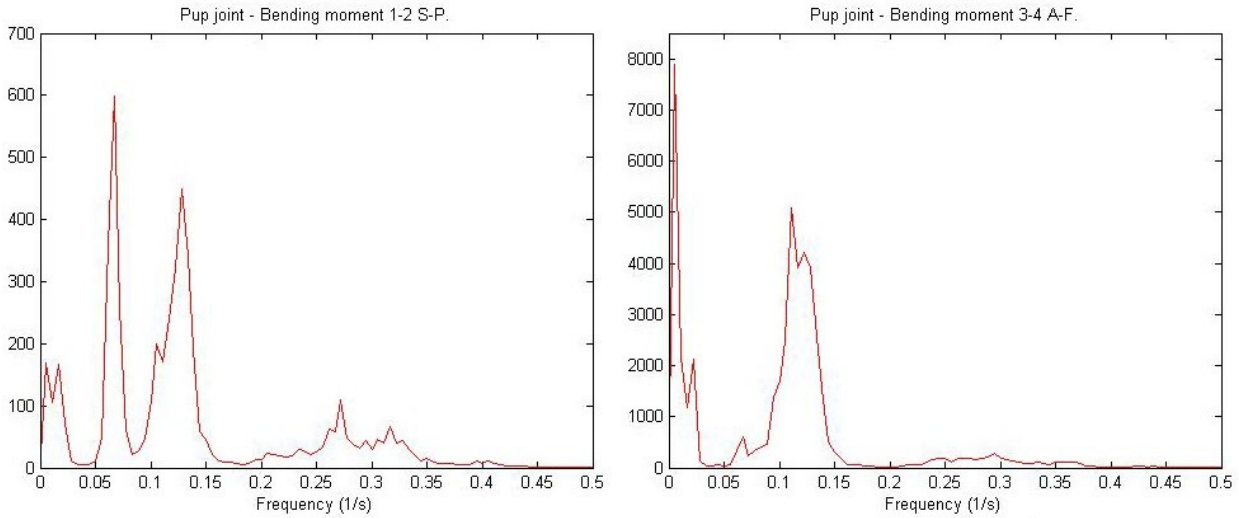

Figure D-8: Energy spectrum for the bending moment 1-2 S-P (left) corresponding to the moment about the x–axis and the bending moment 3-4 A-F (right) corresponding to the moment about the y–axis in the pup joint for case 2.

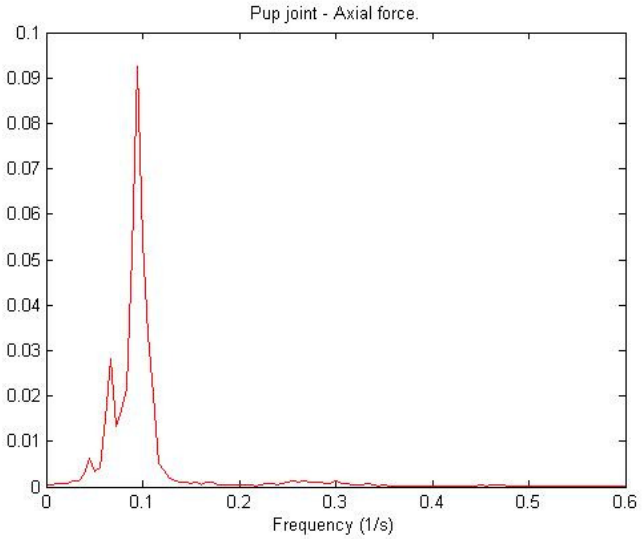

Figure D-9: Energy spectrum for the axial force in the pup joint for case 2.

Appendix E DVD

The files used in the thesis are included on the DVD attached at the back of this report.

Contents DVD:

- OrcaFlex files .dat and .sim for each run, where .dat is the model and .sim is the simulation file
- RAO input file for OrcaFlex: “DSA Displacement RAO for Import.txt”
- Excel sheets for calculation of input to OrcaFlex: “Input_calculation.xlsx”
- Input for calculation of soil stiffness: “soil_stiffness_respons_whdatum.txt “
- Excel sheets for calculation of analysis results in wellhead: “Calculation_of_analysis_results_in_wellhead.xls”
- Results from calculation of analysis results, used as input for time history and spectrum plot: “Case1_results_orcaflex_xymoment_aforce.txt” and “Case2_results_orcaflex_xymoment_aforce.txt”
- MATLAB files used for generation of spectrum and plotting: “SPEGEN_T.M”, “plot_energy_spectrum.m” and “plot_timehistory.m”. NB! The plotting files have been used for several plots and the input and structure may differ, but the general setup is the same.
- The logs used to find sequences for measurements to compare results with: “Run 2 - Sequence Logg.xlsx”
- The measurement data used in the comparison. For Case 1: “measurements_case1_part1.txt” and “measurements_case1_part2.txt”. For Case 2: “measurements_case2_part1.txt” and “measurements_case2_part2.txt”.
- In addition the list here is added on the DVD: “read_me.txt”